

BACTERIAL CARBOHYDRATES TRIGGER
***CANDIDA ALBICANS* VIRULENCE**

by

Jason Burch

A dissertation submitted to the Faculty of the University of Delaware in partial fulfillment of the requirements for the degree of Doctor of Philosophy in Chemistry and Biochemistry

Fall 2018

© 2018 Jason Burch
All Rights Reserved

BACTERIAL CARBOHYDRATES TRIGGER

CANDIDA ALBICANS VIRULENCE

by

Jason Burch

Approved: _____
Brian Bahnson, Ph.D.
Chair of the Department of Chemistry and Biochemistry

Approved: _____
John Pelesko, Ph.D.
Interim Dean of the College of Arts and Sciences

Approved: _____
Douglas Doren, Ph.D.
Interim Vice Provost for Graduate and Professional Education

I certify that I have read this dissertation and that in my opinion it meets the academic and professional standard required by the University as a dissertation for the degree of Doctor of Philosophy.

Signed:

Catherine Leimkuhler Grimes, Ph.D.
Professor in charge of dissertation

I certify that I have read this dissertation and that in my opinion it meets the academic and professional standard required by the University as a dissertation for the degree of Doctor of Philosophy.

Signed:

Neal Zondlo, Ph.D.
Member of dissertation committee

I certify that I have read this dissertation and that in my opinion it meets the academic and professional standard required by the University as a dissertation for the degree of Doctor of Philosophy.

Signed:

Sharon Rozovsky, Ph.D.
Member of dissertation committee

I certify that I have read this dissertation and that in my opinion it meets the academic and professional standard required by the University as a dissertation for the degree of Doctor of Philosophy.

Signed:

Ramona Neunuebel, Ph.D.
Member of dissertation committee

ACKNOWLEDGMENTS

As in all aspects of science, the path to a PhD is a collaborative and cannot be accomplished without the help and support of those around you. I considered myself lucky to be surrounded by those who were willing to help in the journey in both large and small ways. First and foremost, I would like to thank my advisor Dr. Catherine Leimkuhler Grimes, who gave a volunteer researcher from a post-bac medical program the opportunity to research in her lab. With your support and guidance I would not be the scientist I am today.

I would like to thank my committee members, Sharon Rozovsky, Neal Zondlo, and Ramona Neunuebel, for their support and guidance.

I am appreciative of all the past and current members of the Grimes group, who provided support and assistance in this journey. I would like to thank synthetic chemists in the group: Dr. James Melnyk, Kristen DeMeester, Klare Lazor, Siaviash Masayekh, and Junhui Zhou. They were also willing to answer any synthetic question I had no matter how simple and provided many of the molecules that were critical to my work. I like to thank Amy Schaefer and Elizabeth D'Ambrosio as those I could always talk to troubleshoot problem I was experience. Finally, I would like to thank Geneva Crump for continuing the work on this project and always making the group room fun.

I need thank my collaborators Dr. Dennis Wykoff and Alize Marangoz. I am greatly thankful for the guidance of Dr. Dennis Wykoff, who taught me many microbiology and yeast culture and was always willing to offer advice. I am grateful for opportunity to work with a talented scientist such Alize, who exposed me to many techniques that I otherwise would not have seen in my graduate career.

I need to thank the support staff, especially Susan Cheadle, Moiscell Robinson, and John Famiglietti; who were always immensely helpful when issues arose.

I would not be here today with the support of friend's family and friends I need to thank my mom and dad for always believing in me. I would like to thank my two wonderful dogs, Yogi and Casey, for always be happy to see at the end of a long day.

Finally, I need to thank my wife Amber with out whose love and support, this would not be possible. Lastly, I would like to thank my daughter, Jordan, for not being born until I finished my defense was done.

TABLE OF CONTENTS

LIST OF TABLES	x
LIST OF FIGURES	xi
ABSTRACT	xvi

Chapter

1	INTRODUCTION	1
1.1	The Human Microbiome	1
1.1.1	The Mycobiome.....	2
1.2	<i>Candida Albicans</i>	5
1.2.1	<i>C. Albicans</i> Hyphae	7
1.3	Cyr1	10
1.3.1	Leucine Rich Repeat (LRR) Domains.....	14
1.3.2	Carbohydrate Binding Proteins	18
1.4	Dissertation Overview	19
	REFERENCES	21
2	CHARACTERIZATION OF THE LUECINE RICH REPEAT DOMAIN OF THE <i>CANDIDA ALBICANS</i> ADENYLY CYCLASE (<i>CaCYR1</i>).....	35
2.1	Introduction	35
2.2	Materials and Methods	38
2.2.1	Materials	38
2.2.2	Amplification of CYR1 gene.....	38
2.2.3	Molecular Cloning of LRR construct	39
2.2.4	Expression and Purification of GST-LRR construct	39
2.2.5	Expression of MBP LRR.....	40
2.2.6	Purification of MBP-LRR	41

2.2.7	Characterization of CaCYR1-LRR.....	42
2.2.7.1	SDS PAGE Analysis	42
2.2.7.2	Circular Dichroism (CD).....	42
2.2.7.3	Protein Mass Spectrometry.....	43
2.2.7.4	pH stability screen	43
2.3	Results	44
2.3.1	Expression and Purification of GST-LRR.....	44
2.3.2	Expression and Purification of MBP-LRR.....	47
2.3.3	Characterization of GST-LRR.....	50
2.3.4	Characterization of MBP-LRR.....	52
2.3.4.1	Circular Dichroism	52
2.3.4.2	Mass Spectrometry Identification of MBP-LRR.....	53
2.3.4.3	MBP-LRR is Unstable in Acidic Conditions	55
2.4	Conclusion.....	56
	REFERENCES	59
3	BACTERIAL DERIVED CARBOHYDRATES TRIGGER HYPHAE FORMATION IN <i>C. ALBICANS</i>	64
3.1	Introduction	64
3.2	Materials and Methods	66
3.2.1	Materials.....	66
3.2.2	Hyphae Growth Assay.....	67
3.2.2.1	Initial Screen.....	67
3.2.2.2	Quantification of Hyphae Growth	67
3.2.3	Cyclic AMP ELISA.....	68
3.2.3.1	Time Course Assay.....	68
3.2.3.2	Effects of Ligand Concentration on cAMP Levels	68
3.2.3.3	cAMP Extraction	69
3.2.3.4	ELISA Protocol	69
3.2.3.5	Data Analysis.....	70
3.2.4	Quantitative PCR.....	70
3.2.4.1	Assay	70

3.2.4.2	RNA Extraction	71
3.2.4.3	cDNA Synthesis	71
3.2.4.4	qPCR Reaction	72
3.2.4.5	Data Analysis.....	73
3.3	Results and Discussion	73
3.3.1	Hyphae Growth	73
3.3.1.1	MDP Fragment Screen	73
3.3.1.2	Quantification of Hyphae Formation in Response to Bacterial Carbohydrates	77
3.3.2	cAMP Elisa.....	79
3.3.2.1	Carbohydrate Induced Increases In cAMP Levels Are Time Dependent	79
3.3.2.2	Cyclic AMP Levels Are Not Dependent on the Concentration of Stimulating Molecules	80
3.3.3	qPCR.....	81
3.4	Conclusions and Future Directions	85
REFERENCES		89
4	CACYR1-LRR BINDS BACTERIAL DERIVED CARBOHYDRATES	94
4.1	Introduction	94
4.2	Materials and Methods	96
4.2.1	Materials	96
4.2.2	Protein Expression and Purification	96
4.2.2.1	MBP-LRR.....	96
4.2.2.2	Free MBP-tag expression and purification.....	96
4.2.3	Surface Plasmon Resonance.....	97
4.2.3.1	Preparation of Gold Thiol Chip (Mixed SAM)	98
4.2.3.2	Immobilization of Compounds.....	98
4.2.3.3	Equilibrium Analysis.....	99
4.2.3.4	Equilibrium Binding Analysis	99
4.2.3.5	Competition Assays	99

4.2.4	Fluorescence Polarization.....	100
4.2.4.1	Assay Setup	100
4.2.4.2	Data Analysis.....	101
4.3	Results and Discussion	101
4.3.1	Fluorescence Polarization.....	101
4.3.2	Surface Plasmon Resonance (SPR).....	104
4.3.2.1	Assay Design	104
4.3.2.2	Chip Generation.....	106
4.3.2.3	MTP and Daunosamine binding.....	108
4.3.2.4	MBP Control	109
4.3.2.5	Competition assay	111
4.3.2.6	Nonbinding Competition Control.....	116
4.4	Conclusions	118
REFERENCES	121
5	CONCLUSIONS AND FUTURE DIRECTIONS	123
5.1	Introduction	123
5.2	Conclusions	124
5.2.1	Characterization of the Leucine Rich Repeat (LRR) Domain of the <i>Candida Albicans</i> Adenylyl Cyclase (<i>CaCyr1</i>).....	124
5.2.2	Bacterial Derived Carbohydrates Trigger Hyphae Formation in <i>C. albicans</i>	125
5.2.3	CaCYR1-LRR Binds Bacterial Derived Carbohydrates	128
5.3	Future Directions	131
5.3.1	Improved LRR Solubility	131
5.3.2	Predicting the Carbohydrate Binding Pocket	132
5.3.3	Photoactivatable Crosslinking	134
5.4	Summary.....	135
REFERENCES	137
Appendix		
A	REPRINT PERMISSIONS	143

LIST OF TABLES

Table 1.1 – Conditions associated with fluctuations in the microbiome.....	2
Table 1.2 – Selected TLRs/NLRs and associated MAMPs.....	15
Table 2.1 – Experimental parameters for CD experiments	43
Table 3.1 – Primer sequences for qPCR reactions	72
Table 3.2 – Thermocycling protocol	72
Table 3.3 – Effects of MDP structural components on hyphae formation in <i>C. albicans</i>	75
Table 5.1 – Bacterial molecules demonstrated to effect <i>C. albicans</i> growth and morphology	127

LIST OF FIGURES

Figure 1.1 – Papers in the PubMed database referencing the ‘mycobiome’ has increased exponentially since the term was first used in 2010.....	3
Figure 1.2 – <i>C. albicans</i> is capable of growing as budding yeast (A), pseudohyphae (B), or filamentous hyphae (C). Images were taken at 40x magnification for cultures grown overnight in YPD.....	8
Figure 1.3 – Cyr1 acts as a signal integrator responding to environmental cues to activate the cAMP-PKA pathway. G α : G alpha RA: Ras association; LRR: 14 leucine rich repeats PP2C: protein phosphatase 2C; CYCc: catalytic cyclase (Figure adapted from Yue Wang, <i>PLoS Pathog</i> , 2013 ⁸⁰).....	11
Figure 1.4 – Peptidoglycan is carbohydrate polymer comprised of alternating units of <i>N</i> -Acetyl-Glucosamine and <i>N</i> -acetyl-Muramic Acid cross-linked by a peptide chain. A D-Ala-m-DAP linkage connects the polymers in Gram- positive species the polymers. In Gram-negative species, this connection is made by L-Lys linked to D-Ala through a penta-Gly linker. Small synthetic fragments of peptidoglycan, such as MDP shown in red, can elicit an immune response in mammals.	12
Figure 1.5 – Synthetic peptidoglycan ligands tested for the ability to elicit hyphae formation in <i>C. albicans</i> . I ₅₀ values represent the amount of concentration of compound needed for 50% of cells to demonstrate hyphae formation ⁹²	13
Figure 1.6 – Biotinylated MDP used to demonstrate to the interaction between Cyr1 and peptidoglycan ⁹²	14
Figure 1.7 – Crystal structure of porcine ribonuclease inhibitor (PDB ID: 2BNH) ¹¹² demonstrating the conserved structure of LRR domains demonstrating featuring a horse shaped tertiary structure with β -strands lining the concave surface and α -helices on the convex face.....	17
Figure 2.1 - Initial purification of GST-LRR contained two additional protein bands when analyzed by SDS-PAGE. Mass spectrometry identified the impurities as the chaperone proteins, DnaK and GroEL.....	46

Figure 2.2 - GST-LRR was purified using glutathione resin and the column washed with buffers containing ATP. Lane 1: Lysate; Lane 2: Pellet; Lane 3: Supernatant; Lane 4: ATP wash flowthrough; Lane 5: purified GST-LRR	47
Figure 2.3 - MBP-LRR expression in <i>E. coli</i> leads to the formation of inclusion bodies. Lane 1: Lysate; Lane 2: Supernatant; Lane 3: Pellet; Lane 4: Inclusion Body.	49
Figure 2.4 - MBP-LRR was purified from urea solubilized inclusion bodies using a Ni-NTA column attached to a NGC quest FPLC system. Fractions showing absorbance at 280 nm were analyzed by SDS-PAGE. Fractions contained a single protein band between the 75 kDa and 100 kDa molecular weight markers, consistent with the 90 kDa molecular weight of MBP-LRR.	50
Figure 2.5 - A circular dichroism spectrum of 3 μ M GST-LRR in 10 mM sodium phosphate buffer, pH 7.4, containing 50 mM NaCl was obtained using a JASCO J810 spectropolarimeter. The observed spectrum is the result of the accumulation of 3 scans. Analysis by the K2D3 ³⁷ webserver predicts 66.1% α -helical and 11.0% β -strand secondary structure.	51
Figure 2.6 - CD spectra for MBP-LRR obtained from the soluble lysate fraction (red) and refolded MBP-LRR (blue). The observed spectra are the result of the accumulation of 3 scans. Mean residue ellipticity at 240 nm was normalized to 0. Analysis using the K2D3 webserver predicts 60.3% α -helical and 16.7% β -strand secondary structure for both the soluble and refolded LRR, indicating the proper conformation was obtained after refolding.	53
Figure 2.7 - Intact protein mass spectrometry analysis of MBP-LRR. Predicted mass: 91,048 Da, Observed: 91,030 Da	54
Figure 2.8 – After refolding MBP-LRR aggregates when dialyzed against acidic buffers. Lane 1: Refolding buffer; Lane 2: pH 5.5; Lane 3: pH 6.0; Lane 4: pH 6.5; Lane 5: pH 7.0; Lane 6: pH 7.5.....	55
Figure 2.9 – Homology model of Cyr1 created using the I-TASSER database using Arabidopsis FLS2 (PDB ID: 4MN8A) as a template ⁴³ . Residues 480-900 (red) indicate the predicted LRR domain from the SMART database. Residues 370 -1135 (green) show secondary characteristics that could be important in protein folding.....	57

Figure 3.1 - Muramyl Dipeptide Fragment Library used to screen for hyphae growth in <i>C. albicans</i> . Compounds 3.02-3.05 were used to examine how peptide stem stereochemistry effects hyphae formation. The impact of the length of the peptide stem was examine by truncating then eliminating it in compounds 3.02, 3.06, and 3.08 . Individual carbohydrates 3.10 - 3.13 were also examined.	74
Figure 3.2 – Carbohydrates derived from bacterial sources (Figure 3.1) are capable of eliciting hyphae formation in <i>C. albicans</i> . Changing amino acid stereochemistry from the naturally occurring LD to LL did not effect hyphae formation (3.02-3.05). The carbohydrate was necessary, as the dipeptide (3.14) alone did not trigger hyphae formation. Carbohydrates not found in peptidoglycan, daunosamine (3.13) also caused hyphae formation.	76
Figure 3.3 – Quantification of hyphae growth. A) Anthracycline and peptidoglycan carbohydrate B) <i>C. albicans</i> cultures were treated with 1 mM of the indicated compound and incubated at 37 °C overnight. Cells were visualized at 40 × magnification and images containing approximately 100 cells were blindly scored for hyphae characteristics. Hyphae formation is reported as percent hyphae calculated by dividing cells expressing hyphae characteristics divided by total cells.	78
Figure 3.4 – <i>C. albicans</i> cultures were treated 100 μM of the indicated compound and aliquots were taken at fifteen intervals from 0 to 60 minutes after treatment. Cyclic AMP was extracted and quantified using cAMP Biotrack EIA. cAMP levels increased upon exposure to MTP (3.17) and daunosamine (3.13) peaking at 30 minutes.	80
Figure 3.5 – <i>C. albicans</i> cultures were treated with either 10 μM or 100 μM of the indicated compounds for 30 minutes. Cyclic AMP was extracted and quantified using cAMP Biotrack EIA. No significant difference in cAMP levels was observed between culutres treated with either 10 μM or 100 μM daunosamine or MTP.	81
Figure 3.6 – Peptidoglycan Fragments and Bacterial Natural products tested for their effects on <i>ECE1</i> and <i>HWPI</i> expression. Peptidoglycan fragments were chosen to determine the how varying the peptide stem effects gene expression. The natural products looked to established the dependence of daunosamine in anthracyclines to elicit hyphae responses.	83

Figure 3.7 – Bacterial natural products increase expression levels of hypha-specific genes. <i>C. albicans</i> cultures were treated with 100 μ M of each compound. <i>ECE1</i> and <i>HWPI</i> expression levels were normalized to actin. Relative expression were determined comparing mRNA levels of each sample to the control sample treated with H ₂ O, set to an expression level equal to 1. Two samples were measured from two biological replicates for each compound.	85
Figure 4.1 – Bacterial derived carbohydrates used in SPR assay.....	100
Figure 4.2 – 6-Bodipy-MDP (4.8) was used as a fluorophore in the FP assay.	102
Figure 4.3- Results of Fluorescence polarization binding assay. A) Total and nonspecific binding anisotropy B) Specific Binding Anisotropy. The lack of change in anisotropy indicates the 6-bodipy MDP is not specifically binding MBP-LRR.....	103
Figure 4.4 – SPR Assay. The bacterial carbohydrates are covalently coupled to the gold surface. The LRR domain is flowed over the chip and binding events are detected by measuring the change in refractive index occurring at the surface solution interface. Figure adapted from Cooper, <i>Nat Rev Drug Discov</i> ¹⁴	106
Figure 4.5 – Attachment of MTP and Daunosamine utilizing NHS/EDC coupling chemistry.	107
Figure 4.6 - Raw Sensogram of MBP-LRR binding to A) MTP (4.1) and B) daunosamine (4.2).	108
Figure 4.7 – MBP-LRR binds to MTP (4.1) ($K_D = 176 \pm 68$ nM) and to daunosamine (4.2) ($K_D = 287 \pm 88$ nM) with nanomolar affinity.....	109
Figure 4.8 – Purified MBP-tag. Protein bands between the 37 kDa and 50 kDa molecular weight markers are consistent with the 42 kDa molecular weight of MBP. Lane 1: supernatant; Lanes 2-9: Free MBP-tag.....	110
Figure 4.9 – Raw sensogram shows decreased binding of free MBP-tag to either A) MTP or B) Daunosamine	111
Figure 4.10 – Experimental design of competition assay. A) With no free ligand present the LRR can bind carbohydrates tethered to the surface. B) Preincubation with free ligand inhibits LRR binding to the surface C) Preincubation with a small molecule that does not bind the LRR has not effect on surface binding	111

Figure 4.11- Preincubation with A) MTP or B) Daunomycin is capable of decreasing MBP-LRR binding by 50%. Binding was reported as a relative response, dividing each sample by the response of apo MBP-LRR (no preincubation with ligands). The relative response was set to 1 and values less than one indicate that the compound is capable of competing binding.	113
Figure 4.12- MBP-LRR binding to MTP and daunomycin can be competed away by A) MDP and B) Doxorubicin. Binding was reported as a relative response, dividing each sample by the response of apo MBP-LRR (no preincubation with ligands). The relative response was set to 1 and values less than one indicate that the compound is capable of competing binding.	115
Figure 4.13- Chloramphenicol, a natural product for <i>Streptomyces</i> not containing a carbohydrate, and the individual amino acids (alanine and glutamate) forming the peptide stem of MDP were tested for the ability to inhibit MBP-LRR binding to carbohydrates.	116
Figure 4.14 –MBP-LRR was incubated with 9.6 μ M of each compound prior to being used in the SPR assay. Results were reported as the % binding to the surface. Calculated by dividing each sample by the response of control (no ligand). The control sample was set to 100% and values less than 100% indicate that the compound is capable of inhibiting binding. The non-carbohydrate compound did not inhibit binding.	118
Figure 5.1 – The LRR domain of Cyr1 contains 14 phenylalanine residues (blue) and 1 tryptophan residue (red) organized into three hydrophobic clusters. Due the reliance of CH- π interactions to stabilize carbohydrate-protein binding, these hydrophobic pockets potentially form Cyr1’s binding site.	130
Figure 5.2 – Homology model of Cyr1. Residues 480-900 (red) indicate the predicted LRR domain from the SMART database. Residues 370 - 1135 (green) show repeats truncated in the purified construct	132
Figure 5.3 – The LRR domain of Cyr1 contains a single tryptophan residue at position 730. Mutational analysis can be employed to assess the importance of this residue in carbohydrate binding.	133
Figure 5.4 – Proposed mass spectrometry experiments to identify the MDP’s binding site on Cyr1. The LRR domain would be incubated with photoactivatable MDP. After exposure to UV light, the protein will be digested with trypsin and analyzed by proteomic mass spectrometry ..	135

ABSTRACT

The human body is home to a diverse ecosystem containing trillions of microorganisms collectively referred to as the microbiome. Interactions between bacterial and fungal species have been correlated to the progression of cancer and Crohn's disease. Despite the implications for human health, there is a lack of molecular understanding of how fungi recognize and respond to bacteria. It has been demonstrated that normally benign *Candida albicans* turns pathogenic when exposed to fragments of the bacterial cell wall. However, the molecular mechanism of this interaction is not well characterized. The work described in this dissertation improves the molecular understanding of how *Candida albicans* is capable of recognizing molecules of bacterial origin and demonstrates for the first time that the Cyr1 can bind diverse bacterial carbohydrates to initiate hyphae growth. Importantly, the work described is the first to determine the strength of the interaction between Cyr1 and the peptidoglycan fragment, MTP, and the first report of Cyr1 binding the anthracycline, doxorubicin, and its carbohydrate moiety, daunosamine.

In the larger biological landscape; this dissertation adds another level of molecular understanding used by the LRR domain. Purification of the LRR domain of Cyr1 allowed the successful development of a surface plasmon resonance assay to characterize the binding of bacterial derived carbohydrates. The mid-nanomolar binding affinities for MTP and daunosamine offer unique examples of strong protein-monosaccharide interactions. By comparing these molecular details, insight can be

gained into how one domain can respond to a variety of ligands. Overall, this dissertation provides new tools to study the LRR domain and molecular level insight for carbohydrate – protein interactions

Chapter 1

INTRODUCTION

1.1 The Human Microbiome

The human body is host to trillions of microorganisms collectively referred to as the microbiome. The microbiome is a diverse ecosystem with an estimated 1,000 bacterial species present at any given time¹. In fact, there are as many bacterial cells present in and on the human body as there are “human” cells². The importance of the microbiome to human health came into focus in 2008, when the National Institute of Health launched the human microbiome project³. The microbes are often site specific, as different bacteria inhabit various locations of the body with dramatic shifts between areas often observed⁴. Interestingly, the microbiome is largely individualized as even identical twins have different bacterial compositions⁵. While the microbiome is largely inherited at birth⁶, the composition is dynamic, changing in response to a variety of influences through out life. Diet⁷, antibiotics⁸, and even cohabitation with pets⁹ have been demonstrated to affect the bacteria present in the microbiome.

The microbiome has a symbiotic relationship with the human host aiding in digestion, nutrition, and the development of a healthy immune system¹⁰. A stable and diverse community of commensal bacteria helps protect the host from the proliferation of pathogenic bacteria¹¹. Fluctuations in microbiome composition has been implicated in disease states (Table 1.1), such as inflammatory bowel disease,

cancer, and asthma¹². With its immense role in human health, it is easy to see the importance of understanding the composition, recognition, and regulation of the microbiome.

Table 1.1 – Conditions associated with fluctuations in the microbiome

Condition	Significance of the microbiome
Acne	Increase in <i>Propionibacterium acnes</i> leading to inflammation ¹³
HIV	Increase in the ratio of <i>Firmicutes</i> to <i>Bacteroidetes</i> ¹⁴
Asthma	<i>Proteobacteria</i> more common in asthmatics compared to healthy individuals ¹⁵
Autism	Lower populations of <i>Akkermansia</i> and <i>Bifidobacterium</i> ¹⁶
Allergies	Decreases in <i>Bacteroidetes</i> , <i>Proteobacteria</i> , and <i>Actinobacteria</i> ¹⁷
Cancer	Elimination of <i>H.pylori</i> , <i>C. psittaci</i> , or <i>B. burghorferi</i> lead to a regression of lymphoma and gastric cancers ¹⁸
Crohn's Disease	Decreases in <i>Bacteroidetes</i> and <i>Firmicutes</i> . Increases in <i>Proteobacteria</i> and <i>Fusobacteriaceae</i> ¹⁹
Obesity	Increased <i>Firmicutes</i> to <i>Bacteroidetes</i> ratio ¹²
Diabetes	Lower Diversity of bacteria species is correlated to an increase risk of Type 2 diabetes ²⁰

1.1.1 The Mycobiome

While the importance of the bacteria species in the microbiome cannot be understated, there is also a significant population of fungi, called the ‘mycobiome’. The mycobiome is considered to be a minor component of the microbiome, accounting for approximately 0.1% of the total microorganisms present in the human body²¹. However there are reasons to believe that these populations have been underestimated.

Shotgun sequencing identifies microorganisms and results are matched to reference genomes available in annotated databases. However, fungal species are often underrepresented in these databases. In 2014 the NCBI Genome database contained only 57 fungal genome compared to the nearly 3,000 complete bacterial genomes²²⁻²³. Using these annotated databases, it is easy to see how some fungal species could be missed. However, much like the microbiome in the early part of the decade, the importance of the mycobiome is gaining appreciation. Since the first mention in the literature a decade ago, the number of papers studying the mycobiome has increased exponentially (Figure 1.1).

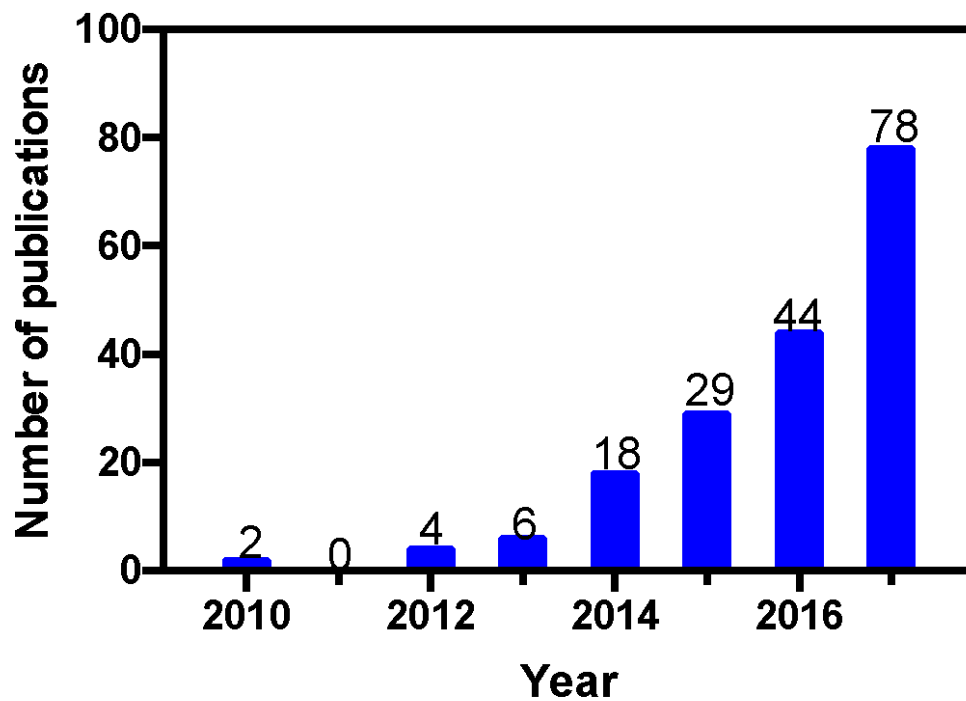


Figure 1.1 – Papers in the PubMed database referencing the ‘mycobiome’ has increased exponentially since the term was first used in 2010

Similar to bacteria, identity and density of fungal species vary by location in and on the human body. The intestinal tract is rich in fungi, hosting more than 50 species with large populations of *Candida*, *Saccharomyces*, and *Cladosporium*²⁴. The concentration of each is greatly influenced by diet, as increases in *Candida* species were observed after ingestion of carbohydrates²⁵. The oral cavity is home to the most diverse composition of fungi, hosting more than 75 genera. The largest populations found in the mouth include *Candida*, *Cladosporium*, and *Aspergillus*²⁶. The fungal populations of the skin vary greatly by location, with *Malassezia* dominating the hands and arms and *Aspergillus* found in higher concentrations on the feet²⁷⁻²⁸.

Despite being only a small percentage of the microbiome, fungi have a large impact on human health. While there are few reported beneficial roles of fungi species, this can be attributed to the deficiency of research. One of the few examples in the literature, *Saccharomyces boulardii* has been demonstrated to provide relief of gastroenteritis²⁹. Though largely commensal, the greatest impact on health is the mycobiome relationship to various disease states. Being that many of these fungi are opportunistic pathogens, the most common issues are overgrowth of fungal species which leads to infection. In immunocompromised patients, such as those with HIV, *Candida*, *Aspergillus*, and *Fusarium* are more prevalent in the oral cavity. This causes frequent oral infections, which may lead to more serious esophageal and bloodstream infections³⁰. Also, the weakened immune system in individuals receiving chemotherapy has been shown to put them at an increased risk of developing *Candida* infections³¹⁻³².

Interestingly, fungal infections are often correlated to changes in the bacterial composition of the microbiome. In mouse models, mice that are germ-free or those that have undergone antibiotic treatment are highly susceptible to *Candida* infections^{24, 33-35}. In human subjects, dysbiosis of the bacterial populations lead to increased colonization of the gut by *Candida albicans*³⁶. Studies have shown that the interaction between fungi and bacteria is especially important in patients with Crohn's disease (CD)³⁷⁻³⁸. In CD patients, increases in *Serratia marcescens* and *E. coli* populations were observed in tandem with decreases in beneficial bacteria. Additionally, an increased abundance of *Candida tropicalis* was correlated to an increase in anti-*Saccharomyces cerevisiae* antibodies³⁹. With its immense role in human health, it is easy to see why the mycobiome is rapidly gaining attention.

1.2 *Candida Albicans*

Despite being one of the most prevalent members of the mycobiome, *Candida albicans* is the most common cause of fungal infections in human. This normally commensal species can be found in the oral cavity of approximately 75% of all people⁴⁰. For the healthy individuals this fungus will cause no problems; however, those with weakened immune systems can experience uncontrolled growth of the fungi leading to infections. Two of the most common human fungal infections, thrush and yeast infections, are caused by the overgrowth of *C. albicans*. Uncommon in healthy adults, thrush (oral candidiasis) is more typically seen in the young and elderly. Symptoms are generally mild and can include dry mouth and a temporary loss of taste. Commonly referred to as a "yeast infection", vulvovaginal candidiasis is the most recognizable fungal infection in humans. It has been estimated that nearly 75%

of women will experience vulvovaginal candidiasis at least once in their lifetime⁴¹. Both of these conditions are generally mild and are treatable with oral doses of the antifungal agent, fluconazole⁴².

Unfortunately, these minor infections are not the only conditions caused by *C. albicans*. When *C. albicans* enters the blood stream, a condition known as candidemia, patient prognoses are usually much worse. Regrettably, candidemia is not uncommon and it the cause of 9% of hospital-acquired blood stream infections⁴³⁻⁴⁴. Candidemia often occurs in those suffering from AIDS or cancer making it difficult to determine symptoms associated with the infection rather than the pre-existing condition of the patient. Sadly, candidemia is difficult to treat due to *C. albicans* ability to develop resistance to common azole drugs⁴⁵. The need to develop new therapeutics is highlighted by the 30% mortality associated with the infection⁴⁶.

Interestingly, the bacterial composition of the microbiome affects the ability of *C. albicans* to become pathogenic. The presence of certain bacteria can promote co-infections, as evidenced by mixed biofilms identified in clinical isolates. In many hospital acquired infections *Pseudomonas aeruginosa* is often isolated with *C. albicans*⁴⁷⁻⁴⁸. Additionally mixed biofilms containing *Staphylococcus epidermis*⁴⁹, *Staphylococcus aureus*⁵⁰, and *Streptococcus mutans*⁵¹ have been identified. Bacterial populations in the microbiome are also affected by *C. albicans*. Following antibiotic treatment, the presence of *C. albicans* promotes the recovery of *Bacteroidetes* and *Enterococcus faecalis* populations, while inhibiting *Lactobacillus*^{33, 36}. There is a reciprocal relationship, as *C. albicans* growth is inhibited by *Lactobacillus*

*acidophilus*⁵². To development more efficient treatments, it is necessary to understand how *C. albicans* becomes pathogenic.

1.2.1 *C. Albicans* Hyphae

Candida albicans is a polymorphic fungus capable of growing as budding yeast, pseudohypha, or filamentous hypha (Figure 1.2)⁵³⁻⁵⁵. Hyphae formation is necessary for *C. albicans* virulence, with the most direct evidence coming from studies examining the cyclin related protein, HGC1. Deletion of the gene results in *C. albicans* cells incapable of hyphal growth, despite normal expression of other hyphae specific genes including HWP1, ECE1, and HYR1. When mice were infected with strains deficient in Hgc1, all mice were alive at 20 days post infection. In control samples infected with wild-type strains, all mice were dead by seven day post-infection⁵⁶.

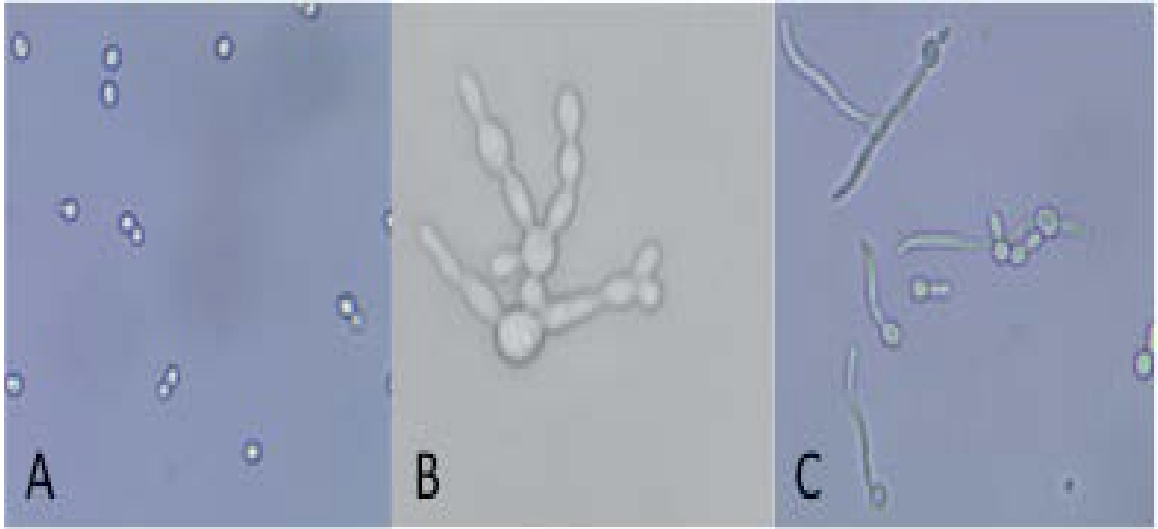


Figure 1.2 – *C. albicans* is capable of growing as budding yeast (A), pseudohyphae (B), or filamentous hyphae (C). Images were taken at 40x magnification for cultures grown overnight in YPD.

The first step in *C. albicans* infection is adherence to the surface of epithelial cells. Adherence is mediated through the expression of glycosylphosphatidylinositol (GPI)-linked adhesin proteins on the external hyphae surfaces⁵⁷⁻⁶⁰. The ALS (agglutinin-like sequence) class mediates adherence by binding epithelial cell surface proteins, such as N-cadherins and the epidermal growth factor receptor⁶¹⁻⁶². One adhesin of particular note is hyphal wall protein 1 (Hwp1). Instead of recognizing proteins on the epithelial cell surface, the N-terminal domain acts as a substrate for epithelial transglutaminases, which covalently cross-link it to receptors on the surface epithelial cells⁵⁸⁻⁶⁰. Interestingly, Hwp1 can interact with ALS adhesins to form biofilms that have been demonstrated to increase drug resistance⁶³⁻⁶⁴.

Like adherence, hyphae are essential to the invasion of epithelial cells. There are two distinct mechanisms by which *C. albicans* invade epithelial cells: active

penetration and induced endocytosis⁶⁵. Although the mechanism has not been entirely elucidated, active penetration is likely mediated by the expression of secreted aspartyl proteases (SAPs) on hyphae surfaces. These proteases degrade E-cadherin weakening the tight junctions between epithelial cells allowing *C. albicans* to pass through the epithelium⁶⁶. Invasin proteins expressed on the filamentous hyphae mediate induced endocytosis. The presence of the proteins alone are enough to activate invasion, as beads coated with recombinant invasins are actively endocytosed⁶⁷⁻⁶⁸.

Hyphae formation is a complex biological process regulated by the interplay of numerous signaling pathways. Each pathway responds to unique environmental signals to regulate *C. albicans* morphology. The MAPK (mitogen-activated protein kinase) pathway was the first signaling cascade correlated to *C. albicans* morphology⁶⁹. The MAPK signaling pathway is the primary pathway determining cell morphology in times of nutrient limitation⁷⁰⁻⁷¹. Since this discovery, numerous other effectors of *C. albicans* morphology had been identified. Basic pH activates the Rim101 transcription factor (pH pathway) inducing the expression of Phr1, which is involved in hyphae maintenance⁷²⁻⁷³.

Perhaps the most complex and well-studied pathway involved in *C. albicans* morphology is the cAMP-PKA (cyclic AMP – protein kinase A) signaling cascade. The pathway is critical to *C. albicans* virulence as several of the pathway regulators and genes induced are essential for hyphae formation⁶². Increases in cAMP levels activate PKA, which phosphorylates and activates the transcription factor, Efg1. Efg1 in turn induces the transcription of hyphae specific genes: Hwp1, Hgc1 and Als3⁷⁴⁻⁷⁵. Cyclic AMP levels are regulated by the phosphodiesterases, Pde1 and Pde2, and the adenylyl

cyclase, Cyr1. Deletion of Pde2 leads to the increased hyphae formation, highlighting the importance of high cAMP in *C. albicans* morphology⁷⁶. As the main activator of the cAMP-PKA pathway, Cyr1 is of critical importance.

1.3 Cyr1

Cyr1 is the lone adenylyl cyclase present in *C. albicans* and it is essential to regulating *C. albicans* morphology. In 2001, elegant experiments from Leberer and co-worker demonstrated that hyphae formation was abolished when the CDC35 gene – encoding for Cyr1 – is knocked out⁷⁷. Although no crystal structure is available, sequence analysis predicts five domains that are highly conserved among fungal adenylyl cyclases in the 1690 amino acid protein (Figure 1.3)⁷⁸⁻⁷⁹. The protein acts as a signal integrator responding to a plethora of environmental signals to activate the cAMP-PKA pathway, with each domain recognizing a unique set of cues⁸⁰. In response to glucose and amino acids, the G-protein-coupled receptor Gpr1 activates Gpa2, which binds to the G α domain enhancing the production of cAMP⁸¹⁻⁸². Ras1 directly binds the RA domains. Mutations in the RA domain blocks Ras1-Cyr1 binding, inhibiting adenylyl cyclase activity⁸³. Exposure to temperatures above 37°C induces hyphae formation, through the direct interaction of Heat shock protein 90/Sgt1 complex with Cyr1⁸⁴⁻⁸⁵. The catalytic domain is not only responsible for converting AMP to cAMP, but it can directly respond to high CO₂ concentrations to induce hyphae formation⁸⁶. Farnesol, a quorum-sensing molecule produced by *C. albicans*, inhibits cAMP synthesis through direct interaction with the CYCc domain⁸⁷⁻⁹⁰. Interestingly, the catalytic domain can also recognize the *Pseudomonas aeruginosa* quorum-sensing molecule, 3-oxo-C12-homoserine lactone. The interactions decrease

cAMP synthesis and therefore inhibit hyphae formation⁸⁸. The ability of bacterial quorum-sensing molecules to repress hyphae formation may partially explain why antibiotics increase *C. albicans* colonization.

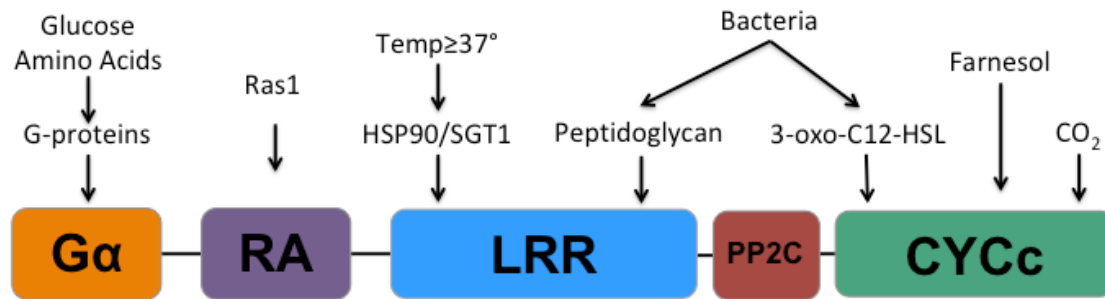


Figure 1.3 – Cyr1 acts as a signal integrator responding to environmental cues to activate the cAMP-PKA pathway. Gα: G alpha RA: Ras association; LRR: 14 leucine rich repeats PP2C: protein phosphatase 2C; CYCc: catalytic cyclase (Figure adapted from Yue Wang, *PLoS Pathog*, **2013**⁸⁰)

Since the 1950's, serum has been known to induce hyphae formation⁹¹. However it would be more than fifty years until the molecular identity of the compound responsible for the observed morphological switch would be identified. In 2009, a seminal discovery pointed to bacterial cell wall fragments as the element of serum responsible for the hyphal phenotype⁹². More specifically, it was shown that peptidoglycan fragments were the activators. Peptidoglycan is a large polymer comprised of two conserved carbohydrates (*N*-Acetyl-Glucosamine and *N*-acetyl-Muramic Acid) linked together by penta-peptide cross-linking chains, which can vary in composition and linker type⁹³ (Figure 1.4). A variety of synthetic ligands (Figure 1.5) were used to assess which portions of the polymer were capable of activation. It was found that 2-amino muramyl dipeptide (MDP) – a small peptidoglycan fragment

and Nod2 ligand – and 1,6-anhydro-MDP readily activated the growth phenotype; whereas glucosamine, a sugar found in eukaryotes and bacteria did not. The potency of the MDP derivative was influenced by the terminal peptide was isoglutamine, MAiGN, or glutamine, Mur-L-Ala-D-Glu. Mur-L-Ala-D-Glu. Interestingly, these differences are related to the bacterial source, as glutamine is found in Gram-negative species and isoglutamine is present in Gram-positive species⁹⁴.

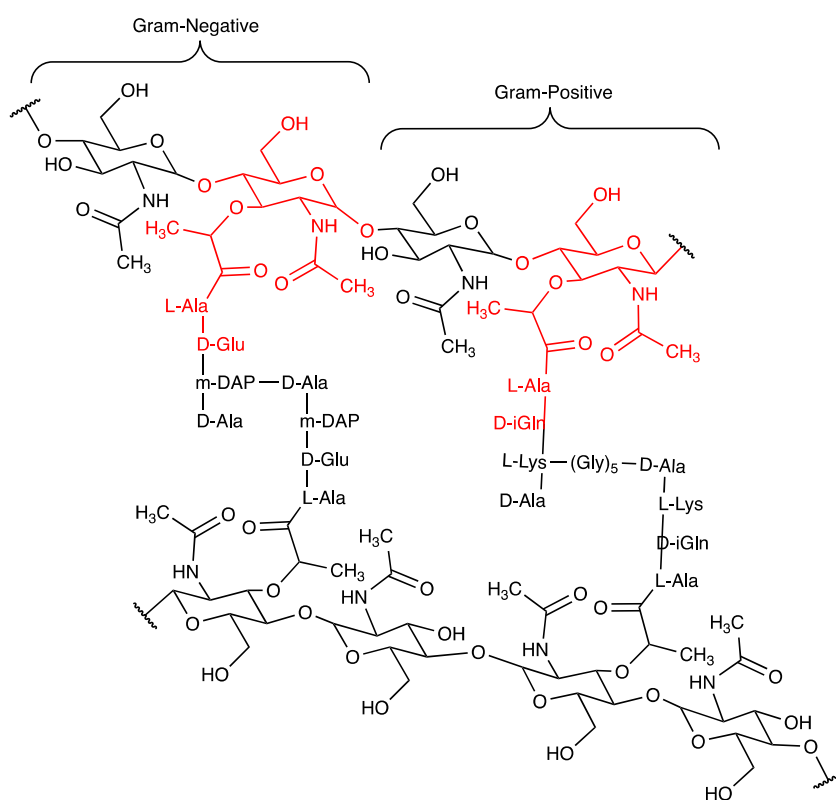


Figure 1.4 – Peptidoglycan is carbohydrate polymer comprised of alternating units of *N*-Acetyl-Glucosamine and *N*-acetyl-Muramic Acid cross-linked by a peptide chain. A D-Ala-m-DAP linkage connects the polymers in Gram-positive species the polymers. In Gram-negative species, this connection is made by L-Lys linked to D-Ala through a penta-Gly linker. Small synthetic fragments of peptidoglycan, such as MDP shown in red, can elicit an immune response in mammals.

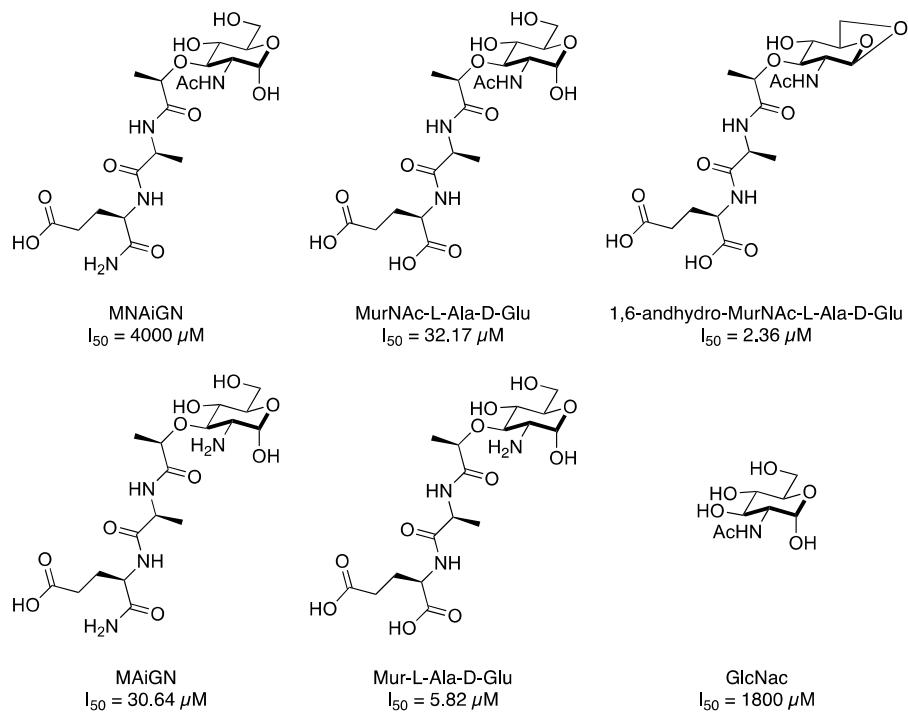


Figure 1.5 – Synthetic peptidoglycan ligands tested for the ability to elicit hyphae formation in *C. albicans*. I_{50} values represent the amount of concentration of compound needed for 50% of cells to demonstrate hyphae formation⁹².

In order to understand the molecular mechanism of this phenotypical switch, proteins that were known at the time to respond to peptidoglycan fragments were analyzed. In the human innate immune system, peptidoglycan is known to activate a variety of innate immune receptors which contain leucine rich repeat (LRR) domains⁹⁵. It was hypothesized that *C. albicans* was recognizing peptidoglycan via this domain. Using the LRR domain of Nod1 and Nod2 as a template, the *C. albicans* genome was searched for homologous proteins; a protein with 40% sequence similarity, Cyr1, was identified. Utilizing a biotinylated MDP moiety (Figure 1.6) in an affinity purification assay, Cyr1 was putatively shown to bind peptidoglycan through its LRR domain⁹². The data suggest that the LRR domain is the binding to PG

viruses⁹⁸. Currently, there are over 60,000 LRR containing proteins identified in SMART's nrdb (non-redundant database) database⁹⁹. LRR containing proteins are important in numerous biological processes, including cell adhesion, neuronal development, RNA processing, hormone signaling, and pathogenicity in bacteria¹⁰⁰⁻¹⁰³. In spite of their numerous roles, the domains are perhaps most recognized for the importance to innate immunity in plants and animals⁹⁶⁻⁹⁷. In mammals, toll-like receptors (TLRs) and NOD-like receptors (NLRs) utilize LRRs to respond to microbe-associated molecular patterns (MAMPS) –such as peptidoglycan – to initiate an immune response and protect the host from invading pathogens (Table 1.2)⁹⁷. Interestingly, in plants, LRR containing proteins play a similar role detecting the presence of pathogens and activating the plants immune responses¹⁰⁴.

Table 1.2 – Selected TLRs/NLRs and associated MAMPs

PRR	MAMP
Nod1	γ -D-Glu-mDAP (iE-DAP)
Nod2	MDP
IPAF	Flagellin
NALP3	Bacterial RNA and MDP
TLR1	Triacyl lipopeptide
TLR4	Lipopolysaccharide (LPS)
TLR5	Flagellin
TLR7	ssRNA

Table adapted from Istomin, *BMC Immunology*¹⁰⁵

Despite being found in functionally diverse proteins, all LRRs share similar domain architectures. LRR domains are comprised of repeating 20-30 residue motifs comprised of a highly conserved and a variable segment. The highly conserved

segment consists of an 11 residue, LxxLxLxxNxL, or a 12 residue, LxxLxLxxCxxL, consensus sequence, where “L” is leucine, isoleucine, valine, or phenylalanine, “N” is asparagine, threonine, serine, or cysteine, and “C” is cysteine, serine, or asparagine⁹⁸. Residues 3-5 of these conserved segments form a short β -strand. Connected by β -turns, the variable segments form diverse helical structures, such as α -helices, 3_{10} helices, or polyproline II helices¹⁰⁶. These motifs arrange parallel to a single axis, resulting in a horseshoe-shaped fold with the β -strands lining the concave surface and helical structures on the convex face (Figure 1.7)¹⁰⁷⁻¹⁰⁸. The conserved structure was initially identified in porcine ribonuclease inhibitor, the first LRR containing protein to be crytalyzed¹⁰⁹.

The stability of the LRR domain is largely conferred by the ability to shield hydrophobic residues from solvent exposure. Leucine and other aliphatic residues are oriented to fill the space between the β -strands and helical structures forming a hydrophobic core. Side chains from neighboring repeats fill holes in the hydrophobic core, ensuring stability along the length of the domain. Hydrophobic residues in the first and last repeats are protected by N-terminal and C-terminal capping motifs. Commonly, these capping motifs contain cysteine rich regions that form disulfide bonds to stabilize the repeats^{106, 110}. Courtemanche and Barrick highlighted the importance of these capping domains by demonstrating the mutations in the N-terminal capping motif of Internalin B slowed the rate at which the LRR domain folded¹¹¹. Overall, this is an extremely complicated domain, the stability of which can vary from protein to protein.

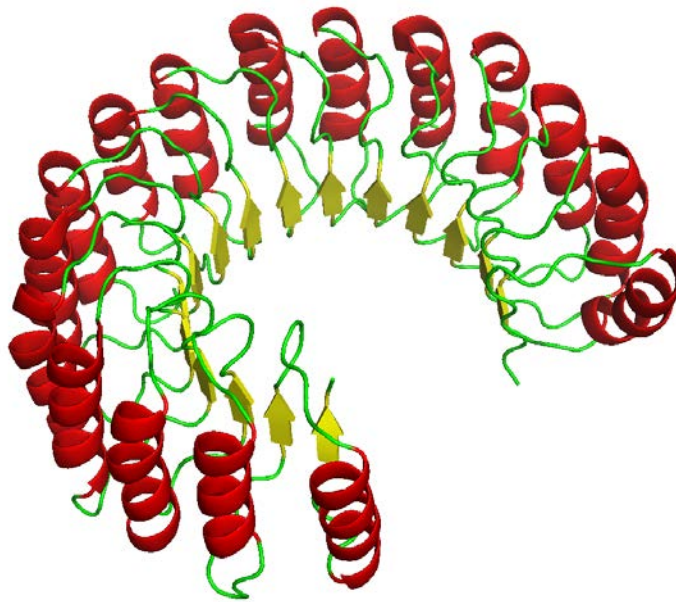


Figure 1.7 – Crystal structure of porcine ribonuclease inhibitor (PDB ID: 2BNH)¹¹² demonstrating the conserved structure of LRR domains demonstrating featuring a horse shaped tertiary structure with β -strands lining the concave surface and α -helices on the convex face.

The discovery of LRR proteins role in innate immunity by Charles Janeway and co-workers ushered in a new way of thinking about the LRR domain¹¹³. While initially thought to be involved in only protein-protein interactions, 2011 Nobel prize winning work by Bruce Beutler and Jules Hoffmann demonstrated that the LRR containing Toll-like receptors (TLR) were responsible for recognizing and mounting a response to pathogens in both *Drosophila* and mammals¹¹⁴⁻¹¹⁵. Since lipopolysaccharide (LPS) was first shown to activate TLR4¹¹⁶, the diversity of MAMPs demonstrated to activate an immune response through binding of LRR containing proteins has greatly expanded. MAMPs vary greatly in size and composition, ranging from the 30 kDa protein, flagellin¹¹⁷, to the 493 Da carbohydrate

muramyl dipeptide¹¹⁸. It is very impressive that one protein domain is able to recognize and respond to a wide variety of signals. To date however, there is no detailed characterization of molecular mechanism by which the LRR for Cyl1 binds its ligands.

1.3.2 Carbohydrate Binding Proteins

As one of the building blocks of life, carbohydrates are vastly important in numerous biological processes. Carbohydrates are critical in energy production, cellular structures, and modifications post-translational modifications of lipids and proteins¹¹⁹. Interactions between carbohydrates and proteins are often the first step in the signaling cascade leading to the activation of complex biological events including fertilization, cancer development, and the activation of the innate immune system¹²⁰. Carbohydrates are essential to many PAMPs including LPS, peptidoglycan, viral nucleic acids, CpG rich DNA, and β – glucans. With the exception of flagellin and a few pure lipids, carbohydrates are present in nearly all PAMPs¹²¹. In order to recognize and respond to these PAMPs, both animals and plants have evolved a series of pattern recognition receptors (PRR) that bind carbohydrates. LRR containing proteins in mammals, such as TLRs and NOD-like receptors (NLRs), are capable of binding diverse carbohydrate based PAMPs (Table 1.2)¹²². Although most are believed to be protein-protein activator molecules, homologous receptors in plants bind LPS and peptidoglycan¹²³. Interestingly, several fungal species possess proteins capable of binding the same PAMPs; modulating morphology or the production of antimicrobial natural products¹²⁴. In spite of the vast knowledge of the biological

importance of these interactions, molecular characterization has been difficult to obtain due to the challenges in crystalizing carbohydrates¹²⁵.

Despite structural differences, all carbohydrates contain hydroxyl and C-H bond functional groups. These groups are important for protein binding because the hydroxyl groups can form hydrogen bonds with polar amino acids and the C-H bond can contribute to the binding affinity through the formation of hydrophobic interactions with non-polar amino acids¹²⁶. Due to the reliance of the weak interactions, binding energies for individual carbohydrates are small and it thought multivalent interactions with oligosaccharides are often required for biological relevance¹²⁷. In addition to the hydrogen bonding and hydrophobic interactions, CH- π interactions with aromatic residues are imperative in carbohydrate-protein binding. The partial positive proton of the C-H bond forms a favorable electrostatic interaction with the partial negative π -systems above and below the aromatic residue, stabilizing the protein-carbohydrate interaction¹²⁸. The importance of these CH- π interactions is highlighted by the fact the most common amino acids found in carbohydrate binding pocket are tryptophan, tyrosine, and histidine¹²⁹. Looking for pockets of aromatic residues in Cyr1 could potentially lead to the identification of a binding site for peptidoglycan fragments. Identifying the residues responsible for binding MDP will add to the understanding of how monosaccharides can cause significant biological responses.

1.4 Dissertation Overview

Interactions between the bacteria and fungi species of the microbiome are critical to human health, as they have been linked to a variety of disease states. Despite

the importance, there is a lack of molecular understanding of how fungi recognize and respond to bacteria. The major goal of this dissertation is to improve the molecular understanding of how *Candida albicans* is capable of recognizing molecules of bacterial origin. In the larger biological landscape; this thesis aims to add another level of molecular understanding used by the LRR domain. By comparing these molecular details, we can begin to understand how one domain can respond to a variety of ligands. Chapter 2 details the purification and characterization of the elusive leucine rich repeat (LRR) domain of Cyr1. Chapter 3 discusses the development of three assays to determine the ability of a small library of bacterial derived carbohydrates to elicit a hyphae response in *C. albicans*. Chapter 4 details the successful development of a surface plasmon resonance assay to characterize the binding of Cyr1-LRR to bacterial derived carbohydrates. Overall, this thesis provides new tools to study the LRR domain and molecular level insight for LRR binding to carbohydrates.

REFERENCES

1. Gilbert, J. A.; Blaser, M. J.; Caporaso, J. G.; Jansson, J. K.; Lynch, S. V.; Knight, R., Current understanding of the human microbiome. *Nat Med* **2018**, *24* (4), 392-400. DOI: 10.1038/nm.4517.
2. Chen, J.; Ren, J. A.; Gu, G. S.; Wang, G. F.; Wu, X. W.; Yan, D. S.; Liu, S.; Li, J. S., Crohn's disease and polymorphism of heat shock protein gene HSP70-2 in the Chinese population. *Journal of Gastroenterology and Hepatology* **2013**, *28* (5), 814-818. DOI: 10.1111/jgh.12163.
3. Peterson, J.; Garges, S.; Giovanni, M.; McInnes, P.; Wang, L.; Schloss, J. A.; Bonazzi, V.; McEwen, J. E.; Wetterstrand, K. A.; Deal, C.; Baker, C. C.; Di Francesco, V.; Howcroft, T. K.; Karp, R. W.; Lunsford, R. D.; Wellington, C. R.; Belachew, T.; Wright, M.; Giblin, C.; David, H.; Mills, M.; Salomon, R.; Mullins, C.; Akolkar, B.; Begg, L.; Davis, C.; Grandison, L.; Humble, M.; Khalsa, J.; Little, A. R.; Peavy, H.; Pontzer, C.; Portnoy, M.; Sayre, M. H.; Starke-Reed, P.; Zakhari, S.; Read, J.; Watson, B.; Guyer, M., The NIH Human Microbiome Project. *Genome research* **2009**, *19* (12), 2317-23. DOI: 10.1101/gr.096651.109.
4. Grice, E. A.; Segre, J. A., The skin microbiome. *Nat Rev Microbiol* **2011**, *9* (4), 244-53. DOI: 10.1038/nrmicro2537.
5. Goodrich, J. K.; Waters, J. L.; Poole, A. C.; Sutter, J. L.; Koren, O.; Blekhman, R.; Beaumont, M.; Van Treuren, W.; Knight, R.; Bell, J. T.; Spector, T. D.; Clark, A. G.; Ley, R. E., Human genetics shape the gut microbiome. *Cell* **2014**, *159* (4), 789-99. DOI: 10.1016/j.cell.2014.09.053.
6. Ley, R. E.; Lozupone, C. A.; Hamady, M.; Knight, R.; Gordon, J. I., Worlds within worlds: evolution of the vertebrate gut microbiota. *Nature reviews. Microbiology* **2008**, *6* (10), 776-88. DOI: 10.1038/nrmicro1978.
7. Albenberg, L. G.; Wu, G. D., Diet and the intestinal microbiome: associations, functions, and implications for health and disease. *Gastroenterology* **2014**, *146* (6), 1564-72. DOI: 10.1053/j.gastro.2014.01.058.
8. Modi, S. R.; Collins, J. J.; Relman, D. A., Antibiotics and the gut microbiota. *J Clin Invest* **2014**, *124* (10), 4212-8. DOI: 10.1172/JCI72333.

9. Song, S. J.; Lauber, C.; Costello, E. K.; Lozupone, C. A.; Humphrey, G.; Berg-Lyons, D.; Caporaso, J. G.; Knights, D.; Clemente, J. C.; Nakielny, S.; Gordon, J. I.; Fierer, N.; Knight, R., Cohabiting family members share microbiota with one another and with their dogs. *Elife* **2013**, *2*, e00458. DOI: 10.7554/eLife.00458.
10. Littman, D. R.; Pamer, E. G., Role of the commensal microbiota in normal and pathogenic host immune responses. *Cell Host Microbe* **2011**, *10* (4), 311-23. DOI: 10.1016/j.chom.2011.10.004.
11. Kennedy, T. A.; Naeem, S.; Howe, K. M.; Knops, J. M.; Tilman, D.; Reich, P., Biodiversity as a barrier to ecological invasion. *Nature* **2002**, *417* (6889), 636-8. DOI: 10.1038/nature00776.
12. Cho, I.; Blaser, M. J., The human microbiome: at the interface of health and disease. *Nat Rev Genet* **2012**, *13* (4), 260-70. DOI: 10.1038/nrg3182.
13. Rocha, M. A.; Bagatin, E., Skin barrier and microbiome in acne. *Arch Dermatol Res* **2018**, *310* (3), 181-185. DOI: 10.1007/s00403-017-1795-3.
14. Ling, Z.; Jin, C.; Xie, T.; Cheng, Y.; Li, L.; Wu, N., Alterations in the Fecal Microbiota of Patients with HIV-1 Infection: An Observational Study in A Chinese Population. *Sci Rep* **2016**, *6*, 30673. DOI: 10.1038/srep30673.
15. Huang, Y. J.; Boushey, H. A., The microbiome in asthma. *The Journal of allergy and clinical immunology* **2015**, *135* (1), 25-30. DOI: 10.1016/j.jaci.2014.11.011.
16. Wang, L.; Christophersen, C. T.; Sorich, M. J.; Gerber, J. P.; Angley, M. T.; Conlon, M. A., Low relative abundances of the mucolytic bacterium *Akkermansia muciniphila* and *Bifidobacterium* spp. in feces of children with autism. *Appl Environ Microbiol* **2011**, *77* (18), 6718-21. DOI: 10.1128/AEM.05212-11.
17. Ling, Z.; Li, Z.; Liu, X.; Cheng, Y.; Luo, Y.; Tong, X.; Yuan, L.; Wang, Y.; Sun, J.; Li, L.; Xiang, C., Altered fecal microbiota composition associated with food allergy in infants. *Appl Environ Microbiol* **2014**, *80* (8), 2546-54. DOI: 10.1128/AEM.00003-14.
18. Schwabe, R. F.; Jobin, C., The microbiome and cancer. *Nature reviews. Cancer* **2013**, *13* (11), 800-12. DOI: 10.1038/nrc3610.
19. Lauro, M. L.; Burch, J. M.; Grimes, C. L., The effect of NOD2 on the microbiota in Crohn's disease. *Current Opinion in Biotechnology* **2016**, *40*, 97-102. DOI: <http://dx.doi.org/10.1016/j.copbio.2016.02.028>.

20. Wang, B.; Yao, M.; Lv, L.; Ling, Z.; Li, L., The Human Microbiota in Health and Disease. *Engineering* **2017**, *3* (1), 71-82. DOI: <https://doi.org/10.1016/J.ENG.2017.01.008>.
21. Arumugam, M.; Raes, J.; Pelletier, E.; Le Paslier, D.; Yamada, T.; Mende, D. R.; Fernandes, G. R.; Tap, J.; Bruls, T.; Batto, J. M.; Bertalan, M.; Borruel, N.; Casellas, F.; Fernandez, L.; Gautier, L.; Hansen, T.; Hattori, M.; Hayashi, T.; Kleerebezem, M.; Kurokawa, K.; Leclerc, M.; Levenez, F.; Manichanh, C.; Nielsen, H. B.; Nielsen, T.; Pons, N.; Poulain, J.; Qin, J.; Sicheritz-Ponten, T.; Tims, S.; Torrents, D.; Ugarte, E.; Zoetendal, E. G.; Wang, J.; Guarner, F.; Pedersen, O.; de Vos, W. M.; Brunak, S.; Dore, J.; Meta, H. I. T. C.; Antolin, M.; Artiguenave, F.; Blottiere, H. M.; Almeida, M.; Brechot, C.; Cara, C.; Chervaux, C.; Cultrone, A.; Delorme, C.; Denariáz, G.; Dervyn, R.; Foerstner, K. U.; Friss, C.; van de Guchte, M.; Guedon, E.; Haimet, F.; Huber, W.; van Hylekama-Vlieg, J.; Jamet, A.; Juste, C.; Kaci, G.; Knol, J.; Lakhdari, O.; Layec, S.; Le Roux, K.; Maguin, E.; Merieux, A.; Melo Minardi, R.; M'Rini, C.; Muller, J.; Oozeer, R.; Parkhill, J.; Renault, P.; Rescigno, M.; Sanchez, N.; Sunagawa, S.; Torrejon, A.; Turner, K.; Vandemeulebrouck, G.; Varela, E.; Winogradsky, Y.; Zeller, G.; Weissenbach, J.; Ehrlich, S. D.; Bork, P., Enterotypes of the human gut microbiome. *Nature* **2011**, *473* (7346), 174-80. DOI: 10.1038/nature09944.
22. Underhill, D. M.; Iliev, I. D., The mycobiota: interactions between commensal fungi and the host immune system. *Nature reviews. Immunology* **2014**, *14* (6), 405-16. DOI: 10.1038/nri3684.
23. Cui, L.; Morris, A.; Ghedin, E., The human mycobiome in health and disease. *Genome medicine* **2013**, *5* (7), 63. DOI: 10.1186/gm467.
24. Dollive, S.; Chen, Y. Y.; Grunberg, S.; Bittinger, K.; Hoffmann, C.; Vandivier, L.; Cuff, C.; Lewis, J. D.; Wu, G. D.; Bushman, F. D., Fungi of the murine gut: episodic variation and proliferation during antibiotic treatment. *PloS one* **2013**, *8* (8), e71806. DOI: 10.1371/journal.pone.0071806.
25. Huseyin, C. E.; O'Toole, P. W.; Cotter, P. D.; Scanlan, P. D., Forgotten fungi- the gut mycobiome in human health and disease. *FEMS Microbiol Rev* **2017**, *41* (4), 479-511. DOI: 10.1093/femsre/fuw047.
26. Ghannoum, M. A.; Jurevic, R. J.; Mukherjee, P. K.; Cui, F.; Sikaroodi, M.; Naqvi, A.; Gillevet, P. M., Characterization of the oral fungal microbiome (mycobiome) in healthy individuals. *PLoS Pathog* **2010**, *6* (1), e1000713. DOI: 10.1371/journal.ppat.1000713.
27. Findley, K.; Oh, J.; Yang, J.; Conlan, S.; Deming, C.; Meyer, J. A.; Schoenfeld, D.; Nomicos, E.; Park, M.; Program, N. I. H. I. S. C. C. S.; Kong, H. H.;

- Segre, J. A., Topographic diversity of fungal and bacterial communities in human skin. *Nature* **2013**, *498* (7454), 367-70. DOI: 10.1038/nature12171.
28. Roth, R. R.; James, W. D., Microbial ecology of the skin. *Annu Rev Microbiol* **1988**, *42*, 441-64. DOI: 10.1146/annurev.mi.42.100188.002301.
29. Huffnagle, G. B.; Noverr, M. C., The emerging world of the fungal microbiome. *Trends Microbiol* **2013**, *21* (7), 334-41. DOI: 10.1016/j.tim.2013.04.002.
30. Seed, P. C., The human mycobiome. *Cold Spring Harb Perspect Med* **2014**, *5* (5), a019810. DOI: 10.1101/cshperspect.a019810.
31. Karabinis, A.; Hill, C.; Leclercq, B.; Tancrede, C.; Baume, D.; Andreumont, A., Risk factors for candidemia in cancer patients: a case-control study. *J Clin Microbiol* **1988**, *26* (3), 429-32.
32. Teoh, F.; Pavelka, N., How Chemotherapy Increases the Risk of Systemic Candidiasis in Cancer Patients: Current Paradigm and Future Directions. *Pathogens* **2016**, *5* (1). DOI: 10.3390/pathogens5010006.
33. Mason, K. L.; Erb Downward, J. R.; Mason, K. D.; Falkowski, N. R.; Eaton, K. A.; Kao, J. Y.; Young, V. B.; Huffnagle, G. B., Candida albicans and bacterial microbiota interactions in the cecum during recolonization following broad-spectrum antibiotic therapy. *Infect Immun* **2012**, *80* (10), 3371-80. DOI: 10.1128/IAI.00449-12.
34. Naglik, J. R.; Fidel, P. L., Jr.; Odds, F. C., Animal models of mucosal Candida infection. *FEMS microbiology letters* **2008**, *283* (2), 129-39. DOI: 10.1111/j.1574-6968.2008.01160.x.
35. Noverr, M. C.; Falkowski, N. R.; McDonald, R. A.; McKenzie, A. N.; Huffnagle, G. B., Development of allergic airway disease in mice following antibiotic therapy and fungal microbiota increase: role of host genetics, antigen, and interleukin-13. *Infect Immun* **2005**, *73* (1), 30-8. DOI: 10.1128/IAI.73.1.30-38.2005.
36. Erb Downward, J. R.; Falkowski, N. R.; Mason, K. L.; Muraglia, R.; Huffnagle, G. B., Modulation of post-antibiotic bacterial community reassembly and host response by Candida albicans. *Sci Rep* **2013**, *3*, 2191. DOI: 10.1038/srep02191.
37. Chow, J.; Tang, H.; Mazmanian, S. K., Pathobionts of the gastrointestinal microbiota and inflammatory disease. *Curr Opin Immunol* **2011**, *23* (4), 473-80. DOI: 10.1016/j.coi.2011.07.010.

38. Pothoulakis, C., Review article: anti-inflammatory mechanisms of action of *Saccharomyces boulardii*. *Aliment Pharmacol Ther* **2009**, *30* (8), 826-33. DOI: 10.1111/j.1365-2036.2009.04102.x.
39. Hoarau, G.; Mukherjee, P. K.; Gower-Rousseau, C.; Hager, C.; Chandra, J.; Retuerto, M. A.; Neut, C.; Vermeire, S.; Clemente, J.; Colombel, J. F.; Fujioka, H.; Poulain, D.; Sendid, B.; Ghannoum, M. A., Bacteriome and Mycobiome Interactions Underscore Microbial Dysbiosis in Familial Crohn's Disease. *MBio* **2016**, *7* (5). DOI: 10.1128/mBio.01250-16.
40. M., R., Skin and mucous membrane infections. In *Candida and Candidiasis*, Calderone, R., Ed. ASM Press: Washington, DC, 2002; pp 307-325.
41. Sobel, J. D., Vaginitis. *N Engl J Med* **1997**, *337* (26), 1896-903. DOI: 10.1056/NEJM199712253372607.
42. Pappas, P. G.; Kauffman, C. A.; Andes, D. R.; Clancy, C. J.; Marr, K. A.; Ostrosky-Zeichner, L.; Reboli, A. C.; Schuster, M. G.; Vazquez, J. A.; Walsh, T. J.; Zaoutis, T. E.; Sobel, J. D., Clinical Practice Guideline for the Management of Candidiasis: 2016 Update by the Infectious Diseases Society of America. *Clin Infect Dis* **2016**, *62* (4), e1-50. DOI: 10.1093/cid/civ933.
43. Morgan, J.; Meltzer, M. I.; Plikaytis, B. D.; Sofair, A. N.; Huie-White, S.; Wilcox, S.; Harrison, L. H.; Seaberg, E. C.; Hajjeh, R. A.; Teutsch, S. M., Excess mortality, hospital stay, and cost due to candidemia: a case-control study using data from population-based candidemia surveillance. *Infect Control Hosp Epidemiol* **2005**, *26* (6), 540-7. DOI: 10.1086/502581.
44. Wisplinghoff, H.; Bischoff, T.; Tallent, S. M.; Seifert, H.; Wenzel, R. P.; Edmond, M. B., Nosocomial bloodstream infections in US hospitals: analysis of 24,179 cases from a prospective nationwide surveillance study. *Clin Infect Dis* **2004**, *39* (3), 309-17. DOI: 10.1086/421946.
45. Shapiro, R. S.; Robbins, N.; Cowen, L. E., Regulatory circuitry governing fungal development, drug resistance, and disease. *Microbiology and molecular biology reviews : MMBR* **2011**, *75* (2), 213-67. DOI: 10.1128/membr.00045-10.
46. Cleveland, A. A.; Farley, M. M.; Harrison, L. H.; Stein, B.; Hollick, R.; Lockhart, S. R.; Magill, S. S.; Derado, G.; Park, B. J.; Chiller, T. M., Changes in incidence and antifungal drug resistance in candidemia: results from population-based laboratory surveillance in Atlanta and Baltimore, 2008-2011. *Clin Infect Dis* **2012**, *55* (10), 1352-61. DOI: 10.1093/cid/cis697.

47. Pierce, G. E., *Pseudomonas aeruginosa*, *Candida albicans*, and device-related nosocomial infections: implications, trends, and potential approaches for control. *J Ind Microbiol Biotechnol* **2005**, *32* (7), 309-18. DOI: 10.1007/s10295-005-0225-2.
48. Hogan, D. A.; Kolter, R., *Pseudomonas-Candida* interactions: an ecological role for virulence factors. *Science* **2002**, *296* (5576), 2229-32. DOI: 10.1126/science.1070784.
49. Adam, B.; Baillie, G. S.; Douglas, L. J., Mixed species biofilms of *Candida albicans* and *Staphylococcus epidermidis*. *J Med Microbiol* **2002**, *51* (4), 344-9. DOI: 10.1099/0022-1317-51-4-344.
50. Schlecht, L. M.; Peters, B. M.; Krom, B. P.; Freiberg, J. A.; Hansch, G. M.; Filler, S. G.; Jabra-Rizk, M. A.; Shirtliff, M. E., Systemic *Staphylococcus aureus* infection mediated by *Candida albicans* hyphal invasion of mucosal tissue. *Microbiology* **2015**, *161* (Pt 1), 168-181. DOI: 10.1099/mic.0.083485-0.
51. Metwalli, K. H.; Khan, S. A.; Krom, B. P.; Jabra-Rizk, M. A., *Streptococcus mutans*, *Candida albicans*, and the human mouth: a sticky situation. *PLoS Pathog* **2013**, *9* (10), e1003616. DOI: 10.1371/journal.ppat.1003616.
52. Fitzsimmons, N.; Berry, D. R., Inhibition of *Candida albicans* by *Lactobacillus acidophilus*: evidence for the involvement of a peroxidase system. *Microbios* **1994**, *80* (323), 125-33.
53. Sudbery, P. E., Growth of *Candida albicans* hyphae. *Nature reviews. Microbiology* **2011**, *9* (10), 737-48. DOI: 10.1038/nrmicro2636.
54. Gow, N. A. R.; Yadav, B., Microbe Profile: *Candida albicans*: a shape-changing, opportunistic pathogenic fungus of humans. *Microbiology* **2017**, *163* (8), 1145-1147. DOI: 10.1099/mic.0.000499.
55. Soll, D. R., High-frequency switching in *Candida albicans*. *Clin Microbiol Rev* **1992**, *5* (2), 183-203.
56. Zheng, X.; Wang, Y.; Wang, Y., Hgc1, a novel hypha-specific G1 cyclin-related protein regulates *Candida albicans* hyphal morphogenesis. *The EMBO Journal* **2004**, *23* (8), 1845-1856.
57. Heilmann, C. J.; Sorgo, A. G.; Siliakus, A. R.; Dekker, H. L.; Brul, S.; de Koster, C. G.; de Koning, L. J.; Klis, F. M., Hyphal induction in the human fungal pathogen *Candida albicans* reveals a characteristic wall protein profile. *Microbiology* **2011**, *157* (Pt 8), 2297-2307. DOI: 10.1099/mic.0.049395-0.

58. Ponniah, G.; Rollenhagen, C.; Bahn, Y. S.; Staab, J. F.; Sundstrom, P., State of differentiation defines buccal epithelial cell affinity for cross-linking to *Candida albicans* Hwp1. *J Oral Pathol Med* **2007**, *36* (8), 456-67. DOI: 10.1111/j.1600-0714.2007.00565.x.
59. Staab, J. F.; Bradway, S. D.; Fidel, P. L.; Sundstrom, P., Adhesive and mammalian transglutaminase substrate properties of *Candida albicans* Hwp1. *Science* **1999**, *283* (5407), 1535-8.
60. Staab, J. F.; Sundstrom, P., Genetic organization and sequence analysis of the hypha-specific cell wall protein gene HWP1 of *Candida albicans*. *Yeast* **1998**, *14* (7), 681-6. DOI: 10.1002/(sici)1097-0061(199805)14:7<681::aid-yea256>3.0.co;2-8.
61. da Silva Dantas, A.; Lee, K. K.; Raziunaite, I.; Schaefer, K.; Wagener, J.; Yadav, B.; Gow, N. A., Cell biology of *Candida albicans*-host interactions. *Curr Opin Microbiol* **2016**, *34*, 111-118. DOI: 10.1016/j.mib.2016.08.006.
62. Hogan, D. A.; Sundstrom, P., The Ras/cAMP/PKA signaling pathway and virulence in *Candida albicans*. *Future microbiology* **2009**, *4* (10), 1263-70. DOI: 10.2217/fmb.09.106.
63. Nobile, C. J.; Schneider, H. A.; Nett, J. E.; Sheppard, D. C.; Filler, S. G.; Andes, D. R.; Mitchell, A. P., Complementary adhesin function in *C. albicans* biofilm formation. *Curr Biol* **2008**, *18* (14), 1017-24. DOI: 10.1016/j.cub.2008.06.034.
64. Sardi, J. C.; Scorzoni, L.; Bernardi, T.; Fusco-Almeida, A. M.; Mendes Giannini, M. J., *Candida* species: current epidemiology, pathogenicity, biofilm formation, natural antifungal products and new therapeutic options. *J Med Microbiol* **2013**, *62* (Pt 1), 10-24. DOI: 10.1099/jmm.0.045054-0.
65. Dalle, F.; Wachtler, B.; L'Ollivier, C.; Holland, G.; Bannert, N.; Wilson, D.; Labruere, C.; Bonnin, A.; Hube, B., Cellular interactions of *Candida albicans* with human oral epithelial cells and enterocytes. *Cell Microbiol* **2010**, *12* (2), 248-71. DOI: 10.1111/j.1462-5822.2009.01394.x.
66. Frank, C. F.; Hostetter, M. K., Cleavage of E-cadherin: a mechanism for disruption of the intestinal epithelial barrier by *Candida albicans*. *Translational research : the journal of laboratory and clinical medicine* **2007**, *149* (4), 211-22. DOI: 10.1016/j.trsl.2006.11.006.
67. Park, H.; Myers, C. L.; Sheppard, D. C.; Phan, Q. T.; Sanchez, A. A.; J, E. E.; Filler, S. G., Role of the fungal Ras-protein kinase A pathway in governing epithelial cell interactions during oropharyngeal candidiasis. *Cell Microbiol* **2005**, *7* (4), 499-510. DOI: 10.1111/j.1462-5822.2004.00476.x.

68. Phan, Q. T.; Myers, C. L.; Fu, Y.; Sheppard, D. C.; Yeaman, M. R.; Welch, W. H.; Ibrahim, A. S.; Edwards, J. E., Jr.; Filler, S. G., Als3 is a *Candida albicans* invasin that binds to cadherins and induces endocytosis by host cells. *PLoS Biol* **2007**, *5* (3), e64. DOI: 10.1371/journal.pbio.0050064.
69. Monge, R. A., The MAP kinase signal transduction network in *Candida albicans*. *Microbiology* **2006**, *152* (4), 905-912. DOI: 10.1099/mic.0.28616-0.
70. Leberer, E.; Harcus, D.; Broadbent, I. D.; Clark, K. L.; Dignard, D.; Ziegelbauer, K.; Schmidt, A.; Gow, N. A.; Brown, A. J.; Thomas, D. Y., Signal transduction through homologs of the Ste20p and Ste7p protein kinases can trigger hyphal formation in the pathogenic fungus *Candida albicans*. *Proceedings of the National Academy of Sciences of the United States of America* **1996**, *93* (23), 13217-22.
71. Liu, H.; Kohler, J.; Fink, G. R., Suppression of hyphal formation in *Candida albicans* by mutation of a STE12 homolog. *Science* **1994**, *266* (5191), 1723-6.
72. Calderon, J.; Zavrel, M.; Ragni, E.; Fonzi, W. A.; Rupp, S.; Popolo, L., PHR1, a pH-regulated gene of *Candida albicans* encoding a glucan-remodelling enzyme, is required for adhesion and invasion. *Microbiology* **2010**, *156* (Pt 8), 2484-94. DOI: 10.1099/mic.0.038000-0.
73. Buffo, J.; Herman, M. A.; Soll, D. R., A characterization of pH-regulated dimorphism in *Candida albicans*. *Mycopathologia* **1984**, *85* (1-2), 21-30.
74. Bockmuhl, D. P.; Krishnamurthy, S.; Gerads, M.; Sonneborn, A.; Ernst, J. F., Distinct and redundant roles of the two protein kinase A isoforms Tpk1p and Tpk2p in morphogenesis and growth of *Candida albicans*. *Mol Microbiol* **2001**, *42* (5), 1243-57.
75. Leberer, E.; Harcus, D.; Dignard, D.; Johnson, L.; Ushinsky, S.; Thomas, D. Y.; Schroppel, K., Ras links cellular morphogenesis to virulence by regulation of the MAP kinase and cAMP signalling pathways in the pathogenic fungus *Candida albicans*. *Mol Microbiol* **2001**, *42* (3), 673-87.
76. Jung, W. H.; Stateva, L. I., The cAMP phosphodiesterase encoded by CaPDE2 is required for hyphal development in *Candida albicans*. *Microbiology* **2003**, *149* (Pt 10), 2961-76. DOI: 10.1099/mic.0.26517-0.
77. Rocha, C. R.; Schroppel, K.; Harcus, D.; Marcil, A.; Dignard, D.; Taylor, B. N.; Thomas, D. Y.; Whiteway, M.; Leberer, E., Signaling through adenylyl cyclase is essential for hyphal growth and virulence in the pathogenic fungus *Candida albicans*. *Mol Biol Cell* **2001**, *12* (11), 3631-43.

78. Finn, R. D.; Attwood, T. K.; Babbitt, P. C.; Bateman, A.; Bork, P.; Bridge, A. J.; Chang, H. Y.; Dosztanyi, Z.; El-Gebali, S.; Fraser, M.; Gough, J.; Haft, D.; Holliday, G. L.; Huang, H.; Huang, X.; Letunic, I.; Lopez, R.; Lu, S.; Marchler-Bauer, A.; Mi, H.; Mistry, J.; Natale, D. A.; Necci, M.; Nuka, G.; Orengo, C. A.; Park, Y.; Pesseat, S.; Piovesan, D.; Potter, S. C.; Rawlings, N. D.; Redaschi, N.; Richardson, L.; Rivoire, C.; Sangrador-Vegas, A.; Sigrist, C.; Sillitoe, I.; Smithers, B.; Squizzato, S.; Sutton, G.; Thanki, N.; Thomas, P. D.; Tosatto, S. C.; Wu, C. H.; Xenarios, I.; Yeh, L. S.; Young, S. Y.; Mitchell, A. L., InterPro in 2017-beyond protein family and domain annotations. *Nucleic acids research* **2017**, *45* (D1), D190-d199. DOI: 10.1093/nar/gkw1107.
79. Schultz, J.; Copley, R. R.; Doerks, T.; Ponting, C. P.; Bork, P., SMART: a web-based tool for the study of genetically mobile domains. *Nucleic acids research* **2000**, *28* (1), 231-4.
80. Wang, Y., Fungal adenylyl cyclase acts as a signal sensor and integrator and plays a central role in interaction with bacteria. *PLoS Pathog* **2013**, *9* (10), e1003612. DOI: 10.1371/journal.ppat.1003612.
81. Maidan, M. M.; De Rop, L.; Serneels, J.; Exler, S.; Rupp, S.; Tourneau, H.; Thevelein, J. M.; Van Dijck, P., The G protein-coupled receptor Gpr1 and the Galpha protein Gpa2 act through the cAMP-protein kinase A pathway to induce morphogenesis in *Candida albicans*. *Mol Biol Cell* **2005**, *16* (4), 1971-86. DOI: 10.1091/mbc.e04-09-0780.
82. Maidan, M. M.; Thevelein, J. M.; Van Dijck, P., Carbon source induced yeast-to-hypha transition in *Candida albicans* is dependent on the presence of amino acids and on the G-protein-coupled receptor Gpr1. *Biochem Soc Trans* **2005**, *33* (Pt 1), 291-3. DOI: 10.1042/BST0330291.
83. Fang, H. M.; Wang, Y., RA domain-mediated interaction of Cdc35 with Ras1 is essential for increasing cellular cAMP level for *Candida albicans* hyphal development. *Mol Microbiol* **2006**, *61* (2), 484-96. DOI: 10.1111/j.1365-2958.2006.05248.x.
84. Shapiro, R. S.; Uppuluri, P.; Zaas, A. K.; Collins, C.; Senn, H.; Perfect, J. R.; Heitman, J.; Cowen, L. E., Hsp90 orchestrates temperature-dependent *Candida albicans* morphogenesis via Ras1-PKA signaling. *Curr Biol* **2009**, *19* (8), 621-9. DOI: 10.1016/j.cub.2009.03.017.
85. Shapiro, R. S.; Zaas, A. K.; Betancourt-Quiroz, M.; Perfect, J. R.; Cowen, L. E., The Hsp90 co-chaperone Sgt1 governs *Candida albicans* morphogenesis and drug resistance. *PLoS one* **2012**, *7* (9), e44734. DOI: 10.1371/journal.pone.0044734.

86. Klengel, T.; Liang, W. J.; Chaloupka, J.; Ruoff, C.; Schroppel, K.; Naglik, J. R.; Eckert, S. E.; Mogensen, E. G.; Haynes, K.; Tuite, M. F.; Levin, L. R.; Buck, J.; Muhlschlegel, F. A., Fungal adenylyl cyclase integrates CO₂ sensing with cAMP signaling and virulence. *Curr Biol* **2005**, *15* (22), 2021-6. DOI: 10.1016/j.cub.2005.10.040.
87. Davis-Hanna, A.; Piispanen, A. E.; Stateva, L. I.; Hogan, D. A., Farnesol and dodecanol effects on the *Candida albicans* Ras1-cAMP signalling pathway and the regulation of morphogenesis. *Mol Microbiol* **2008**, *67* (1), 47-62. DOI: 10.1111/j.1365-2958.2007.06013.x.
88. Hall, R. A.; Turner, K. J.; Chaloupka, J.; Cottier, F.; De Sordi, L.; Sanglard, D.; Levin, L. R.; Buck, J.; Muhlschlegel, F. A., The quorum-sensing molecules farnesol/homoserine lactone and dodecanol operate via distinct modes of action in *Candida albicans*. *Eukaryot Cell* **2011**, *10* (8), 1034-42. DOI: 10.1128/EC.05060-11.
89. Langford, M. L.; Atkin, A. L.; Nickerson, K. W., Cellular interactions of farnesol, a quorum-sensing molecule produced by *Candida albicans*. *Future microbiology* **2009**, *4* (10), 1353-62. DOI: 10.2217/fmb.09.98.
90. Lindsay, A. K.; Deveau, A.; Piispanen, A. E.; Hogan, D. A., Farnesol and cyclic AMP signaling effects on the hypha-to-yeast transition in *Candida albicans*. *Eukaryot Cell* **2012**, *11* (10), 1219-25. DOI: 10.1128/EC.00144-12.
91. Reynolds, R., The filament inducing property of blood for *Candida albicans* : its nature and significance. *Clin. Res. Proc.* **1956**, *4*, 40.
92. Xu, X. L.; Lee, R. T.; Fang, H. M.; Wang, Y. M.; Li, R.; Zou, H.; Zhu, Y.; Wang, Y., Bacterial peptidoglycan triggers *Candida albicans* hyphal growth by directly activating the adenylyl cyclase Cyr1p. *Cell Host Microbe* **2008**, *4* (1), 28-39. DOI: 10.1016/j.chom.2008.05.014.
93. Rogers, H. J., Peptidoglycans (mucopeptides): structure, function, and variations. *Ann N Y Acad Sci* **1974**, *235* (0), 29-51.
94. Royet, J.; Dziarski, R., Peptidoglycan recognition proteins: pleiotropic sensors and effectors of antimicrobial defences. *Nature Reviews Microbiology* **2007**, *5*, 264. DOI: 10.1038/nrmicro1620.
95. McDonald, C.; Inohara, N.; Nunez, G., Peptidoglycan signaling in innate immunity and inflammatory disease. *The Journal of biological chemistry* **2005**, *280* (21), 20177-80. DOI: 10.1074/jbc.R500001200.

96. Caplan, J.; Padmanabhan, M.; Dinesh-Kumar, S. P., Plant NB-LRR immune receptors: from recognition to transcriptional reprogramming. *Cell Host Microbe* **2008**, *3* (3), 126-35. DOI: 10.1016/j.chom.2008.02.010.
97. Ng, A.; Xavier, R. J., Leucine-rich repeat (LRR) proteins: integrators of pattern recognition and signaling in immunity. *Autophagy* **2011**, *7* (9), 1082-4.
98. Matsushima, N.; Miyashita, H., Leucine-Rich Repeat (LRR) Domains Containing Intervening Motifs in Plants. *Biomolecules* **2012**, *2* (2), 288-311. DOI: 10.3390/biom2020288.
99. Letunic, I.; Bork, P., 20 years of the SMART protein domain annotation resource. *Nucleic acids research* **2018**, *46* (D1), D493-D496. DOI: 10.1093/nar/gkx922.
100. Bierne, H.; Sabet, C.; Personnic, N.; Cossart, P., Internalins: a complex family of leucine-rich repeat-containing proteins in *Listeria monocytogenes*. *Microbes and infection / Institut Pasteur* **2007**, *9* (10), 1156-66. DOI: 10.1016/j.micinf.2007.05.003.
101. Winther, M.; Walmod, P. S., Neural cell adhesion molecules belonging to the family of leucine-rich repeat proteins. *Advances in neurobiology* **2014**, *8*, 315-95.
102. Kresse, H.; Schonherr, E., Proteoglycans of the extracellular matrix and growth control. *Journal of cellular physiology* **2001**, *189* (3), 266-74. DOI: 10.1002/jcp.10030.
103. Kobe, B.; Deisenhofer, J., The leucine-rich repeat: a versatile binding motif. *Trends in biochemical sciences* **1994**, *19* (10), 415-21.
104. Jones, D. A.; Jones, J. D. G., The Role of Leucine-Rich Repeat Proteins in Plant Defences. *Advances in botanical research*. **1997**, *24*, 90.
105. Istomin, A. Y.; Godzik, A., Understanding diversity of human innate immunity receptors: analysis of surface features of leucine-rich repeat domains in NLRs and TLRs. *BMC Immunol* **2009**, *10*, 48. DOI: 10.1186/1471-2172-10-48.
106. Bella, J.; Hindle, K. L.; McEwan, P. A.; Lovell, S. C., The leucine-rich repeat structure. *Cell Mol Life Sci* **2008**, *65* (15), 2307-33. DOI: 10.1007/s00018-008-8019-0.
107. Kobe, B.; Kajava, A. V., The leucine-rich repeat as a protein recognition motif. *Curr Opin Struct Biol* **2001**, *11* (6), 725-32.

108. Enkhbayar, P.; Kamiya, M.; Osaki, M.; Matsumoto, T.; Matsushima, N., Structural principles of leucine-rich repeat (LRR) proteins. *Proteins* **2004**, *54* (3), 394-403. DOI: 10.1002/prot.10605.
109. Kobe, B.; Deisenhofer, J., Crystal structure of porcine ribonuclease inhibitor, a protein with leucine-rich repeats. *Nature* **1993**, *366*, 751. DOI: 10.1038/366751a0.
110. McEwan, P. A.; Scott, P. G.; Bishop, P. N.; Bella, J., Structural correlations in the family of small leucine-rich repeat proteins and proteoglycans. *Journal of structural biology* **2006**, *155* (2), 294-305. DOI: 10.1016/j.jsb.2006.01.016.
111. Courtemanche, N.; Barrick, D., The leucine-rich repeat domain of Internalin B folds along a polarized N-terminal pathway. *Structure* **2008**, *16* (5), 705-14. DOI: 10.1016/j.str.2008.02.015.
112. Kobe, B.; Deisenhofer, J., Mechanism of ribonuclease inhibition by ribonuclease inhibitor protein based on the crystal structure of its complex with ribonuclease A. *J Mol Biol* **1996**, *264* (5), 1028-43. DOI: 10.1006/jmbi.1996.0694.
113. Charles A. Janeway, J.; Medzhitov, R., Innate Immune Recognition. *Annual Review of Immunology* **2002**, *20* (1), 197-216. DOI: 10.1146/annurev.immunol.20.083001.084359.
114. Lemaitre, B.; Nicolas, E.; Michaut, L.; Reichhart, J. M.; Hoffmann, J. A., The dorsoventral regulatory gene cassette spatzle/Toll/cactus controls the potent antifungal response in *Drosophila* adults. *Cell* **1996**, *86* (6), 973-83.
115. Poltorak, A.; He, X.; Smirnova, I.; Liu, M. Y.; Van Huffel, C.; Du, X.; Birdwell, D.; Alejos, E.; Silva, M.; Galanos, C.; Freudenberg, M.; Ricciardi-Castagnoli, P.; Layton, B.; Beutler, B., Defective LPS signaling in C3H/HeJ and C57BL/10ScCr mice: mutations in Tlr4 gene. *Science* **1998**, *282* (5396), 2085-8.
116. Kim, H. M.; Park, B. S.; Kim, J. I.; Kim, S. E.; Lee, J.; Oh, S. C.; Enkhbayar, P.; Matsushima, N.; Lee, H.; Yoo, O. J.; Lee, J. O., Crystal structure of the TLR4-MD-2 complex with bound endotoxin antagonist Eritoran. *Cell* **2007**, *130* (5), 906-17. DOI: 10.1016/j.cell.2007.08.002.
117. Murthy, K. G.; Deb, A.; Goonesekera, S.; Szabo, C.; Salzman, A. L., Identification of conserved domains in *Salmonella muenchen* flagellin that are essential for its ability to activate TLR5 and to induce an inflammatory response in vitro. *The Journal of biological chemistry* **2004**, *279* (7), 5667-75. DOI: 10.1074/jbc.M307759200.

118. Grimes, C. L.; Ariyananda, L. D.; Melnyk, J. E.; O'Shea, E. K., The Innate Immune Protein Nod2 Binds Directly to MDP, a Bacterial Cell Wall Fragment. *Journal of the American Chemical Society* **2012**, *134* (33), 13535-13537. DOI: 10.1021/ja303883c.
119. Gabius, H. J.; Andre, S.; Jimenez-Barbero, J.; Romero, A.; Solis, D., From lectin structure to functional glycomics: principles of the sugar code. *Trends in biochemical sciences* **2011**, *36* (6), 298-313. DOI: 10.1016/j.tibs.2011.01.005.
120. Malik, A.; Baig, M. H.; Manavalan, B., Protein-Carbohydrate Interactions. In *Reference Module in Life Sciences*, 2018. DOI: 10.1016/b978-0-12-809633-8.20661-4.
121. Mahla, R.; Reddy, C.; Prasad, D.; Kumar, H., Sweeten PAMPs: Role of sugar complexed PAMPs in innate immunity and vaccine biology. *Frontiers in immunology* **2013**, *4* (248). DOI: 10.3389/fimmu.2013.00248.
122. Brubaker, S. W.; Bonham, K. S.; Zanoni, I.; Kagan, J. C., Innate Immune Pattern Recognition: A Cell Biological Perspective. *Annual Review of Immunology* **2015**, *33* (1), 257-290. DOI: 10.1146/annurev-immunol-032414-112240.
123. De Schutter, K.; Van Damme, E. J., Protein-carbohydrate interactions as part of plant defense and animal immunity. *Molecules (Basel, Switzerland)* **2015**, *20* (5), 9029-53. DOI: 10.3390/molecules20059029.
124. Kunzler, M., Hitting the sweet spot-glycans as targets of fungal defense effector proteins. *Molecules (Basel, Switzerland)* **2015**, *20* (5), 8144-67. DOI: 10.3390/molecules20058144.
125. Agirre, J.; Davies, G. J.; Wilson, K. S.; Cowtan, K. D., Carbohydrate structure: the rocky road to automation. *Curr Opin Struct Biol* **2017**, *44*, 39-47. DOI: 10.1016/j.sbi.2016.11.011.
126. Hudson, K. L., Introduction. In *Carbohydrate-Based Interactions at the Molecular and the Cellular Level*, 2018; pp 1-34. DOI: 10.1007/978-3-319-77706-1_1.
127. Reynolds, M.; Pérez, S., Thermodynamics and chemical characterization of protein-carbohydrate interactions: The multivalency issue. *Comptes Rendus Chimie* **2011**, *14* (1), 74-95. DOI: <https://doi.org/10.1016/j.crci.2010.05.020>.
128. Nishio, M.; Umezawa, Y.; Fantini, J.; Weiss, M. S.; Chakrabarti, P., CH-pi hydrogen bonds in biological macromolecules. *Physical chemistry chemical physics : PCCP* **2014**, *16* (25), 12648-83. DOI: 10.1039/c4cp00099d.

129. Hudson, K. L.; Bartlett, G. J.; Diehl, R. C.; Agirre, J.; Gallagher, T.; Kiessling, L. L.; Woolfson, D. N., Carbohydrate-Aromatic Interactions in Proteins. *J Am Chem Soc* **2015**, *137* (48), 15152-60. DOI: 10.1021/jacs.5b08424.

Chapter 2

CHARACTERIZATION OF THE LUECINE RICH REPEAT DOMAIN OF THE *CANDIDA ALBICANS* ADENYLY CYCLASE (CACYR1)

2.1 Introduction

Candida albicans is one of the most common members of the human mycobiome¹. While typically acting as a commensal species, *C. albicans* is also the most prevalent human fungal pathogen. This fungi is responsible for both minor infections - such as oral candidiasis (thrush) or vaginal candidiasis (yeast infection)² – and major diseases such as candidemia, which has associated mortality rates approaching 30%³. In order to effectively prevent these infections, it is imperative to understand the mechanism by which *C. albicans* becomes pathogenic. Critical to becoming pathogenic is a morphological switch from budding yeast to filamentous hyphae⁴. These hyphae are essential for *C. albicans* virulence, regulating the infection process by modulating adhesion to and penetration of epithelial cells.⁵

C. albicans morphogenesis is a vastly complex biological process which is modulated by numerous environmental cues including nutrient depletion, elevated temperatures, low pH, and the presence of quorum sensing molecules⁶. The morphological response to these stimuli are regulated by the interaction of several signaling cascades including the cAMP-PKA, MAPK, cell cycle arrest, and pH pathways⁷. The cAMP-PKA is of central importance as several studies have shown that the addition of the exogenous cAMP to *C. albicans* cultures induces the formation

of hyphae⁸⁻⁹. Increased cAMP levels lead to the activation of protein kinase A (PKA), which then phosphorylates the transcription factor, Efg1, resulting in the increased expression of hyphae specific genes¹⁰.

Cyclic AMP levels in *C. albicans* are regulated by the phosphodiesterases, Pde1 and Pde2, and the adenylyl cyclase, Cyr1¹¹. Cyr1 is of central importance to the cAMP-PKA pathway as it is the only adenylyl cyclase present in *C. albicans*. This enzyme has demonstrated to be essential for virulence, as its deletion abolishes the ability to form filamentous hyphae¹². Not only does the protein catalyze the synthesis of cAMP from ATP, but it also functions as a signal integrator, regulating the formation of hyphae¹³. The activity of Cyr1 is affected by diverse signals including Ras proteins, Hsp90, and quorum sensing molecules¹⁴⁻¹⁶.

Although no crystal structure currently exists for Cyr1, sequence analysis using the SMART database predicts five domains conserved domains in Cyr1: a N-terminal G α domain, a Ras association domain (RA), a protein phosphatase 2C domain (PP2C), the catalytic domain, and a cluster of 14 leucine rich repeats spanning amino acids 489 to 898¹⁷. Different domains have been demonstrated to respond to unique signals to regulate hyphae growth. The RA domain binds Ras1, which in its GTP-bound state stimulates cAMP production^{16, 18}. The G α domain binds the Gpa2, which is activated by the G-protein-coupled receptor Gpr1 that senses glucose and amino acid concentrations¹⁹. Interestingly, the catalytic domain not only converts ATP to cAMP but also recognizes concentrations of carbon dioxide and farnesol to regulate this reaction²⁰⁻²¹.

Perhaps the most interesting part of Cyr1 is the presence of an LRR domain due to the ability of these domains in homologous proteins to bind vastly different ligands, such as small molecule carbohydrates, and serve as scaffolding for protein-protein interactions²². These LRR domains are commonly associated with innate immune receptors where they bind to microbe associated molecular patterns (MAMPs) to initiate an immune response²³. Wang and coworkers highlighted the similarity between Cyr1 and an innate immune receptor in a 2008 Cell Host Microbe report²⁴. After observing that peptidoglycan trigger hyphae growth, Wang and colleagues hypothesized that there is protein in *C. albicans* performing a similar function as the innate immune receptor, Nod2. Using the sequence of Nod2's LRR to search the *C. albicans* genome, they identified Cyr1 as having 40% sequence similarity to Nod2. Using a biotinylated MDP enrichment assay, the Wang and colleagues confirmed their hypothesis demonstrating that like Nod2 the LRR domain of Cyr1 directly binds MDP. Despite showing an interaction does occur, no further characterization of the binding was offered. Based on this observation, we hypothesized the LRR domain of Cyr1 may be acting as a fungal immune receptor and sought to further investigate and understand this unique interaction.

In order to explore our hypothesis, I sought to develop a more quantitative assay to better understand the importance of this interaction and identify other ligands that are binding the LRR domain. To achieve this, it was first necessary to express and purify the LRR domain. Although, the Wang and colleagues reported using a GST-LRR fusion protein expressed in *E. coli*, no method of purification or characterization of the protein was provided. This was troublesome as there are several examples in the literature demonstrating that recombinant LRR expressed in *E.coli* can form inclusion

bodies²⁵⁻²⁶. In this chapter, I describe my development of purification protocols for recombinant Cyr1-LRR utilizing an *E. coli* expression system.

2.2 Materials and Methods

2.2.1 Materials

Primers were purchased from MWG Operon. Restriction endonucleases were purchased from New England Biolabs. The pGEX-6P-1 vector was purchased from GE Healthcare Life Sciences. A modified pMAL-c5x vector with a hexahistidine tag inserted between I3 and E4 of the maltose binding protein was obtained from Prof. Sharon Rozovsky's lab at the University of Delaware²⁷. Antibiotics and IPTG were purchased from Gold Biotechnology.

2.2.2 Amplification of CYR1 gene

C. albicans genomic DNA was extracted following the protocol developed by Looke and coworkers²⁸. A YPD agar plate was streaked with *C. albicans* from a glycerol stock and incubated at 37 °C overnight. The following day a single colony was selected and suspended in 100 µL of 200 mM LiOAc with 1% SDS. The sample was then heated to 70 °C for 15 min. 300 µL of 96% ethanol was added to the cell suspension and the mixture was centrifuged at 15,000 rpm for 15 min. The supernatant was discarded and the pellet was washed with 500 µL of 70% ethanol and centrifuged again at 15,000 rpm for 15 min. The pellet was suspended in 100 µL ddH₂O and centrifuged at 15,000 rpm for 1 min to remove debris. The *CaCYR1* gene was amplified from genomic DNA by PCR. Primers used for PCR were 1) Forward: 5'

ATG AGT TTT TTA AGG GAG 3' and 2) Reverse: 5' CTA TTT AAG TTC ATT AAC TC 3'.

2.2.3 Molecular Cloning of LRR construct

PCR was used to amplify the LRR domain (residues 480-900) from *CaCYR1* DNA and the product inserted into the pGEX-6p1 vector utilizing the BamHI and NotI restriction sites and transformed into DH5 α cells. Primers used for amplification were 3) Forward: 5' ATA GGA TCC AAA TTC CCC AAT AAT TTA TTA GAA GCA CC and 4) Reverse: 5' TAT GCG GCC GCC TAG CTC AAC TCT 3'. DNA encoding Cyr1-LRR was inserted into the modified pMAL-c5x vector utilizing the BamHI and NdeI restriction sites and transformed into DH5 α cells. Primers used for amplification were 5) Forward: 5' AAA CAT ATG AAA TTA TTA GAA GCA CC 3' and 6) Reverse: 5' ATA GGA TCC CTA GCT CAA CTC TGC TGG 3'. Selected colonies were then mini-prepped using a plasmid purification kit (Qiagen) and isolated plasmids were verified by sequencing (Delaware Biotechnology Institute). The plasmid was then transformed into BL21 RIPL-codon plus cells for expression per the manufacturer's instructions (Agilent Technologies).

2.2.4 Expression and Purification of GST-LRR construct

GST-LRR was expressed in 1 L cultures of LB media carbenicillin (100 μ g/mL) and chloramphenicol (34 μ g/mL), at 30 °C until an optical density (OD₆₀₀) of 0.6-0.8 was reached. Protein expression was induced with 200 μ M IPTG overnight at 18 °C. *E.coli* cells were pelleted by centrifugation at 5,000 rpm for 10 minutes. The supernatant was discarded and pellets stored at -80 °C until use.

Three 1 L pellets were combined and suspended in 45 mL lysis buffer (100 mM TEA-HCl, 170 mM NaCl, 1% Triton X-100, 10 mM DTT, pH 7.4, and 3 cOmplete Protease Inhibitor Cocktail tablets). The suspension was lysed on ice using sonication with an amplitude setting of 50% with pulsing 1s on and 1s off for 3 min total. The lysate was cleared by centrifugation at 15,000 rpm for 15 min. 5 mL 10 x ATP Buffer (100 mM TEA-HCl, 100 mM ATP, 200 mM MgCl₂, 500 mM KCl, 10 mM DTT, pH 7.4) was added to the supernatant and the sample was incubated at 37 °C for 10 min. 300 µL of denatured proteins were added and the sample was incubated at 37 °C for 20 min. The supernatant was clarified by centrifugation at 1,500x g for 10 min at 4 °C. The clarified supernatant was applied to a gravity column containing Glutathione Sepharose 4 Fast Flow resin pre-equilibrated with 10 mM ATP wash buffer (100 mM TEA-HCl, 150 mM NaCl, 10 mM ATP, 1% triton X-100, 20 mM MgCl₂, 50 mM KCl, 10 mM DTT, pH 7.4). The column was shaken at room temperature for 40 min. The column was then washed 3 times with 4 column volumes of 10 mM ATP wash buffer followed by 4 column volumes of 5 mM ATP wash buffer (100 mM TEA-HCl, 150 mM NaCl, 5 mM ATP, 20 mM MgCl₂, 50 mM KCl, 10 mM DTT, pH 7.4). GST-LRR was eluted by incubating the column in 10 mL elution buffer (100 mM Tris, 150 mM NaCl, 25 mM Glutathione, pH 8) for 10 min at room temperature.

2.2.5 Expression of MBP LRR

MBP-LRR was expressed in 1 L cultures of LB media containing carbenicillin (100 µg/mL) and chloramphenicol (34 µg/mL), at 30 °C until an optical density

(OD₆₀₀) of 0.8 was reached. Protein expression was induced with 1 mM IPTG overnight at 18 °C. *E.coli* cells were pelleted by centrifugation at 5,000 rpm for 10 minutes. The supernatant was discarded and pellets stored at -80 °C until use.

2.2.6 Purification of MBP-LRR

A 1 L pellet was resuspended in 30 mL lysis buffer (50 mM sodium phosphate, pH 7.9 containing 150 mM NaCl, 1mM DTT, and 5% glycerol) with 2 protease inhibitor tablets. The suspension was lysed on ice using sonication with an amplitude setting of 50% with pulsing 1s on and 1s off for 3 min total. Triton X-100 was added to a final concentration of 1% and the lysate was incubated on ice for 10 minute. Lysate was pelleted at 15,000 rpm for 15 min and the supernatant was discarded. The pellet was washed twice in lysis buffer following the sonication, incubation and centrifugation steps used when lysing the cell culture pellet. 1% Triton-X 100 was added prior to sonication in the first wash step to assist in solubilizing the cell membrane. After the second wash, the resuspension was pelleted at 15,000 rpm for 15 min and the supernatant was discarded. The pellet was resuspended in 15 mL denaturation buffer (50 mM sodium phosphate, pH 7.9 containing 150 mM NaCl, 10 mM imidazole, and 8 M urea) and rotated at 4 °C overnight. The solubilized inclusion body was clarified by centrifugation at 15,000 rpm for 15 min.

The MBP-LRR was purified by Fast-Protein Liquid Chromatography (FPLC) (Biorad) using a 5 mL HisTrap HP column (GE Healthcare). The column was equilibrated with 5 column volumes of denaturation buffer, 5 column volumes of elution buffer (50 mM sodium phosphate, pH 7.9 containing 150 mM NaCl, 10 mM imidazole, and 8 M urea), and finally 10 column volumes of denaturation buffer at a

flow rate of 1 mL/min before the sample was applied. 5 mL of MBP-LRR was applied to the column at a rate of 0.25 mL/min. The column was then washed with 5 column volumes of denaturation buffer at a rate of 1 mL/min. Protein was eluted from the column with 3 column volumes of elution buffer. Fractions containing the MBP-LRR were pooled and dialyzed using SnakeSkin Dialysis Tubing 10K MWCO (Thermo Scientific) against 3 L refolding buffer (50 mM Tris pH 8.2 containing 20 mM NaCl, 1mM DTT, 800 μ M KCl, 800 mM arginine, and 5% glycerol) at 4 °C overnight. Refolded protein was dialyzed against 1 L 50 mM sodium phosphate pH 6.5 with 150 mM NaCl for 4 hours at 4 °C.

2.2.7 Characterization of CaCYR1-LRR

2.2.7.1 SDS PAGE Analysis

20 μ L of the protein samples were mixed with 5 μ L 5X SDS Loading Sample Buffer (250 mM TrisHCl pH 6.8, 10% SDS, 30% glycerol, 5% β -mercaptoethanol, 0.02% bromophenol blue) and heated at 100 °C for 5 min. 15 μ L of each sample was loaded onto a 7.5% SDS Gel. 5 μ L of Precision Plus Protein Dual Color Standards (Bio-Rad) was loaded as a control. The gel was run at 200V for 40 min at room temperature. The gel was the stained with Commassie Blue dye and de-stained prior to analysis on a Gel Doc EZ Imager (Bio-Rad).

2.2.7.2 Circular Dichroism (CD)

CD spectra were taken with a JASCO J810 spectropolarimeter with the protein solution contained in a 0.1 cm path length cylindrical cell. Measurement parameters are listed in table 2.1. Fusion constructs were analyzed in 10 mM sodium phosphate

buffer, pH 7.4, containing 50 mM NaCl. The protein sample was allowed to equilibrate to room temperature before being analyzed at 25 °C in the instrument.

Table 2.1 – Experimental parameters for CD experiments

Start	250 nm
End	200 nm
Scanning Speed	20 nm/min
Data pitch	0.2 nm
Bandwidth	1 nm
Accumulation Times	3

2.2.7.3 Protein Mass Spectrometry

Purified MBP-LRR was concentrated to 20 μ M using an Amicon Ultra-0.5 Centrifugal Filter with a 10 kDa MWCO. Precipitate was removed by centrifugation at 15000 rpm for 15 min. The sample was analyzed by LC-MS/MS using a Xevo G2-S QToF equipped with a Waters UPLC

2.2.7.4 pH stability screen

1 mL aliquots of refolded MBP-LRR was dialyzed using SnakeSkin Dialysis Tubing 10K MWCO against 1 L of 50 mM sodium phosphate containing 150 mM NaCl at pH's 5.5, 6.0, 6.5, 7.0, and 7.5 for 4 hours at 4 °C. After dialysis samples were clarified by centrifugation in a table top centrifuge at 15, 000 rpm for 15 min. Samples were run on an SDS-PAGE gel (Materials and Methods 1.2.7.1) and imaged using on a Gel Doc EZ Imager (Bio-Rad). Using the relative quantity tool, the amount of

soluble MBP-LRR at each pH was compared to MBP-LRR in refolding buffer, set to a quantity of 1.00.

2.3 Results

2.3.1 Expression and Purification of GST-LRR

Previously, Xu and colleagues demonstrated the interaction between MDP and the LRR domain of *CaCyr1* through a biotinylated MDP pull-down assay²⁴. In this assay, they used a GST-LRR (aa 480-900) expressed and purified in *E.coli*. However, no experimental procedures were reported for the purification of this construct. Seeking to develop an assay to quantify the affinity of *CaCyr1*-LRR for bacterial derived ligands, attempts were made to express and purify a similar construct.

CaCyr1-LRR was cloned into a pGEX-6p-1 vector, previously used in our lab for expression of the LRR from Nod2, for expression as a fusion protein with an N-terminal GST tag. Initial attempts to purify GST-LRR were unsuccessful, as two prominent impurities were observed when eluting GST-LRR from the column. Size exclusion and ion exchange chromatography were unable to separate GST-LRR from the impurities. The impurities were identified as the molecular chaperones, GroEL and DnaK, through protein mass spectrometry experiments performed by Leila Choe at the Delaware Biotechnology Institute (Figure 2.1). Co-purification of the chaperones is unsurprising as many LRR containing proteins from eukaryotes have been demonstrated to interact with the Sgt1, Hsp70, and Hsp90 chaperone proteins, which are homologous to bacterial DnaK and GroEL²⁹. In fact Sgt1 and Hsp90 are known to interact with Cyr1 in *C. albicans*³⁰. While the interactions with yeast homologs have

biological relevance, the desire to use these proteins in binding assays required the removal of these contaminants. Co-purification of bacterial chaperones with the yeast transcription factor Gal4 expressed in *E.coli*, decreased the ability of this protein to bind DNA³¹. It is likely that the presence of these chaperones could interfere with Cyr1 binding to peptidoglycan fragments by occluding the binding pocket.

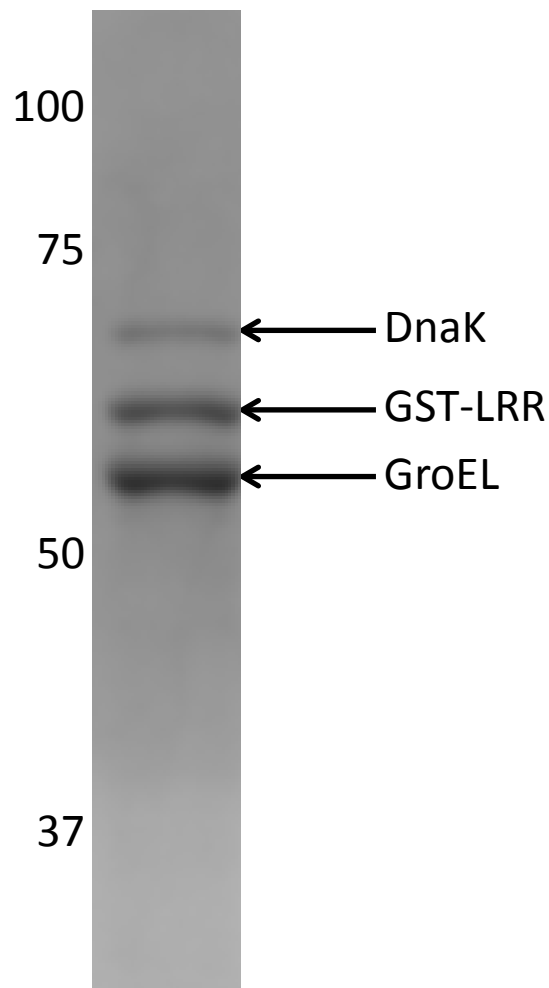
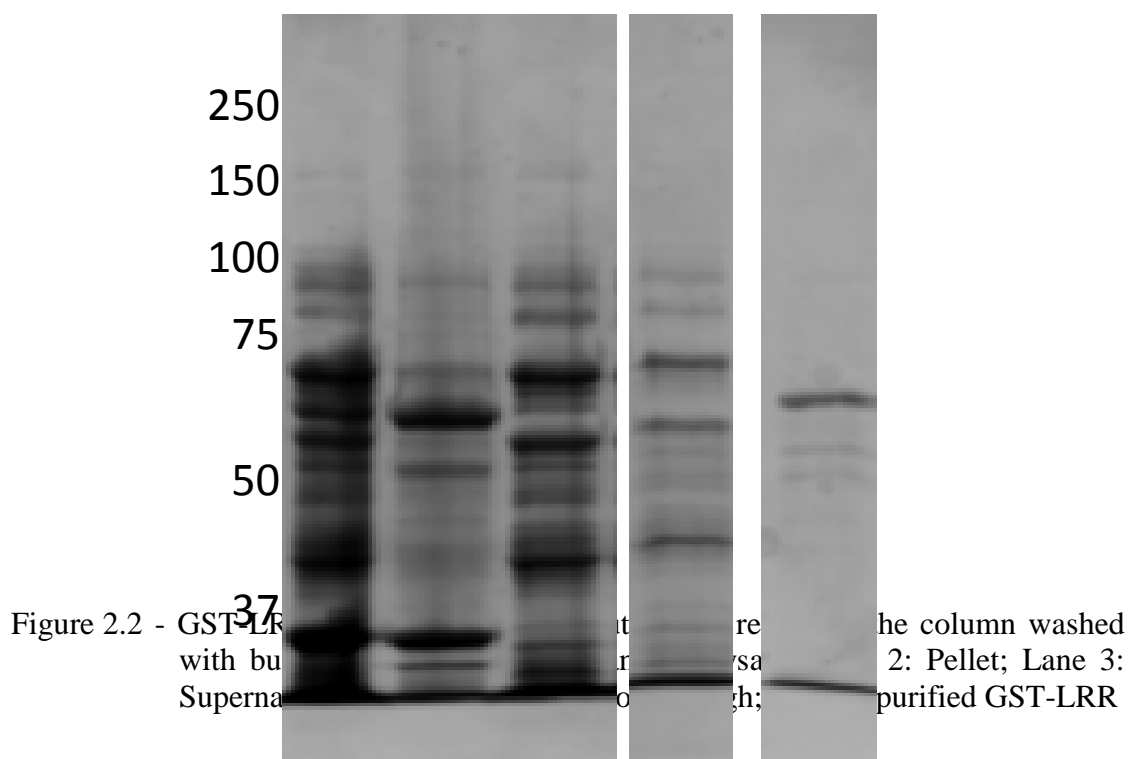


Figure 2.1 - Initial purification of GST-LRR contained two additional protein bands when analyzed by SDS-PAGE. Mass spectrometry identified the impurities as the chaperone proteins, DnaK and GroEL.

To remove the chaperones proteins co-purifying with GST-LRR, a purification method was developed based on the procedure reported by Rohman and Harrison-Lavoieoi³². After clarifying the lysate, a solution of denatured protein was added to the supernatant prior to application to the glutathione resin. Stringent washes containing ATP were performed to remove any chaperones still associating with GST-LRR on the resin (Methods 2.2.4). After eluting with reduced glutathione, pure GST-LRR was obtained at a concentration of 0.5 mg/mL (Figure 2.2). Despite the ability to obtain pure GST-LRR, this purification method proved inefficient, as most of the protein was insoluble and remained in the pellet after lysis.



2.3.2 Expression and Purification of MBP-LRR

To improve the solubility of the LRR protein, the fusion partner was changed from a GST tag to a MBP tag. Maltose binding protein (MBP) has been demonstrated to enhance solubility, improve yield, and promote proper folding of fusion proteins³³. The gene encoding *CaCyr1*-LRR was inserted into a modified pMAL-c5x vector with a his-tag added near the N-terminus of the MBP tag (Methods 1.2.3). The vector was transformed into BL21 RIPL-codon plus cells for protein expression. Although protein expression levels were increased, the MBP fusion partner did not increase solubility of the LRR and much of the protein remained in the pellet.

In order to obtain high yields of MBP-LRR, it was necessary to develop a method to extract the protein from the insoluble fraction. In *E.coli* expression systems, high-levels of recombinant protein expression, like that of MBP-LRR, often cause protein aggregation and inclusion body formation. Recombinant proteins can be recovered by using high concentrations of chaotropic agents, such as urea or guanidine hydrochloride, to solubilize the inclusion body³⁴. Despite adequately solubilizing the protein, the high concentrations of chaotropes resulted in the denaturation of the protein. Refolding the proteins can often prove difficult as the aggregation can reoccur when the chaotrope is removed. Leaving small amounts of the chaotrope or adding detergent has been shown to help in reducing aggregation. Additionally, high concentrations of arginine suppress aggregation during protein refolding, although the mechanism by which this occurs is unknown³⁵.

Modifying a protocol reported by Richard Burgess³⁶, inclusion bodies containing MBP-LRR were obtained from the insoluble fraction of the *E. coli* lysate. Briefly, the insoluble pellet was suspended in lysis buffer containing 1% Triton X-100 to solubilize and remove contaminating membrane proteins and the samples was re-pelleted. After washing to remove residual detergent, the inclusion body was suspended in 8 M urea to solubilize the MBP-LRR (Figure 2.3).

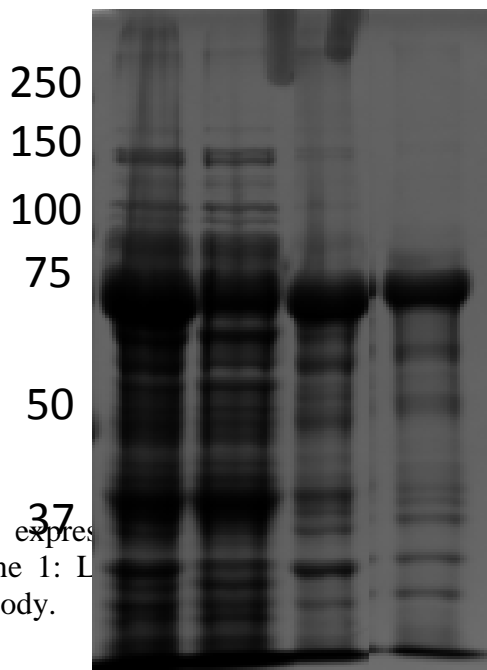
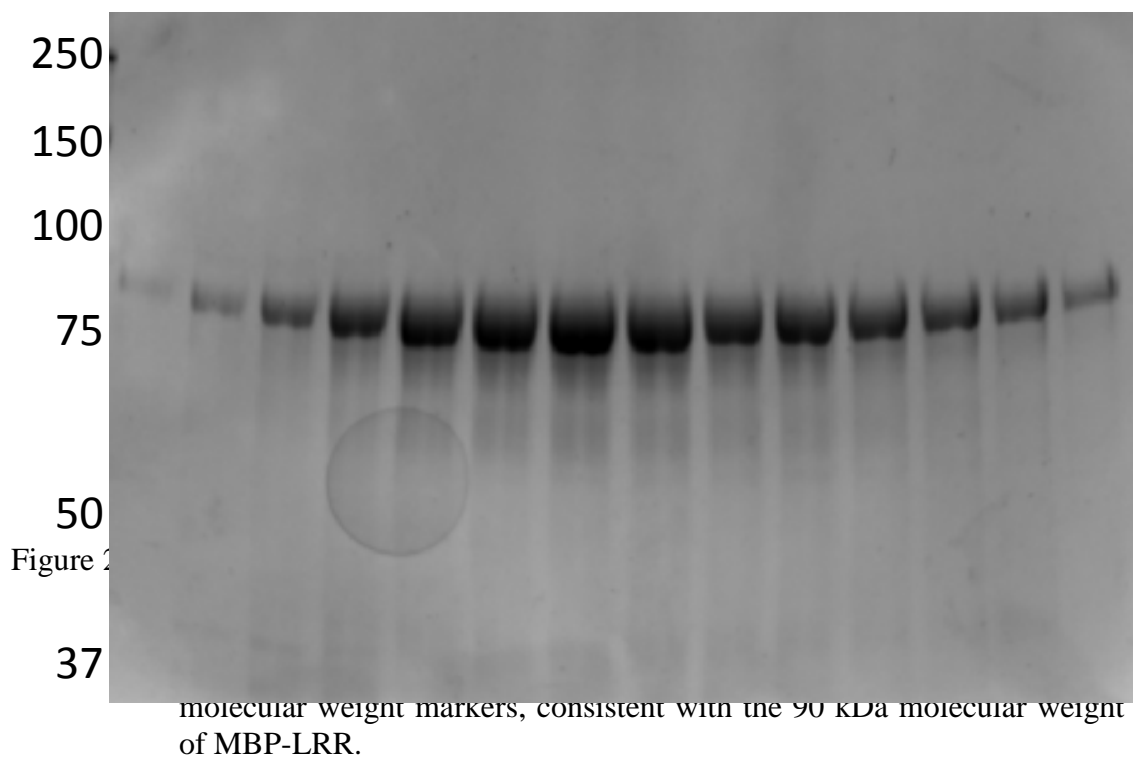


Figure 2.3 - MBP-LRR expression and formation of inclusion bodies. Lane 1: Lysate; Lane 2: Supernatant; Lane 3: Pellet; Lane 4: Inclusion Body.

Following isolation and solubilization of the inclusion body, denatured MBP-LRR was further purified by metal affinity chromatography. Briefly, using a BioRad Quest NGC FPLC system, the denatured MBP-LRR was applied to a Ni-NTA column. The column was washed with buffer containing low concentrations of imidazole to remove non-specific binders. Finally, the MBP-LRR was eluted using an imidazole gradient increasing concentration from 10 mM to 500 mM. Fractions containing protein based on A_{280} , were analyzed by SDS-PAGE (Figure 2.4). Fractions containing MBP-LRR were combined and dialyzed over night against refolding buffer, containing high arginine concentrations to assist refolding and suppress aggregation.



2.3.3 Characterization of GST-LRR

After obtaining pure GST-LRR, circular dichroism (CD) was performed to determine if the protein was folded. GST-LRR was dialyzed in to CD buffer (10 mM sodium phosphate, 50 mM NaCl, pH 7.4). A 3 μ M solution of GST-LRR was used to obtain a CD spectrum (Figure 2.5). Concentration was determined by direct UV absorbance at 280 nm using an aliquot of protein denatured with urea ($\epsilon = 67730 \text{ M}^{-1} \text{ cm}^{-1}$). Analysis of the spectrum using the K2D3 webserver predicts 66.1% α -helical and 11.0% β -strand secondary structure in the protein³⁷. This is consistent with helical

structures commonly observed on the convex surface of other LRR containing proteins²².

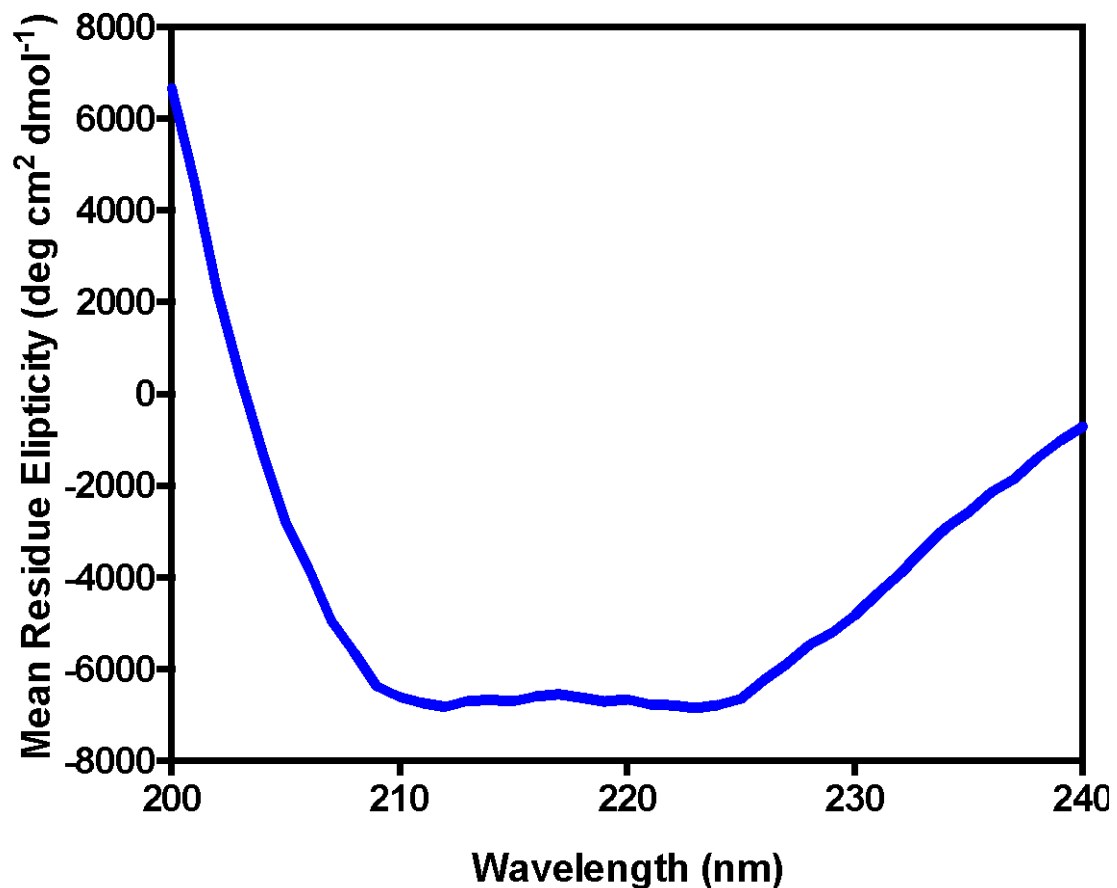


Figure 2.5 - A circular dichroism spectrum of 3 μ M GST-LRR in 10 mM sodium phosphate buffer, pH 7.4, containing 50 mM NaCl was obtained using a JASCO J810 spectropolarimeter. The observed spectrum is the result of the accumulation of 3 scans. Analysis by the K2D3³⁷ webserver predicts 66.1% α -helical and 11.0% β -strand secondary structure.

2.3.4 Characterization of MBP-LRR

2.3.4.1 Circular Dichroism

To confirm that MBP-LRR refolded into the proper conformation, CD spectra was obtained for the refolded protein, as well as MBP-purified from the soluble fraction of the *E. coli* lysate. Refolded and soluble MBP-LRRs were dialyzed against CD buffer (10 mM sodium phosphate, 50 mM NaCl, pH 7.4) and CD spectra were obtained. Molar concentration was determined by direct UV absorbance at 280 nm using an aliquot of protein denatured with urea ($\epsilon = 91595 \text{ M}^{-1} \text{ cm}^{-1}$). Analysis of the spectrum using the K2D3 webserver predicts 60.3% α -helical and 16.7% β -strand secondary structure in both the soluble and refolded MBP-LRR, indicating that the native structure had been achieved after refolding.

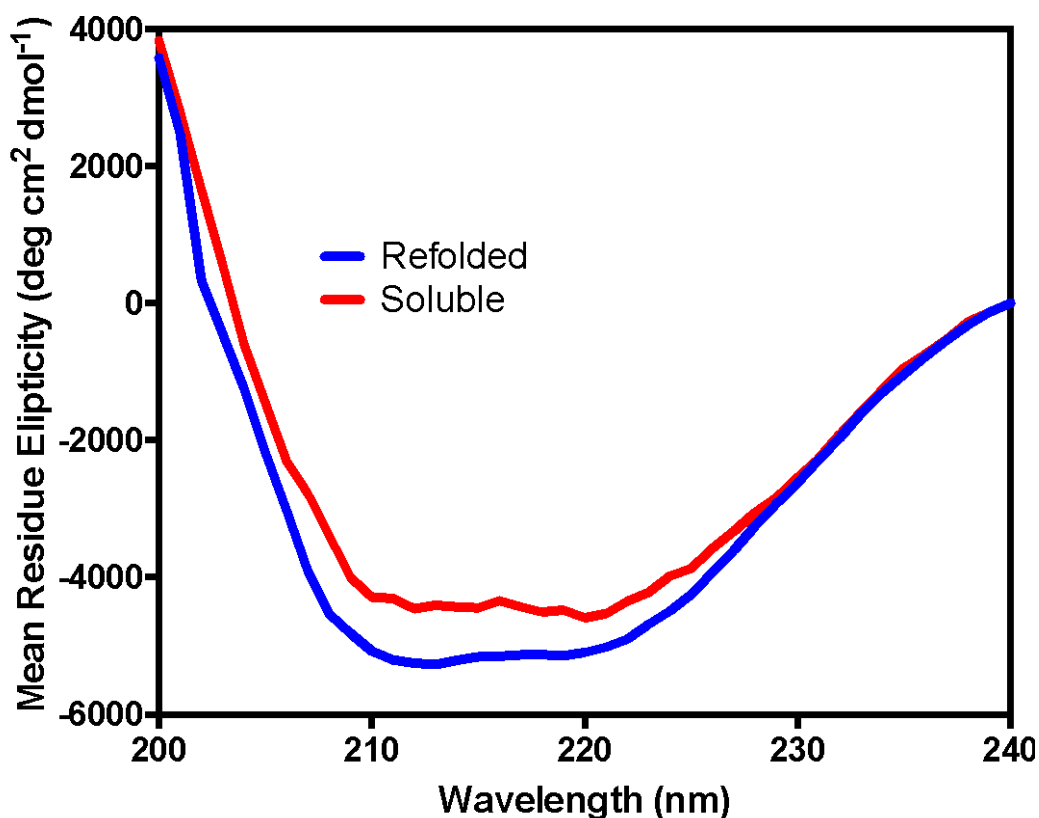


Figure 2.6 - CD spectra for MBP-LRR obtained from the soluble lysate fraction (red) and refolded MBP-LRR (blue). The observed spectra are the result of the accumulation of 3 scans. Mean residue ellipticity at 240 nm was normalized to 0. Analysis using the K2D3 webserver predicts 60.3% α -helical and 16.7% β -strand secondary structure for both the soluble and refolded LRR, indicating the proper conformation was obtained after refolding.

2.3.4.2 Mass Spectrometry Identification of MBP-LRR

Intact mass spectrometry was used to confirm the identity of MBP-LRR. Refolded MBP-LRR in CD buffer was concentrated to 20 μ M using an Amicon spin filter. The sample was analyzed by LC-MS/MS on a Xevo Q-TOF mass spec equipped with a UPLC column. The obtained spectra (Figure 2.7) contained a prominent peak at

91,030 Da, which correlates to the predicted molecular weight of MBP-LRR (91,048 Da) minus water ($M^+ - 18$).

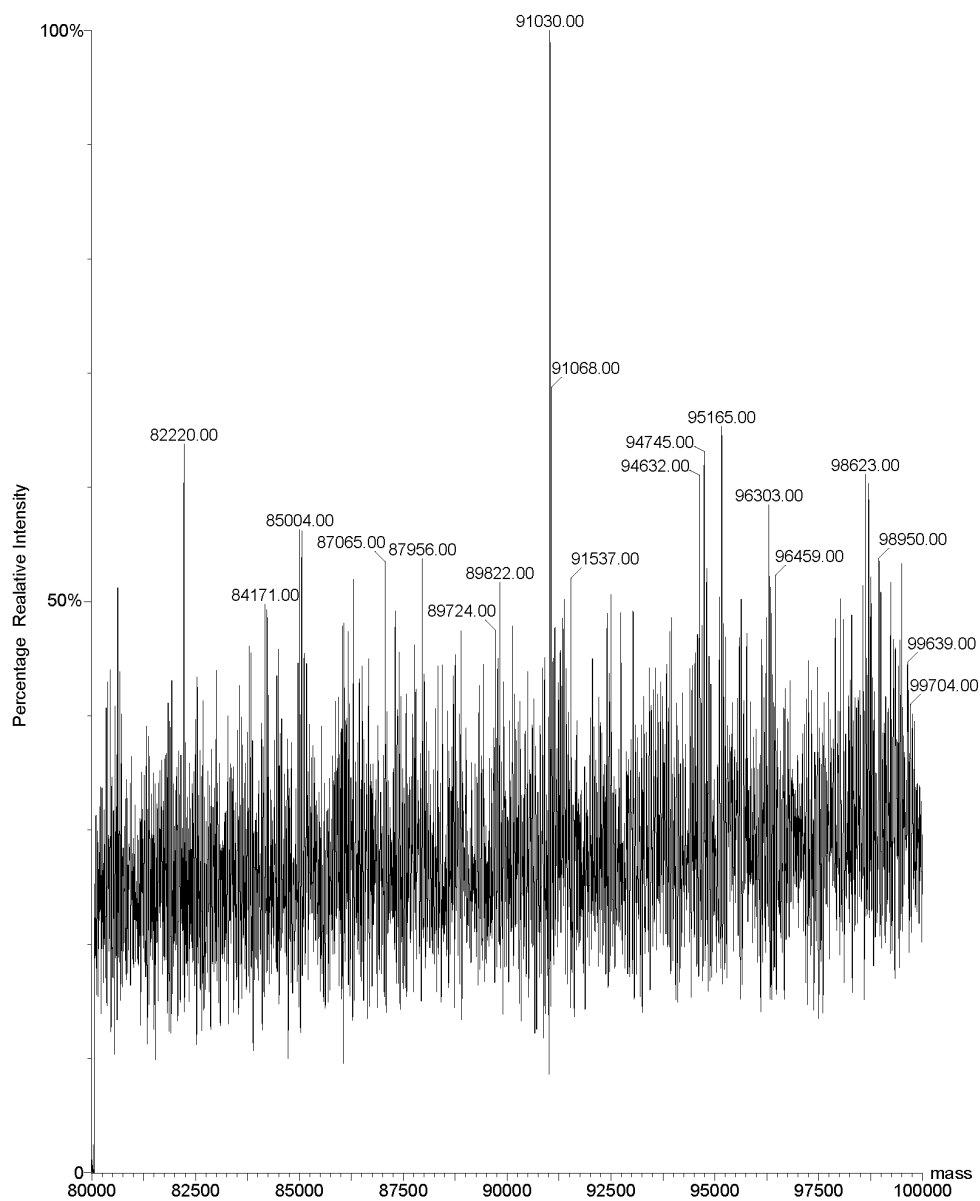


Figure 2.7 - Intact protein mass spectrometry analysis of MBP-LRR. Predicted mass: 91,048 Da, Observed: 91,030 Da

2.3.4.3 MBP-LRR is Unstable in Acidic Conditions

After refolding, purified MBP-LRR was dialyzed into phosphate buffers at pH's 5.5, 6.0, 6.5, 7.0, and 7.5 (Materials and Methods 2.2.7.4). After clarification by centrifugation, soluble fractions were analyzed by SDS-PAGE (Figure 2.8). Compared to MBP-LRR in refolding buffer, protein in acidic buffers showed high amounts of aggregation as only 2% and 7% of the protein remained soluble at pH's 5.0 and 6.0, respectively. Increased solubility was observed when the protein was dialyzed into buffers at pH 6.5, 40% soluble protein, or greater. At pH 7.0 and 7.5 greater than 50% of the protein remained in the soluble fraction.

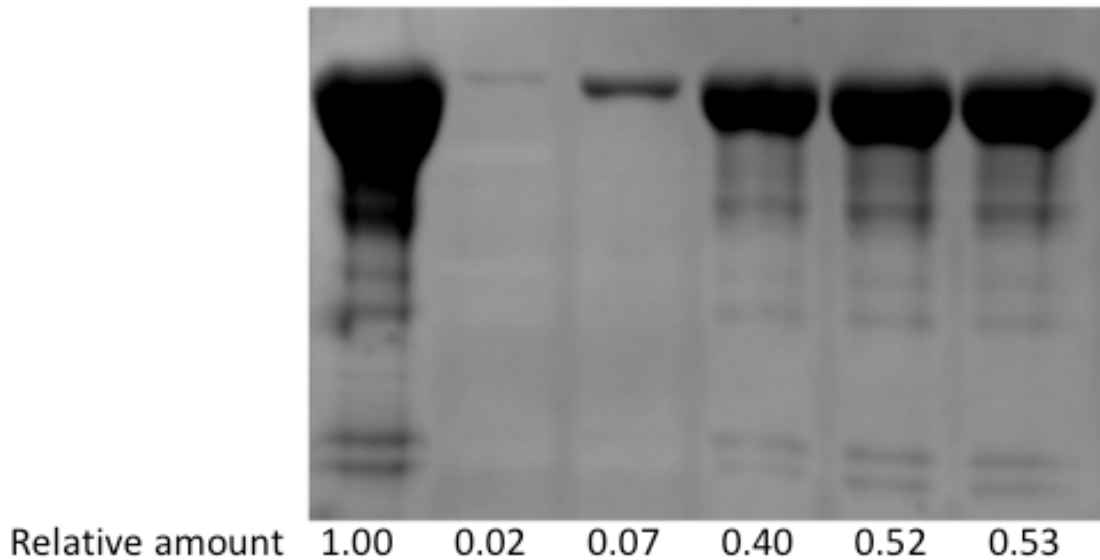


Figure 2.8 – After refolding MBP-LRR aggregates when dialyzed against acidic buffers. Lane 1: Refolding buffer; Lane 2: pH 5.5; Lane 3: pH 6.0; Lane 4: pH 6.5; Lane 5: pH 7.0; Lane 6: pH 7.5

2.4 Conclusion

In order to develop a quantitative assay to characterize the interaction between Cyr1 and peptidoglycan fragments, it was first necessary to find a source of recombinant LRR. With Wang and colleagues previously reporting the use a GST-LRR fusion protein in an enrichment assay²⁴, initial attempts were focused on purifying the same construct. Amino acids 480-900 of Cyr1 were cloned into a pGEX-6p-1 vector and expressed in an *E. coli* system. The initial purification protocol was able to obtain the LRR fusion domain, but two prominent impurities were observed. Through mass spectrometry analysis, these impurities were later identified as the chaperone proteins, GroEl and DnaK. An improved protocol including incubation with denatured proteins and stringent ATP washes was capable of removing the chaperone proteins. As demonstrated by CD, the purified protein showed secondary structure consistent with the predicted structure. Despite obtaining pure protein, yields were low as much of the expressed protein remained in the insoluble fraction. Trials to optimize solubility, including altering expression conditions – time, temperature, and inducer concentration – and the inclusion of detergents in purification buffers, proved unsuccessful.

In order to obtain the LRR in higher yields, the fusion partner was switched from a GST to a MBP tag. Compared to GST tags, MBP tags have been demonstrated increase the soluble fraction of proteins by as much as 50%³⁸. To this end, the LRR was cloned into pMAL-C5X vector modified to include a hexahistidine tag inserted between residues 3 and 4 of the maltose binding protein²⁷. Despite the addition of the MBP fusion partner, a large fraction of the LRR remained in the insoluble pellet.

High level expression of recombinant proteins in *E.coli*, can lead to aggregation and the formation of insoluble inclusion bodies³⁹. This is not an uncommon occurrence when expressing LRRs, as there have been several reports of purifications of LRR containing proteins from inclusion bodies⁴⁰⁻⁴². The inclusion bodies were isolated and solubilized with 8 M urea. The solubilized proteins were purified using a Ni-NTA column attached to an FPLC system. Fractions containing purified LRR were then dialyzed into a buffer with high concentrations of arginine – thought to promote refolding by inhibiting aggregation³⁵ - to refold the protein. CD analysis illustrated the protein regained the same secondary structure as MBP-LRR purified from the soluble fractions.

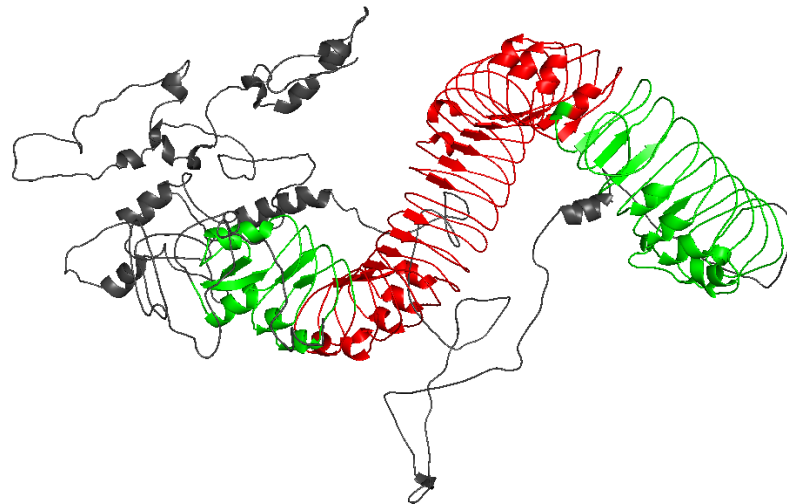


Figure 2.9 – Homology model of Cyr1 created using the I-TASSER database using Arabidopsis FLS2 (PDB ID: 4MN8A) as a template⁴³. Residues 480-900 (red) indicate the predicted LRR domain from the SMART database. Residues 370 -1135 (green) show secondary characteristics that could be important in protein folding.

Efforts are being made to increase the solubility of this protein. Analysis of LRR domain refolding has identified N-terminal capping motifs that promote folding and inhibit aggregation by shielding the hydrophobic face of the LRR domain⁴⁴⁻⁴⁵. Additionally Courtemacne and Barrick demonstrated that LRR folding proceeds via an N-terminal pathway and deleting the first LRR repeat slows the rate of folding⁴⁶. Based on homology modeling performed by I-TASSER⁴³ (Figure 2.9), it appears that the purified LRR construct may be missing the first repeat or the capping motifs. Currently residues 480-900 have been expressed and purified, based on the homology model it appears that 3 alpha helices on the N-terminal may be truncated. In addition to the importance of the first LRR, deletion of the first 18 residues preceding the repeat have been demonstrated to decrease the stability of the domain⁴⁵. To try to increase stability of the LRR, constructs expressing residues 370-1135 are being prepared. A complication to expressing in *E.coli* is the lack of post-translation modifications. In *C. albicans* post-translation modification of Slr1 affects hyphae formations⁴⁷. It is possible the post-translation modification are important for the function of Cyr1. To this end, vectors are being prepared to express the LRR domain in a *Saccharomyces cerevisiae* expression system.

In this chapter I report two methods for obtaining recombinant Cyr1- LRR from *E. coli* sources. These methods can be used to elucidate the structure of the LRR domain and lead to the development of novel therapeutics to treat *C. albicans* infections. Additionally these methods can act as a guide to purify other LRR domains capable of binding peptidoglycan in *E. coli*.

REFERENCES

1. Seed, P. C., The human mycobiome. *Cold Spring Harb Perspect Med* **2014**, *5* (5), a019810. DOI: 10.1101/cshperspect.a019810.
2. Sobel, J. D., Vaginitis. *N Engl J Med* **1997**, *337* (26), 1896-903. DOI: 10.1056/NEJM199712253372607.
3. Cleveland, A. A.; Farley, M. M.; Harrison, L. H.; Stein, B.; Hollick, R.; Lockhart, S. R.; Magill, S. S.; Derado, G.; Park, B. J.; Chiller, T. M., Changes in incidence and antifungal drug resistance in candidemia: results from population-based laboratory surveillance in Atlanta and Baltimore, 2008-2011. *Clin Infect Dis* **2012**, *55* (10), 1352-61. DOI: 10.1093/cid/cis697.
4. Soll, D. R., High-frequency switching in *Candida albicans*. *Clin Microbiol Rev* **1992**, *5* (2), 183-203.
5. Zhu, W.; Filler, S. G., Interactions of *Candida albicans* with epithelial cells. *Cell Microbiol* **2010**, *12* (3), 273-82. DOI: 10.1111/j.1462-5822.2009.01412.x.
6. Sudbery, P. E., Growth of *Candida albicans* hyphae. *Nature reviews. Microbiology* **2011**, *9* (10), 737-48. DOI: 10.1038/nrmicro2636.
7. Shapiro, R. S.; Robbins, N.; Cowen, L. E., Regulatory circuitry governing fungal development, drug resistance, and disease. *Microbiology and molecular biology reviews : MMBR* **2011**, *75* (2), 213-67. DOI: 10.1128/membr.00045-10.
8. Brown, A. J.; Gow, N. A., Regulatory networks controlling *Candida albicans* morphogenesis. *Trends in microbiology* **1999**, *7* (8), 333-8.
9. Morici, P.; Fais, R.; Rizzato, C.; Tavanti, A.; Lupetti, A., Inhibition of *Candida albicans* Biofilm Formation by the Synthetic Lactoferricin Derived Peptide hLF1-11. *PloS one* **2016**, *11* (11), e0167470. DOI: 10.1371/journal.pone.0167470.
10. Hogan, D. A.; Sundstrom, P., The Ras/cAMP/PKA signaling pathway and virulence in *Candida albicans*. *Future microbiology* **2009**, *4* (10), 1263-70. DOI: 10.2217/fmb.09.106.

11. Jung, W. H.; Stateva, L. I., The cAMP phosphodiesterase encoded by CaPDE2 is required for hyphal development in *Candida albicans*. *Microbiology* **2003**, *149* (Pt 10), 2961-76. DOI: 10.1099/mic.0.26517-0.
12. Rocha, C. R.; Schroppel, K.; Harcus, D.; Marcil, A.; Dignard, D.; Taylor, B. N.; Thomas, D. Y.; Whiteway, M.; Leberer, E., Signaling through adenylyl cyclase is essential for hyphal growth and virulence in the pathogenic fungus *Candida albicans*. *Mol Biol Cell* **2001**, *12* (11), 3631-43.
13. Wang, Y., Fungal adenylyl cyclase acts as a signal sensor and integrator and plays a central role in interaction with bacteria. *PLoS Pathog* **2013**, *9* (10), e1003612. DOI: 10.1371/journal.ppat.1003612.
14. Davis-Hanna, A.; Piispanen, A. E.; Stateva, L. I.; Hogan, D. A., Farnesol and dodecanol effects on the *Candida albicans* Ras1-cAMP signalling pathway and the regulation of morphogenesis. *Mol Microbiol* **2008**, *67* (1), 47-62. DOI: 10.1111/j.1365-2958.2007.06013.x.
15. Shapiro, R. S.; Uppuluri, P.; Zaas, A. K.; Collins, C.; Senn, H.; Perfect, J. R.; Heitman, J.; Cowen, L. E., Hsp90 orchestrates temperature-dependent *Candida albicans* morphogenesis via Ras1-PKA signaling. *Curr Biol* **2009**, *19* (8), 621-9. DOI: 10.1016/j.cub.2009.03.017.
16. Leberer, E.; Harcus, D.; Dignard, D.; Johnson, L.; Ushinsky, S.; Thomas, D. Y.; Schroppel, K., Ras links cellular morphogenesis to virulence by regulation of the MAP kinase and cAMP signalling pathways in the pathogenic fungus *Candida albicans*. *Mol Microbiol* **2001**, *42* (3), 673-87.
17. Schultz, J.; Copley, R. R.; Doerks, T.; Ponting, C. P.; Bork, P., SMART: a web-based tool for the study of genetically mobile domains. *Nucleic acids research* **2000**, *28* (1), 231-4.
18. Fang, H. M.; Wang, Y., RA domain-mediated interaction of Cdc35 with Ras1 is essential for increasing cellular cAMP level for *Candida albicans* hyphal development. *Mol Microbiol* **2006**, *61* (2), 484-96. DOI: 10.1111/j.1365-2958.2006.05248.x.
19. Maidan, M. M.; De Rop, L.; Serneels, J.; Exler, S.; Rupp, S.; Tournu, H.; Thevelein, J. M.; Van Dijck, P., The G protein-coupled receptor Gpr1 and the Galpha protein Gpa2 act through the cAMP-protein kinase A pathway to induce morphogenesis in *Candida albicans*. *Mol Biol Cell* **2005**, *16* (4), 1971-86. DOI: 10.1091/mbc.e04-09-0780.

20. Hall, R. A.; Turner, K. J.; Chaloupka, J.; Cottier, F.; De Sordi, L.; Sanglard, D.; Levin, L. R.; Buck, J.; Muhlschlegel, F. A., The quorum-sensing molecules farnesol/homoserine lactone and dodecanol operate via distinct modes of action in *Candida albicans*. *Eukaryot Cell* **2011**, *10* (8), 1034-42. DOI: 10.1128/EC.05060-11.
21. Klengel, T.; Liang, W. J.; Chaloupka, J.; Ruoff, C.; Schroppel, K.; Naglik, J. R.; Eckert, S. E.; Mogensen, E. G.; Haynes, K.; Tuite, M. F.; Levin, L. R.; Buck, J.; Muhlschlegel, F. A., Fungal adenylyl cyclase integrates CO₂ sensing with cAMP signaling and virulence. *Curr Biol* **2005**, *15* (22), 2021-6. DOI: 10.1016/j.cub.2005.10.040.
22. Bella, J.; Hindle, K. L.; McEwan, P. A.; Lovell, S. C., The leucine-rich repeat structure. *Cell Mol Life Sci* **2008**, *65* (15), 2307-33. DOI: 10.1007/s00018-008-8019-0.
23. Ng, A.; Xavier, R. J., Leucine-rich repeat (LRR) proteins: integrators of pattern recognition and signaling in immunity. *Autophagy* **2011**, *7* (9), 1082-4.
24. Xu, X. L.; Lee, R. T.; Fang, H. M.; Wang, Y. M.; Li, R.; Zou, H.; Zhu, Y.; Wang, Y., Bacterial peptidoglycan triggers *Candida albicans* hyphal growth by directly activating the adenylyl cyclase Cyr1p. *Cell Host Microbe* **2008**, *4* (1), 28-39. DOI: 10.1016/j.chom.2008.05.014.
25. Fraiture, M.; Baxter, R. H. G.; Steinert, S.; Chelliah, Y.; Frolet, C.; Quispes-Tintaya, W.; Hoffmann, J. A.; Blandin, S. A.; Levashina, E. A., Two Mosquito LRR Proteins Function as Complement Control Factors in the TEP1-Mediated Killing of Plasmodium. *Cell Host & Microbe* **2009**, *5* (3), 273-284. DOI: <https://doi.org/10.1016/j.chom.2009.01.005>.
26. Afzal, A. J.; Lightfoot, D. A., Soybean disease resistance protein RHG1-LRR domain expressed, purified and refolded from *Escherichia coli* inclusion bodies: Preparation for a functional analysis. *Protein Expression and Purification* **2007**, *53* (2), 346-355. DOI: <https://doi.org/10.1016/j.pep.2006.12.017>.
27. Liu, J.; Srinivasan, P.; Pham, D. N.; Rozovsky, S., Expression and purification of the membrane enzyme selenoprotein K. *Protein Expr Purif* **2012**, *86* (1), 27-34. DOI: 10.1016/j.pep.2012.08.014.
28. Looke, M.; Kristjuhan, K.; Kristjuhan, A., Extraction of genomic DNA from yeasts for PCR-based applications. *Biotechniques* **2011**, *50* (5), 325-8. DOI: 10.2144/000113672.
29. Stuttmann, J.; Parker, J. E.; Noël, L. D., Staying in the fold. *Plant Signaling & Behavior* **2008**, *3* (5), 283-285. DOI: 10.4161/psb.3.5.5576.

30. Shapiro, R. S.; Zaas, A. K.; Betancourt-Quiroz, M.; Perfect, J. R.; Cowen, L. E., The Hsp90 co-chaperone Sgt1 governs *Candida albicans* morphogenesis and drug resistance. *PLoS one* **2012**, *7* (9), e44734. DOI: 10.1371/journal.pone.0044734.
31. Sun, L.; Kodadek, T., Removal of impurities from transcription factor preparations that alter their DNA-binding properties. *Nucleic acids research* **2002**, *30* (16), e88.
32. Rohman, M.; Harrison-Lavoie, K. J., Separation of copurifying GroEL from glutathione-S-transferase fusion proteins. *Protein Expr Purif* **2000**, *20* (1), 45-7. DOI: 10.1006/prep.2000.1271.
33. Sun, P.; Tropea, J. E.; Waugh, D. S., Enhancing the Solubility of Recombinant Proteins in *Escherichia coli* by Using Hexahistidine-Tagged Maltose-Binding Protein as a Fusion Partner. In *Heterologous Gene Expression in E.coli: Methods and Protocols*, Evans, J. T. C.; Xu, M.-Q., Eds. Humana Press: Totowa, NJ, 2011; pp 259-274. DOI: 10.1007/978-1-61737-967-3_16.
34. Singh, A.; Upadhyay, V.; Panda, A. K., Solubilization and refolding of inclusion body proteins. *Methods Mol Biol* **2015**, *1258*, 283-91. DOI: 10.1007/978-1-4939-2205-5_15.
35. Tsumoto, K.; Umetsu, M.; Kumagai, I.; Ejima, D.; Philo, J. S.; Arakawa, T., Role of arginine in protein refolding, solubilization, and purification. *Biotechnology progress* **2004**, *20* (5), 1301-8. DOI: 10.1021/bp0498793.
36. Burgess, R. R., Refolding solubilized inclusion body proteins. *Methods Enzymol* **2009**, *463*, 259-82. DOI: 10.1016/s0076-6879(09)63017-2.
37. Louis-Jeune, C.; Andrade-Navarro, M. A.; Perez-Iratxeta, C., Prediction of protein secondary structure from circular dichroism using theoretically derived spectra. *Proteins* **2012**, *80* (2), 374-81. DOI: 10.1002/prot.23188.
38. Raran-Kurussi, S.; Waugh, D. S., The ability to enhance the solubility of its fusion partners is an intrinsic property of maltose-binding protein but their folding is either spontaneous or chaperone-mediated. *PLoS one* **2012**, *7* (11), e49589. DOI: 10.1371/journal.pone.0049589.
39. Singh, A.; Upadhyay, V.; Upadhyay, A. K.; Singh, S. M.; Panda, A. K., Protein recovery from inclusion bodies of *Escherichia coli* using mild solubilization process. *Microb Cell Fact* **2015**, *14*, 41. DOI: 10.1186/s12934-015-0222-8.

40. Guo, Y.; Bian, W.; Zhang, Y.; Li, H., Expression in Escherichia coli, purification and characterization of LRSAM1, a LRR and RING domain E3 ubiquitin ligase. *Protein Expr Purif* **2017**, *129*, 158-161. DOI: 10.1016/j.pep.2016.05.002.
41. Yang, L.; Hansen Falkesgaard, M.; Thulstrup, P. W.; Walmod, P. S.; Lo Leggio, L.; Krigaars Rasmussen, K., Expression, refolding and spectroscopic characterization of fibronectin type III (FnIII)-homology domains derived from human fibronectin leucine rich transmembrane protein (FLRT)-1, -2, and -3. *PeerJ* **2017**, *5*, e3550. DOI: 10.7717/peerj.3550.
42. Afzal, A. J.; Lightfoot, D. A., Soybean disease resistance protein RHG1-LRR domain expressed, purified and refolded from Escherichia coli inclusion bodies: preparation for a functional analysis. *Protein Expr Purif* **2007**, *53* (2), 346-55. DOI: 10.1016/j.pep.2006.12.017.
43. Yang, J.; Yan, R.; Roy, A.; Xu, D.; Poisson, J.; Zhang, Y., The I-TASSER Suite: protein structure and function prediction. *Nat Methods* **2015**, *12* (1), 7-8. DOI: 10.1038/nmeth.3213.
44. Stumpp, M. T.; Forrer, P.; Binz, H. K.; Plückthun, A., Designing Repeat Proteins: Modular Leucine-rich Repeat Protein Libraries Based on the Mammalian Ribonuclease Inhibitor Family. *Journal of Molecular Biology* **2003**, *332* (2), 471-487. DOI: 10.1016/s0022-2836(03)00897-0.
45. Dao, T. P.; Majumdar, A.; Barrick, D., Capping motifs stabilize the leucine-rich repeat protein PP32 and rigidify adjacent repeats. *Protein science : a publication of the Protein Society* **2014**, *23* (6), 801-11. DOI: 10.1002/pro.2462.
46. Courtemanche, N.; Barrick, D., The leucine-rich repeat domain of Internalin B folds along a polarized N-terminal pathway. *Structure* **2008**, *16* (5), 705-14. DOI: 10.1016/j.str.2008.02.015.
47. Ariyachet, C.; Beissel, C.; Li, X.; Lorrey, S.; Mackenzie, O.; Martin, P. M.; O'Brien, K.; Pholcharee, T.; Sim, S.; Krebber, H.; McBride, A. E., Post-translational modification directs nuclear and hyphal tip localization of *Candida albicans* mRNA-binding protein Slr1. *Mol Microbiol* **2017**, *104* (3), 499-519. DOI: 10.1111/mmi.13643.

Chapter 3

BACTERIAL DERIVED CARBOHYDRATES TRIGGER HYPHAE FORMATION IN *C. ALBICANS*

3.1 Introduction

The human body is host to a diverse ecosystem containing trillions of microorganisms collectively referred to as the microbiome. At any given time, it is estimated that over one thousand unique bacterial species can be found in and on the human body¹. Since the launch of the NIH's human microbiome project in 2008, studies examining the effect of these bacteria on human health have become prevalent in the literature²⁻⁴. Alterations in composition of the microbiome have been implicated in the progression of diseases including cancer, asthma, inflammatory bowel disease, and diabetes^{3, 5-7}. With established connections to multiple disease states, it is easy to see why a focus has been placed on understanding how bacterial populations' effect human health.

While the importance of the bacterial species present in the microbiome can not be overstated, there is a smaller yet not less significant population of fungal species, the mycobiome, whose impact on health has only recently began to be understood⁸. Similar to bacteria, both beneficial and malignant effects have been observed. *Saccharomyces boulardii* has been demonstrated to provide relief of gastroenteritis and has been used as a probiotic to prevent gastrointestinal disorders⁹. Unfortunately, alterations in the composition mycobiome have been implicated in the

progression of Crohn's Disease and cancer¹⁰⁻¹¹. Interestingly, fluctuations in the mycobiome are often correlated to changes in bacterial populations. In Crohn's disease, when compared to healthy family members, patients have increased levels of the fungus *Candida tropicalis* and increased concentrations of the bacterial species *E. coli* and *Serratia marcescens*¹². In oral tumors, increases in *Aspergillus* are correlated to decreases in *Actinomyces*, *Prevtoella*, and *Streptococcus*¹³. With correlations observed in several diseases, it is important to understand how fungi and bacteria are recognizing each other in the human body.

Although normally commensal, *Candida albicans* is the most common human fungal pathogen¹⁴. Interestingly, interactions between this fungi and bacteria have been linked rates of *C. albicans* infections¹⁵. Certain species of bacteria can also promote co-infections demonstrated by the isolation of mixed biofilms from clinical isolates. *Pseudomonas aeruginosa* is commonly identified with *C. albicans* in hospital acquired infections¹⁶⁻¹⁷. Other species identified in mixed biofilms with *C. albicans* include *Staphylococcus epidermis*¹⁸, *Staphylococcus aureus*, and *Streptococcus mutans*¹⁸⁻²⁰. *C. albicans* not only form mixed biofilms with bacteria but can also regulate their populations. After antibiotic treatment, *C. albicans* promote the recovery of *Bacteroidetes* and *Enterococcus faecallis*, while inhibiting *Lactobacillus*^{15,21}. To elucidate the role in disease states, it is necessary to understand how *C. albicans* is recognizing its bacterial neighbors.

Like most microorganisms, *C. albicans* can recognize and respond to the presence of quorum sensing molecules²². *Pseudomonas aeruginosa* produces 3-oxo-C₁₂-homoserine lactone inhibits Cyr1 activity. This leads to inhibition of hyphae

formation and ultimately stops *C. albicans* invasion of epithelial cells²³. However, quorum-sensing molecules are not the only bacterial derived compounds capable of effecting *C. albicans* morphology. In a seminal 2008 publication, Wang and colleagues reported peptidoglycan fragments were capable of causing hyphae growth²⁴. Similar to the human innate immune receptor, Nod2, Cyr1 binds muramyl dipeptide via a leucine rich repeat domain.

Intrigued by the finding that *C. albicans* can recognize pathogen-associated molecular patterns using a similar mechanism as humans, we sought to identify other bacterial derived products that can effect hyphae formation. In this chapter, I discuss the development of three assays to determine the effects of peptidoglycan fragments and bacterial natural products on *C. albicans* morphology. A brightfield microscopy assay was used to determine hyphae formation, RT-PCR was used to examine expression levels of hyphae-specific genes, and an ELISA assay was employed to determine direct effects on the cAMP-PKA pathway.

3.2 Materials and Methods

3.2.1 Materials

All chemicals were purchased unless otherwise noted. Compounds **3.01-3.09** and **3.12** were synthesized by Dr. James Melnyk²⁵. Siavash Mashayekh synthesized **3.17**²⁶. Full characterization details for these molecules can be found in the related publication. Compound **3.16** was purchased from BAchem and compound **3.18** was purchased from CaymenChem. The cAMP Biotrack EIA system was purchased from GE Life Sciences. RNeasy Mini Kit and QuantiTect Reverse Transcription Kit were

purchased from Qiagen. SsoAdvanced universal SYBR Green supermix was purchased from Bio-Rad. Primers for qPCR reactions were synthesized by Eurofins genomics. qPCR reactions were performed on a 7300 Real-Time PCR System from Applied Biosystems.

3.2.2 Hyphae Growth Assay

3.2.2.1 Initial Screen

5 mL of YPD media was inoculated with *C. albicans*, stored as a glycerol stock at -80 °C. The culture was incubated at 30 °C overnight, while shaking at 200 rpm. The next day 3 µL of the *C. albicans* culture was diluted into 285 µL fresh YPD. 15 µL of the 20 mM stocks of each compound (Figure 3.A) were added for a final concentration of 1 mM. The cultures were then incubated overnight at 37 °C, while shaking at 200 rpm. 3 µL of each culture was imaged using bright field microscopy at 40x magnification to examine for the presence of hyphal growth.

3.2.2.2 Quantification of Hyphae Growth

5 mL of YPD media was inoculated with *C. albicans*, stored as a glycerol stock at -80 °C. The culture was incubated at 30 °C overnight, while shaking at 200 rpm. The next day cells were harvest by centrifugation at 150 g x 3 minutes. *C. albicans* cells were washed three times with 5 mL of PBS. Cell pellets were suspended in 5 mL fresh YPS and 10% FBS, 10 mM MTP (**3.17**), 10 mM MDP (**3.16**), 10 mM doxorubicin (**3.15**), or 10 mM daunosamine (**3.13**) was added to 900 µL *C. albicans* cultures. The cultures were grown overnight at 37 °C, while shaking at 200 rpm. 3 µL of each culture was imaged using bright field microscopy at 40x magnification.

Images containing approximately 100 cells were sent to Dennis Wykoff (Villanova University) to score for hyphae formation. Images were scored blindly, i.e. the treating compounds were not identified, to avoid bias. Hyphae formation was reported as a percentage of cells displaying hyphae characteristics compared to total number of cells. Percentages are the average of two independent trails for each compound.

3.2.3 Cyclic AMP ELISA

3.2.3.1 Time Course Assay

10 mL of YPD was inoculated with *C. albicans*, from a glycerol stock stored at -80 °C, and grown at 30 °C for three days with shaking at 200 rpm. Cultures were diluted to 1×10^8 cells/mL. Concentration was determined by absorbance at 540 nanometers²⁷ using the formula: $cells \times 10^3 mL = 64.3 + 8,206(Ab_{540})$. 500 μ L of FBS, 1 mM MTP, or 1 mM daunosamine were added to 5 mL cultures of *C. albicans*. Cultures were then incubated at 37 °C while shaking at 200 rpm. 1 mL aliquots were taken at 0, 15, 30, 45 and 60 minutes after addition of compounds. Cells were harvested by centrifuging at 15,000 rpm for 1 minute in a tabletop centrifuge. Supernatants were discarded and pellets were frozen and stored in liquid nitrogen until use.

3.2.3.2 Effects of Ligand Concentration on cAMP Levels

10 mL of YPD was inoculated with *C. albicans*, from a glycerol stock stored at -80 °C, and grown overnight at 30 °C while shaking at 200 rpm. Cultures were diluted to 1×10^8 cells/mL. Concentration was determined by absorbance at 540 nanometers. Cultures were treated with H₂O (negative control), 10% FBS, and MTP, daunosamine,

and L-alanine at concentrations of 10 μ M and 100 μ M. Cultures were incubated at 37 °C with shaking at 200 rpm for 30 minutes. Cells were harvested by centrifuging at 15,000 rpm for 1 minute in a tabletop centrifuge. Supernatants were discarded and pellets were frozen and stored in liquid nitrogen until use.

3.2.3.3 cAMP Extraction

Cells pellets were thawed and washed with 1 mL H₂O. The pellets were resuspended in 500 μ L H₂O and transferred to 2 mL screw cap vials containing 1 g acid washed beads and 500 μ L trifluoroacetic acid. Samples were vortexed at max speed for 5 minutes at 4 °C. Lysates were clarified by centrifugation at 15,000 rpm for 12 minutes. Supernatants were transferred to clean micro-centrifuge tubes and washed five times with 500 μ L water saturated ether, discarding the organic layer after each wash. After washing the aqueous layer was frozen and lyophilized overnight.

3.2.3.4 ELISA Protocol

cAMP levels were detected with cAMP Biotrack EIA system following the non-acetylation procedure. All reagents were warmed to room temperature prior to starting the assay. Lyophilized samples were dissolved in 500 μ L assay buffer. 200 μ L assay buffer was added to the non-specific binding (NSB) well. 100 μ L assay was added to the zero standard well. 100 μ L of each cAMP standard and sample was pipetted into the appropriate wells. Next, 100 μ L of antiserum was added to all wells except for the blank and non-specific binding wells. The plate was covered and incubated at 4 °C for 2 hours. 50 μ L cAMP-peroxidase was added to all wells excluding the blank and the plate was incubated at 4 °C for 1 hour. All wells were

washed with 400 μL wash buffer four times, blotting with a kimwipe following the last wash to remove residual wash buffer. 150 μL enzyme substrate was added to each well and the plate was shaken at room temperature for 1 hour. The reaction was halted by the addition of 1 M sulphuric acid and the optical density was recorded at 450 nm.

3.2.3.5 Data Analysis

The average optical density of each sample condition run in duplicate was calculated. The percent bound for each sample or standard was determined using the formula: $\%B/B_0 = \frac{(\text{sample OD} - \text{NSB OD})}{(\text{Zero standard OD} - \text{NSB OD})} \times 100$. A standard curve was generated plotting $\%B/B_0$ against the log of the concentration of the samples. Using JMP Pro 13.0, a logarithmic regression equation was obtained from the standard curve. This equation was used to calculate the concentration of cAMP in each sample based on $\%B/B_0$.

3.2.4 Quantitative PCR

3.2.4.1 Assay

50 mL of YPD was inoculated with *C. albicans* from a glycerol stock. The culture was grown overnight at 30 °C while shaking at 200 rpm. The next day, cell density was determined by Ab_{540} , and diluted with YPD to a density of 1×10^8 cells/mL. Cells were divided into 500 μL aliquots and treated with 50 μL of the indicated compound. Samples were incubated at 37 °C for 2 hours while shaking at 200 rpm. Cells were harvested by centrifugation at $15,000 \times g$ for 3 minutes. Supernatant was discarded and pellets were stored at -80 °C until use.

3.2.4.2 RNA Extraction

Total RNA was extracted using a RNeasy Mini Kit (Qiagen). Cell pellets were suspended in 600 μL RLT buffer and transferred to a 2 mL screw cap vial containing 600 μL acid washed beads. Samples were vortexed at max speed for four cycles of 30 seconds at 4 $^{\circ}\text{C}$. 350 μL of lysate was transferred to a clean microcentrifuge tube and centrifuged at 15,000 $\times g$ for 2 minutes. The supernatant was transferred to a clean tube and 350 μL of 70% ethanol was added. Samples were transferred to a spin column and centrifuged at 10,000 $\times g$ for 15 seconds, discarding the flow through. The column was washed with 350 μL RW1 buffer centrifuged at 10,000 $\times g$ for 15 seconds. 80 μL of DNase I mixture was added and the column was incubated at room temperature for 15 minutes. 500 μL of RPW buffer was added and the column centrifuged at 10,000 $\times g$ for 15 seconds. A final wash of 500 μL RPE buffer was added and the column was centrifuged at 10,000 $\times g$ for 2 minutes. The spin column was transferred to a fresh microcentrifuge tube and centrifuged at 10,000 $\times g$ for 1 minute to remove any residual buffer. The spin column was transferred to a clean microcentrifuge tube and RNA was eluted with 50 μL RNase free water by centrifugation at 10,000 rpm $\times g$ for 1 minute. Samples were stored at -80 $^{\circ}\text{C}$.

3.2.4.3 cDNA Synthesis

cDNA was synthesized from RNA samples using QuantiTect Reverse Transcription Kit (Qiagen). 2 μL 7x gDNA Wipeout Buffer was added to 150 ng of RNA in a total volume of 14 μL to remove any contaminating DNA. Samples were heated at 42 $^{\circ}\text{C}$ for 2 minutes and immediately transferred to ice. 1 μL Quantiscript Reverse Transcriptase, 4 μL 5x Quantiscript RT Buffer, and 1 μL RT Primer Mix was

added to the RNA template mixture. Samples were incubated at 42 °C for 15 minutes followed by 3 minutes at 95 °C. Samples were diluted to 50 ng/μL of DNA and stored at -20 °C.

3.2.4.4 qPCR Reaction

Primers sequences were taken from Naseem *et al*²⁸ and are listed in Table 3.1. PCR master mix was prepared by mixing 2x SsoAdvanced universal SYBR Green supermix, 500 nM forward and reverse primers, and H₂O. 18 μL PCR master mix was added to 2 μL 50 ng/μL DNA. Using an Applied Biosystems 7300 Real-Time PCR System, a relative quantification study was performed following the thermocycling protocol in Table 3.2.

Table 3.1 – Primer sequences for qPCR reactions

Primer Name	Sequence
ACT1-F	5' TCC AGA AGC TTT GTT CAG ACC AGC 3'
ACT1-R	5' TGC ATA CGT TCA GCA ATA CCT GGG 3'
ECE1-F	5' TGG CGT TCC AGA TGT TGG CCT-3'
ECE1-R	5' GCT AAG TGCT ACT GAG CCG GCA 3'
HWP1-F	5' GCT CCT GCC ACT GAA CCT TCC C-3'
HWP1-R	5' ACT TGA GCC AGC TGG AGC GG 3'

Table 3.2 – Thermocycling protocol

Step	Temp erature	T ime	C ycles

Polymerase	95 °C	3	1
Activation		0 s	
DNA	95 °C	1	
Denaturation		5 s	2
Annealing/Exte	60 °C	6 ⁰	
nsion		0 s	

3.2.4.5 Data Analysis

Relative gene expression levels were calculated using the $2^{-\Delta\Delta C_t}$ method²⁹. Where $\Delta\Delta C_t$ is the difference between the ΔC_t of the treated sample and the ΔC_t of the control sample. ΔC_t is calculated by subtracting C_t of the house-keeping gene, actin, from the C_t of the gene of interest. C_t was the average of two trials of two biological replicates.

3.3 Results and Discussion

3.3.1 Hyphae Growth

3.3.1.1 MDP Fragment Screen

Since the 1950's it has been known that blood serum has the ability to induce hyphae formation in *C. albicans*³⁰. However, it would be more than 50 years until the identity of the small molecule responsible would be identified. In 2008, Wang and colleagues identified the peptidoglycan as the molecule present in serum that triggers hyphae growth²⁴. To better understand how *C. albicans* is recognizing bacteria, it was

necessary to identify the peptidoglycan portions that are capable of eliciting hyphae formation when exposed to *C. albicans*. Budding yeast cells were exposed to small library of peptidoglycan fragments, (Figure 3.1) – synthesized by Dr. James Melnyk²⁵- at a concentration of 1 mM and incubated at 37 °C overnight. This library was designed to examine the effects of carbohydrate identity (**3.10** - **3.13**) and variations of the peptide stem (**3.02** - **3.08**) on hyphae formations. The importance of the peptide stem was tested by altering the stereochemistry naturally occurring LD (**3.02**) to LL (**3.04**) conformation and progressively truncating it from a dipeptide (**3.02**) to a mono-peptide (**3.06**) to containing no amino acid (**3.08**). The next day cultures were visualized by bright field microscopy to assay hyphae formation.

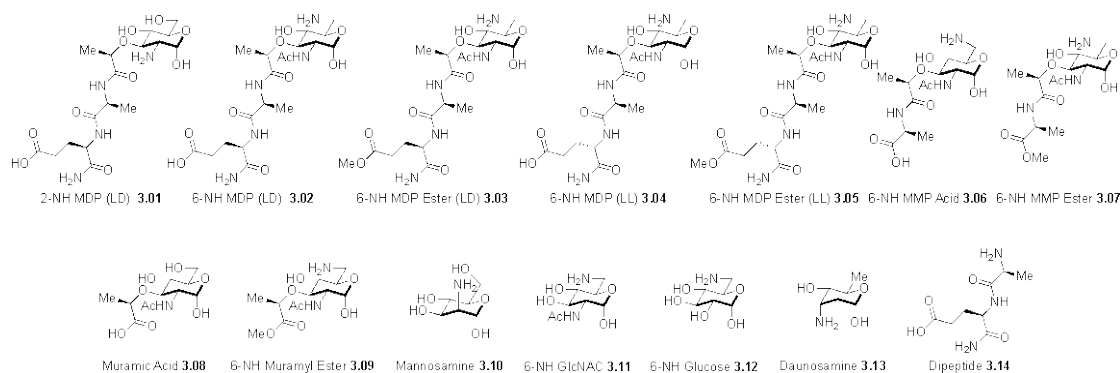


Figure 3.1 - Muramyl Dipeptide Fragment Library used to screen for hyphae growth in *C. albicans*. Compounds **3.02-3.05** were used to examine how peptide stem stereochemistry effects hyphae formation. The impact of the length of the peptide stem was examine by truncating then eliminating it in compounds **3.02**, **3.06**, and **3.08**. Individual carbohydrates **3.10** - **3.13** were also examined.

Hyphae formation was induced by a variety of peptidoglycan derivatives (Figure 3.2). The carbohydrate moiety was essential as LD-Dipeptide (**3.14**) was

unable to induce hyphae formation. Modifications on the peptide stem were well tolerated as the natural occurring LD stereochemistry (**3.02**) and LL stereochemistry (**3.04**) both triggered hyphae growth. Acetyl groups on the amine at the 2 position of the carbohydrate (**3.02-3.05**) decrease the amount of cells displaying hyphae characteristics compared to an unprotected amine (**3.01**). Carbohydrates found in the peptidoglycan backbone were also capable of inducing hyphae formation even in the absence of the peptide stem (**3.08, 3.10, and 3.11**). Due to the increased hyphae formation in cultures treated with 2-NH MDP (**3.01**), we hypothesized that a free amine on the carbohydrate was sufficient for hyphae formation. However, *C. albicans* grown in the presence of 6-NH glucose (**3.12**) did not exhibit hyphae formation disproving this postulation. Surprisingly, daunosamine (**3.13**) elicited high amounts of hyphae formation in the *C. albicans* culture. Table 3.3 summarizes the effects of the components of MDP on *C. albicans* hyphae formation.

Table 3.3 – Effects of MDP structural components on hyphae formation in *C. albicans*

Component	Effect
Carbohydrate	Necessary for hyphae growth
Amine at 2 position	Acetyl capping decreases hyphae growth
Peptide Stem	Does not affect hyphae growth

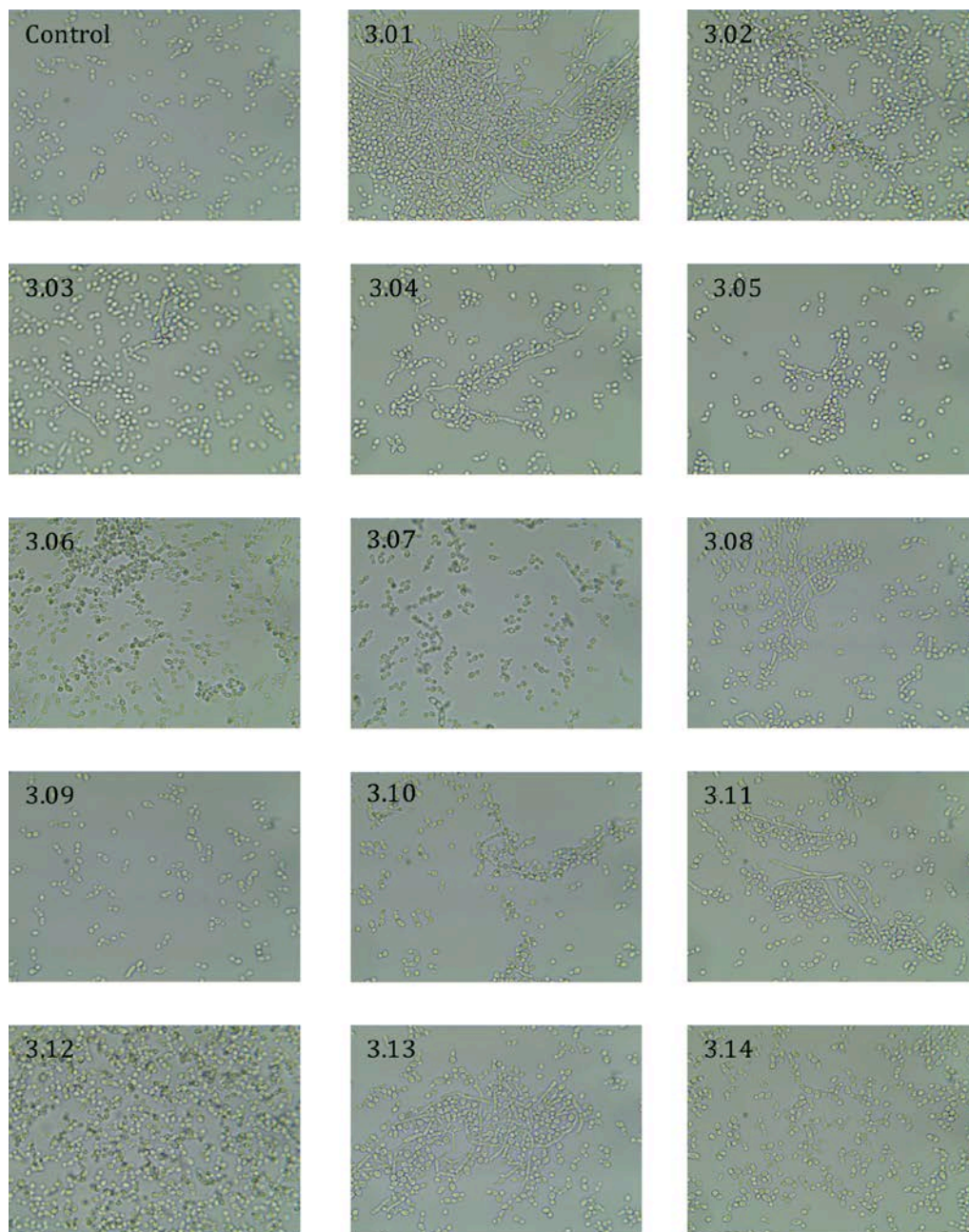


Figure 3.2 – Carbohydrates derived from bacterial sources (Figure 3.1) are capable of eliciting hyphae formation in *C. albicans*. Changing amino acid stereochemistry from the naturally occurring LD to LL did not effect hyphae formation (3.02-3.05). The carbohydrate was necessary, as the dipeptide (3.14) alone did not trigger hyphae formation. Carbohydrates not found in peptidoglycan, daunosamine (3.13) also caused hyphae formation.

3.3.1.2 Quantification of Hyphae Formation in Response to Bacterial Carbohydrates

The results of daunosamine treatment were surprising, as the sugar is not found in peptidoglycan but still able to induce hyphae formation in *C. albicans*. A search of the literature identified daunosamine as the carbohydrate present in anthracycline natural products produced by *Streptomyces* bacterium (Figure 3.3A, **3.13-3.14**). These compounds exhibit both antibiotic and antitumor properties through a mechanism of DNA topoisomerase inhibition³¹. Interestingly, this class of compounds has been demonstrated to effect the growth of *C. albicans*³². To better understand how *C. albicans* is responding to diverse bacterial derived carbohydrates quantification of hyphae formation was needed. The hyphal growth assay was repeated with 1mM daunosamine (**3.13**), doxorubicin (**3.15**), MDP (**3.16**), muramyl tripeptide (MTP, **3.17**), and 10% FBS (Figure 3.3A). To avoid bias, cells were imaged and scored blindly by Dennis Wykoff for hyphae characteristics. The average of two trials was reported as a percentage of cells with hyphae characteristics divided by total cells (Figure 3.3B). Both peptidoglycan fragments, MDP (**3.16**) and MTP (**3.17**), strongly induced hyphae formation, with 29% and 41% of cells have hyphae characteristics respectively. MTP was even more effective in inducing hyphae formation than the positive control, FBS, which only induced 37% of cells. Daunosamine (**3.13**) and doxorubicin (**3.15**) were not as potent, only increasing hyphae percentage by 1% and 2% compared to the non-induced control. Despite the small increase in cells showing hyphae characteristics, daunosamine did exhibit true hyphae – long filaments (Figure 3.3B) – that were not observed in the control culture. The doxorubicin (**3.15**) treated culture proved difficult to quantify, as the cell density was lower likely due to the antibiotic properties of the compound.

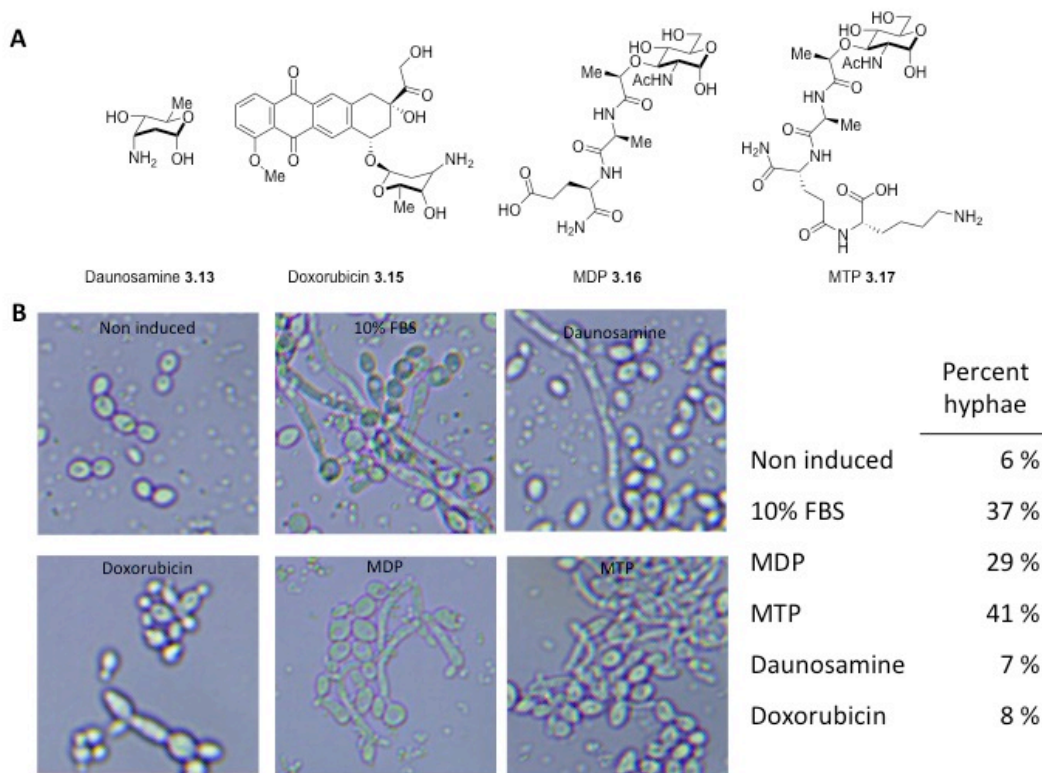


Figure 3.3 – Quantification of hyphae growth. A) Anthracycline and peptidoglycan carbohydrate B) *C. albicans* cultures were treated with 1 mM of the indicated compound and incubated at 37 °C overnight. Cells were visualized at 40 × magnification and images containing approximately 100 cells were blindly scored for hyphae characteristics. Hyphae formation is reported as percent hyphae calculated by dividing cells expressing hyphae characteristics divided by total cells.

3.3.2 cAMP Elisa

3.3.2.1 Carbohydrate Induced Increases In cAMP Levels Are Time Dependent

In order to better identify compounds capable triggering hyphae growth with more confidence, a more stringent and quantitative assay is needed. Since hyphae formation is largely under control of the adenylyl cyclase, CYR1, an assay was needed to accurately quantify cAMP levels in the cell. Using a commercially available ELSIA kit (GE Life Sciences), cAMP levels were determined in response to carbohydrates from bacterial sources. An initial assay was performed to determine the time point at which cAMP levels peak after exposure to various ligands. *C. albican* cultures were treated with 10% FBS, 100 μ M daunosamine (**3.13**), or 100 μ M MTP (**3.17**). Cultures were incubated at 37 °C and aliquots were taken at 15-minute intervals from 0 to 60 minutes after addition of the inducing agents. Cyclic AMP was extracted (Materials and Methods 3.2.3.3) and quantified following the manufacturers instructions. As was seen in the hyphae quantification assay (Results and discussion 3.3.1.2), cAMP levels were similar in samples treated with MTP (**3.17**) and 10% FBS (Figure 3.4). Surprisingly, daunosamine (**3.13**) induced the largest cAMP increases; with levels approximately double that of MTP and FBS. For conditions, peak levels were observed between 30 minutes and 40 minutes with levels decreasing at 60 minutes. The decreased levels of cAMP after 45 minutes can be attributed to increased expression of the cAMP phosphodiesterase, PDE2³³.

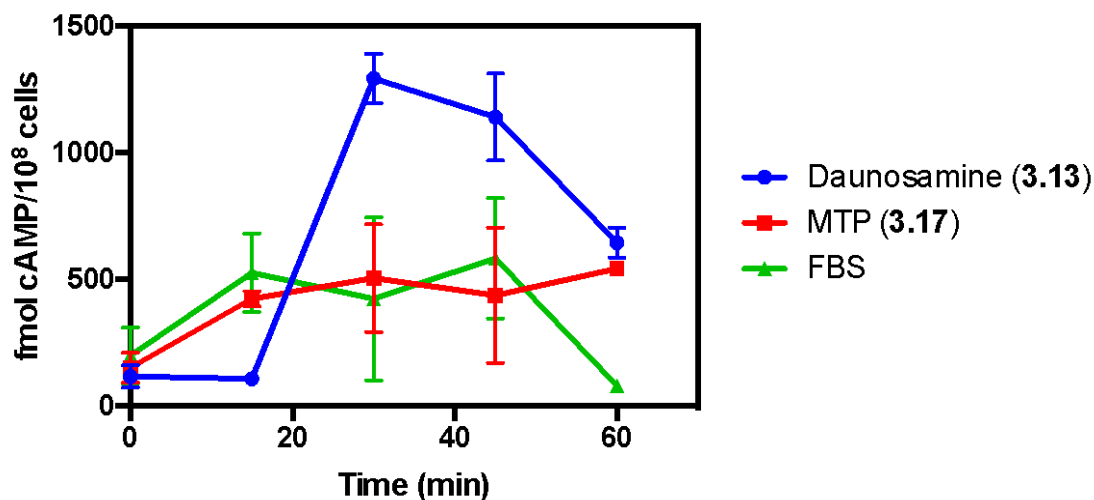


Figure 3.4 – *C. albicans* cultures were treated 100 μ M of the indicated compound and aliquots were taken at fifteen intervals from 0 to 60 minutes after treatment. Cyclic AMP was extracted and quantified using cAMP Biotrack EIA. cAMP levels increased upon exposure to MTP (3.17) and daunosamine (3.13) peaking at 30 minutes.

3.3.2.2 Cyclic AMP Levels Are Not Dependent on the Concentration of Stimulating Molecules

After determining the time at which cAMP levels peak after exposure to MTP (3.17) and daunosamine (3.18), a second ELISA assay was performed to determine if decreasing the concentration of the compound would produce a smaller increase in cAMP levels. Alanine, daunosamine (3.13), and MTP (3.17) were added to cultures of *C. albicans* at concentrations of 10 μ M and 100 μ M. 10% FBS and H₂O were included as positive and negative controls respectively. Cultures were incubated at 37 °C for 30 minutes and cAMP was extracted (Materials and Methods 3.2.3.3). Unfortunately, increases in cAMP levels did not appear to be concentration dependent as there was not a significant difference between any samples. It would appear that the assay was not very robust as there were large standard deviations seen in the replicates of each

sample. To improve this assay, it may be necessary to sync cell growth as hyphae formation is effected by stages of the cell cycle³⁴. In order to be able to accurately quantify the carbohydrates influence on *C. albicans* morphology, a more reliable and high throughput assay is needed.

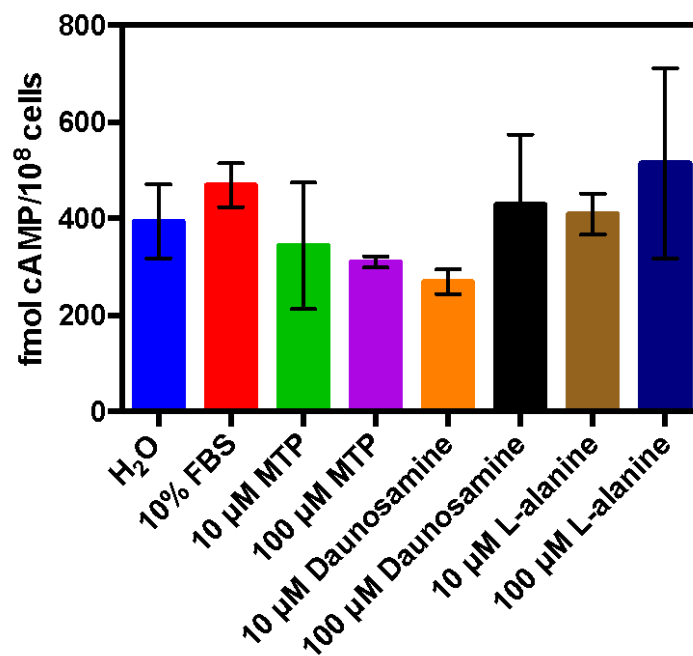


Figure 3.5 – *C. albicans* cultures were treated with either 10 μM or 100 μM of the indicated compounds for 30 minutes. Cyclic AMP was extracted and quantified using cAMP Biotrack EIA. No significant difference in cAMP levels was observed between cultures treated with either 10 μM or 100 μM daunosamine or MTP.

3.3.3 qPCR

C. albicans morphogenesis is regulated by the differential expression of hyphae specific genes. These genes play important roles in hyphae formation,

maintenance, and regulation. Microarray analysis has identified several genes that are highly expressed in response to serum³⁵, including *HWPI*, a cell wall protein responsible for cell-surface adhesion³⁶ only transcribed during the hyphae growth phase³⁷; and *ECE1*, a cytolytic peptide toxin that is only expressed after cells start to form hyphae³⁸⁻³⁹. Expression levels of these genes have been used in assays testing inhibition of hyphae morphogenesis in *C. albicans*^{28, 40}. qPCR studies were performed monitoring the expression levels of these genes to determine how *C. albicans* is responding to peptidoglycan fragments and bacterial natural products. Briefly, 6×10^6 *C. albicans* cells were treated with H₂O, 10% FBS, DMSO, or 100 μ M compounds **3.01**, **3.08**, and **3.13 – 3.19** (Figure 3.6). DMSO was included as the natural products, such as doxorubicinone (**3.18**) and vancomycin (**3.19**), exhibit poor solubility in H₂O. After addition of the compounds cells were incubated at 37 °C for 2 hrs. Total RNA was isolated and cDNA was generated following the protocol in Materials and methods 3.2.4.2 -3.2.4.5.

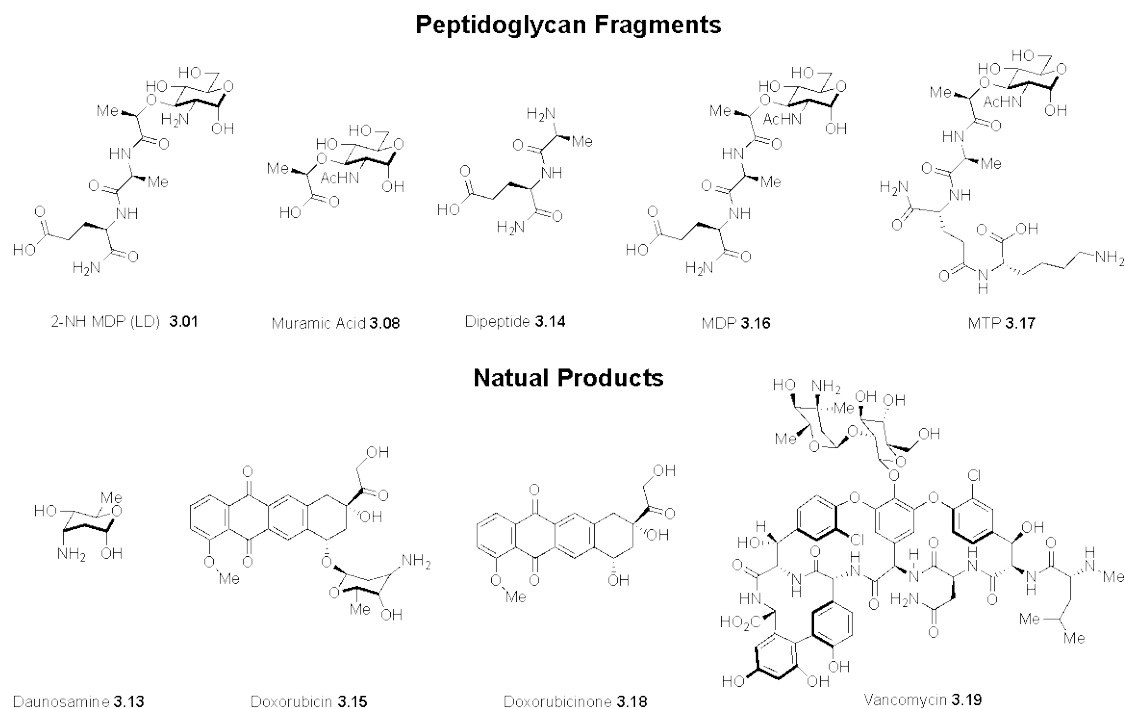


Figure 3.6 – Peptidoglycan Fragments and Bacterial Natural products tested for their effects on *ECE1* and *HWPI* expression. Peptidoglycan fragments were chosen to determine the how varying the peptide stem effects gene expression. The natural products looked to established the dependence of daunosamine in anthracyclines to elicit hyphae responses.

DMSO did not affect expression levels of either *ECE1* or *HWPI*, allowing for the comparison between the peptidoglycan fragments and the bacterial natural products. In agreement with the hyphae formation and increased cAMP observed in the other assays, MTP (**3.17**) and 10% FBS showed similar levels of gene expression with a four-fold increase in *ECE1*. Surprisingly, despite not causing hyphae formation in the microscopy assay, dipeptide (**3.18**) had the highest levels of *ECE1* with a 26-fold increase compared to the non-treated control. A strong hyphal inducer from the cell growth assay, 2-NH MDP (**3.01**) showed little effect on either *ECE1* or *HWPI*, with expression levels at $1.3 \times$ and $0.7 \times$ of the H_2O control respectively. Interestingly,

MDP (**3.16**), which has an acetyl group capping the amine at the 2-position and a weak activator of hyphae formation, decreased *ECE1* expression by half. Vancomycin (**3.19**) was the most potent natural product inducing a 18-fold increase in *ECE1* expression. Doxorubicin (**3.17**) and doxorubicinone (**3.18**) increased *ECE1* levels by approximately 15-fold and 10-fold. With sugar moiety, daunosamine (**3.13**), only exhibiting a 3-fold increase in *ECE1* expression and the aglycone showing comparable expression levels to doxorubicin, it can be concluded the carbohydrate is not necessary for production of the cytolytic toxin. Under all conditions, *ECE1* expression is increased to higher levels than *HWPI*. This is unsurprising as *ECE1* is expressed within 30 minutes of hyphae induction and peak levels of *HWPI* expression were not seen until 6 hours after serum exposure³⁵. With results of the qPCR assay not in agreement with the hyphae assay, it may be necessary to expand the hyphae specific genes being examined. There are over 700 genes differentially expressed during the hyphae formation process³⁵; identifying which are being affected by bacterial carbohydrates can help elucidate the mechanism by which *C. albicans* recognizes its microbial neighbors.

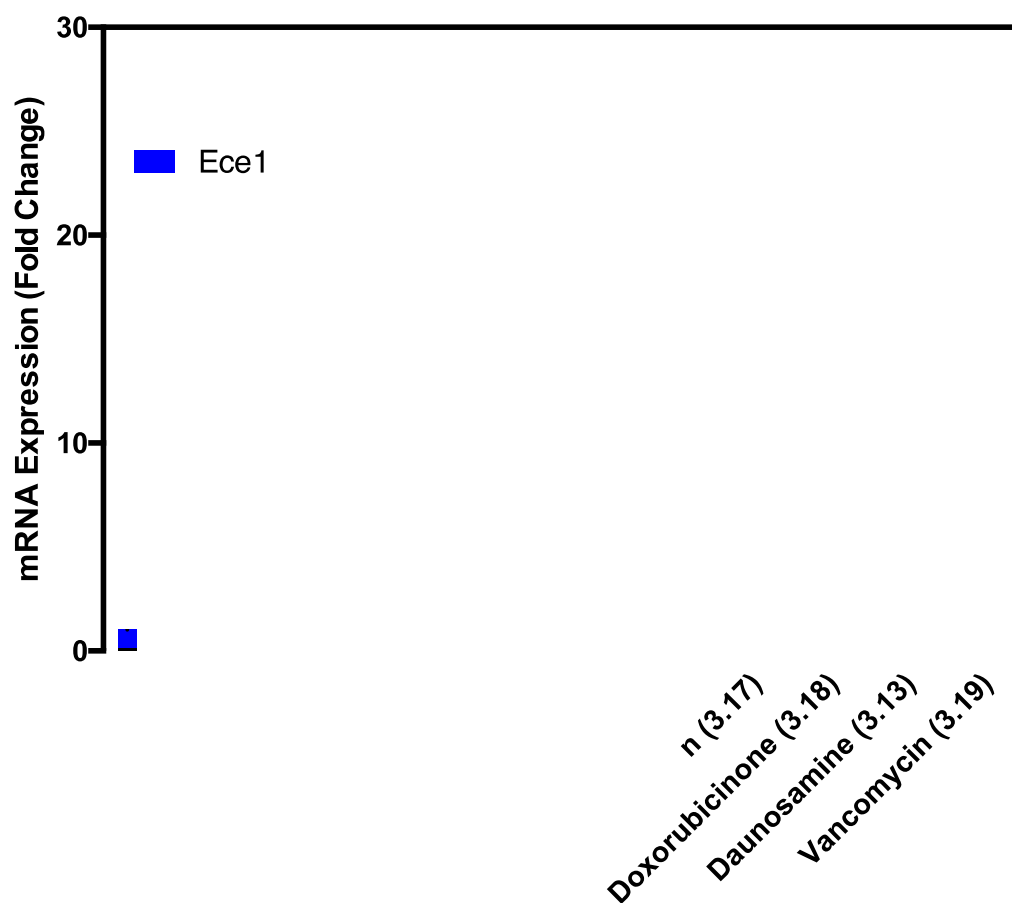


Figure 3.7 – Bacterial natural products increase expression levels of hypha-specific genes. *C. albicans* cultures were treated with 100 μ M of each compound. *ECE1* and *HWPI* expression levels were normalized to actin. Relative expression were determined comparing mRNA levels of each sample to the control sample treated with H₂O, set to an expression level equal to 1. Two samples were measured from two biological replicates for each compound.

3.4 Conclusions and Future Directions

While the peptidoglycan sugar backbone is conserved, many bacterial species have evolved the ability to alter the composition of the peptide stem or acetylate the amine on the sugars in order to avoid detection by host cells⁴¹. While it has been

shown that MDP can induce hyphae, it is possible that some modifications of peptidoglycan can have the opposite effect. In order to understand which portions of peptidoglycan were responsible for hyphae formation, we tested a small library (Figure 3.1) of peptidoglycan fragments for their effect on hyphal activation.

A brightfield microscopy assay identifying hyphae formation after overnight incubation with each compound identified the carbohydrate core of MDP as essential for hyphae growth. Alterations to the peptide stem - including changes in composition, stereochemistry, and even elimination (Figure 3.1, **3.01**, **3.02**, **3.04**, and **3.08**) – did not eliminate hyphae formation. The inability of the dipeptide to induce hyphae provided further evidence of the importance of the carbohydrate. Surprisingly, it was not only peptidoglycan fragments that induced hyphae formation but also the *Streptomyces* natural product, doxorubicin, and its sugar moiety, daunosamine. While the microscopy assay was able to identify bacterial carbohydrates capable of inducing hyphae, it was not without its limitations. The biggest drawback is that the assay is qualitative. While it was possible to count the number of cells displaying hyphae morphology, the difference between pseudohyphae and true hyphae is often hard to distinguish.

In order to quantify the affects of the bacterial product, an RT-PCR assay was performed examining expression levels of hyphae specific genes. *HWPI* and *ECE1* were chosen, as they are highly unregulated during hyphae induction and previous studies have established their utility in RT-PCR assays^{28, 35, 40}. Large variations were not observed in *HWPI* expression levels. This can be attributed to the time point at which mRNA levels were measured. Reports in the literature indicate that peak

express occurs 6 hours after exposure to serum³⁵. Future studies looking at the expression at longer times post induction may be able to observe larger inductions in gene expression. Curiously, the carbohydrate did not appear to be important in inducing the expression of *ECE1*, as dipeptide (**3.14**) and doxorubicinone (**3.18**) produced two of the largest increases. The ability of the compounds to increase *ECE1* but not induce hyphae formation could be due to the complex signaling pathways regulating hyphae growth. After exposure to serum, *ECE1* levels peaks around 60 minutes returning to basal levels within 6 hours³⁵. In addition to inducing the *ECE1*, it is possible to that dipeptide (**3.14**) and doxorubicinone (**3.18**) could be altering the expression genes responsible for production of the quorum-sensing molecule, farnesol. Farnesol is produced by *C. albicans* and has been show to not only inhibit hyphae formation but also promote the switch from hyphae to budding yeast⁴². Examining the expression genes involved in farnesol production provides interesting future targets to understand the balance needed for the formation of hyphae.

With previous reports demonstrating MDP's direct effect on Cyr1, it was important to develop an assay that could directly measure changes in cAMP levels in response to these bacterial carbohydrates. To this end, a commercially available cAMP ELISA assay was employed. This assay has previously been used in studies examining the effects of the deletion of Pde2 and Cyr1^{33, 43}. In agreement with previous reports in the literature^{24, 33, 43}, peak cAMP levels were observed between 15 and 45 minutes after exposure to the FBS, MTP (**3.17**), or daunosamine (**3.13**). Concentration of these compounds did not appear to effect cAMP levels. This could be due to be the transporters proteins being saturated. Identifying the mechanism by which these carbohydrates enter the cell could explain this phenomenon.

In this chapter, I described three assays I developed and used to examine the effects of bacterial derived carbohydrates and natural products on *C. albicans* morphology with emphasis on the cAMP. To truly understand the effects of the molecules, it is necessary to look beyond this single pathway. The formation of hyphae is an enormously complex and important process, essential to *C. albicans* infection and biofilm formation⁴⁴. Transcription profiling performed during the yeast to hyphae transition has identified over 750 genes that are differentially regulated in the process. Their regulation, which is often time dependent, is based on whether they are important in hyphae initiation, maintenance, or even the invasion process³⁵. Future studies employing DNA microarrays can be used to determine which genes each compound regulates, which in turn can help identify the signaling pathway responsible. However, crosstalk between the pathways complicates this analysis. For example, both the cAMP-PKA and pH pathways activate the transcription factor, Efg1³⁴. Identifying how *C. albicans* responds to its bacterial neighbors expands on the growing importance of the interactions between bacteria and fungi in the human microbiome.

REFERENCES

1. Gilbert, J. A.; Blaser, M. J.; Caporaso, J. G.; Jansson, J. K.; Lynch, S. V.; Knight, R., Current understanding of the human microbiome. *Nat Med* **2018**, *24* (4), 392-400. DOI: 10.1038/nm.4517.
2. Young, V. B., The role of the microbiome in human health and disease: an introduction for clinicians. *BMJ* **2017**, *356*. DOI: 10.1136/bmj.j831.
3. Wang, B.; Yao, M.; Lv, L.; Ling, Z.; Li, L., The Human Microbiota in Health and Disease. *Engineering* **2017**, *3* (1), 71-82. DOI: <https://doi.org/10.1016/J.ENG.2017.01.008>.
4. Peterson, J.; Garges, S.; Giovanni, M.; McInnes, P.; Wang, L.; Schloss, J. A.; Bonazzi, V.; McEwen, J. E.; Wetterstrand, K. A.; Deal, C.; Baker, C. C.; Di Francesco, V.; Howcroft, T. K.; Karp, R. W.; Lunsford, R. D.; Wellington, C. R.; Belachew, T.; Wright, M.; Giblin, C.; David, H.; Mills, M.; Salomon, R.; Mullins, C.; Akolkar, B.; Begg, L.; Davis, C.; Grandison, L.; Humble, M.; Khalsa, J.; Little, A. R.; Peavy, H.; Pontzer, C.; Portnoy, M.; Sayre, M. H.; Starke-Reed, P.; Zakhari, S.; Read, J.; Watson, B.; Guyer, M., The NIH Human Microbiome Project. *Genome research* **2009**, *19* (12), 2317-23. DOI: 10.1101/gr.096651.109.
5. Huang, Y. J.; Boushey, H. A., The microbiome in asthma. *The Journal of allergy and clinical immunology* **2015**, *135* (1), 25-30. DOI: 10.1016/j.jaci.2014.11.011.
6. Lauro, M. L.; Burch, J. M.; Grimes, C. L., The effect of NOD2 on the microbiota in Crohn's disease. *Current Opinion in Biotechnology* **2016**, *40*, 97-102. DOI: <http://dx.doi.org/10.1016/j.copbio.2016.02.028>.
7. Schwabe, R. F.; Jobin, C., The microbiome and cancer. *Nature reviews. Cancer* **2013**, *13* (11), 800-12. DOI: 10.1038/nrc3610.
8. Huseyin, C. E.; O'Toole, P. W.; Cotter, P. D.; Scanlan, P. D., Forgotten fungi- the gut mycobiome in human health and disease. *FEMS Microbiol Rev* **2017**, *41* (4), 479-511. DOI: 10.1093/femsre/fuw047.
9. Kelesidis, T.; Pothoulakis, C., Efficacy and safety of the probiotic *Saccharomyces boulardii* for the prevention and therapy of gastrointestinal disorders.

Therapeutic advances in gastroenterology **2012**, 5 (2), 111-25. DOI: 10.1177/1756283x11428502.

10. Nash, A. K.; Auchtung, T. A.; Wong, M. C.; Smith, D. P.; Gesell, J. R.; Ross, M. C.; Stewart, C. J.; Metcalf, G. A.; Muzny, D. M.; Gibbs, R. A.; Ajami, N. J.; Petrosino, J. F., The gut mycobiome of the Human Microbiome Project healthy cohort. *Microbiome* **2017**, 5 (1), 153. DOI: 10.1186/s40168-017-0373-4.

11. Hoarau, G.; Mukherjee, P. K.; Gower-Rousseau, C.; Hager, C.; Chandra, J.; Retuerto, M. A.; Neut, C.; Vermeire, S.; Clemente, J.; Colombel, J. F.; Fujioka, H.; Poulain, D.; Sendid, B.; Ghannoum, M. A., Bacteriome and Mycobiome Interactions Underscore Microbial Dysbiosis in Familial Crohn's Disease. *MBio* **2016**, 7 (5). DOI: 10.1128/mBio.01250-16.

12. Hager, C. L.; Ghannoum, M. A., The mycobiome: Role in health and disease, and as a potential probiotic target in gastrointestinal disease. *Digestive and liver disease : official journal of the Italian Society of Gastroenterology and the Italian Association for the Study of the Liver* **2017**, 49 (11), 1171-1176. DOI: 10.1016/j.dld.2017.08.025.

13. Mukherjee, P. K.; Wang, H.; Retuerto, M.; Zhang, H.; Burkey, B.; Ghannoum, M. A.; Eng, C., Bacteriome and mycobiome associations in oral tongue cancer. *Oncotarget* **2017**, 8 (57), 97273-97289. DOI: 10.18632/oncotarget.21921.

14. M., R., Skin and mucous membrane infections. In *Candida and Candidiasis*, Calderone, R., Ed. ASM Press: Washington, DC, 2002; pp 307-325.

15. Erb Downward, J. R.; Falkowski, N. R.; Mason, K. L.; Muraglia, R.; Huffnagle, G. B., Modulation of post-antibiotic bacterial community reassembly and host response by *Candida albicans*. *Sci Rep* **2013**, 3, 2191. DOI: 10.1038/srep02191.

16. Pierce, G. E., *Pseudomonas aeruginosa*, *Candida albicans*, and device-related nosocomial infections: implications, trends, and potential approaches for control. *J Ind Microbiol Biotechnol* **2005**, 32 (7), 309-18. DOI: 10.1007/s10295-005-0225-2.

17. Hogan, D. A.; Kolter, R., *Pseudomonas-Candida* interactions: an ecological role for virulence factors. *Science* **2002**, 296 (5576), 2229-32. DOI: 10.1126/science.1070784.

18. Adam, B.; Baillie, G. S.; Douglas, L. J., Mixed species biofilms of *Candida albicans* and *Staphylococcus epidermidis*. *J Med Microbiol* **2002**, 51 (4), 344-9. DOI: 10.1099/0022-1317-51-4-344.

19. Schlecht, L. M.; Peters, B. M.; Krom, B. P.; Freiberg, J. A.; Hansch, G. M.; Filler, S. G.; Jabra-Rizk, M. A.; Shirtliff, M. E., Systemic *Staphylococcus aureus* infection mediated by *Candida albicans* hyphal invasion of mucosal tissue. *Microbiology* **2015**, *161* (Pt 1), 168-181. DOI: 10.1099/mic.0.083485-0.
20. Metwalli, K. H.; Khan, S. A.; Krom, B. P.; Jabra-Rizk, M. A., *Streptococcus mutans*, *Candida albicans*, and the human mouth: a sticky situation. *PLoS Pathog* **2013**, *9* (10), e1003616. DOI: 10.1371/journal.ppat.1003616.
21. Mason, K. L.; Erb Downward, J. R.; Mason, K. D.; Falkowski, N. R.; Eaton, K. A.; Kao, J. Y.; Young, V. B.; Huffnagle, G. B., *Candida albicans* and bacterial microbiota interactions in the cecum during recolonization following broad-spectrum antibiotic therapy. *Infect Immun* **2012**, *80* (10), 3371-80. DOI: 10.1128/IAI.00449-12.
22. Han, T. L.; Cannon, R. D.; Villas-Boas, S. G., The metabolic basis of *Candida albicans* morphogenesis and quorum sensing. *Fungal Genet Biol* **2011**, *48* (8), 747-63. DOI: 10.1016/j.fgb.2011.04.002.
23. Hall, R. A.; Turner, K. J.; Chaloupka, J.; Cottier, F.; De Sordi, L.; Sanglard, D.; Levin, L. R.; Buck, J.; Muhlschlegel, F. A., The quorum-sensing molecules farnesol/homoserine lactone and dodecanol operate via distinct modes of action in *Candida albicans*. *Eukaryot Cell* **2011**, *10* (8), 1034-42. DOI: 10.1128/EC.05060-11.
24. Xu, X. L.; Lee, R. T.; Fang, H. M.; Wang, Y. M.; Li, R.; Zou, H.; Zhu, Y.; Wang, Y., Bacterial peptidoglycan triggers *Candida albicans* hyphal growth by directly activating the adenylyl cyclase Cyr1p. *Cell Host Microbe* **2008**, *4* (1), 28-39. DOI: 10.1016/j.chom.2008.05.014.
25. Schaefer, A. K.; Melnyk, J. E.; Baksh, M. M.; Lazor, K. M.; Finn, M. G.; Grimes, C. L., Membrane Association Dictates Ligand Specificity for the Innate Immune Receptor NOD2. *ACS chemical biology* **2017**. DOI: 10.1021/acscchembio.7b00469.
26. Burch, J. M.; Mashayekh, S.; Wykoff, D. D.; Grimes, C. L., Bacterial Derived Carbohydrates Bind Cyr1 and Trigger Hyphal Growth in *Candida albicans*. *ACS Infect Dis* **2018**, *4* (1), 53-58. DOI: 10.1021/acsinfectdis.7b00154.
27. Rodrigues, A.; Vaz, C. P.; da Fonseca, A. F.; de-Oliveira, J. M., Evaluating the concentration of a *Candida albicans* suspension. *Infectious diseases in obstetrics and gynecology* **1993**, *1* (3), 134-6. DOI: 10.1155/s1064744993000304.
28. Naseem, S.; Araya, E.; Konopka, J. B., Hyphal growth in *Candida albicans* does not require induction of hyphal-specific gene expression. *Mol Biol Cell* **2015**, *26* (6), 1174-87. DOI: 10.1091/mbc.E14-08-1312.

29. Livak, K. J.; Schmittgen, T. D., Analysis of relative gene expression data using real-time quantitative PCR and the 2(-Delta Delta C(T)) Method. *Methods (San Diego, Calif.)* **2001**, 25 (4), 402-8. DOI: 10.1006/meth.2001.1262.
30. Reynolds, R., The filament inducing property of blood for *Candida albicans* : its nature and significance. *Clin. Res. Proc.* **1956**, 4, 40.
31. Pang, B.; Qiao, X.; Janssen, L.; Velds, A.; Groothuis, T.; Kerkhoven, R.; Nieuwland, M.; Ovaa, H.; Rottenberg, S.; van Tellingen, O.; Janssen, J.; Huijgens, P.; Zwart, W.; Neefjes, J., Drug-induced histone eviction from open chromatin contributes to the chemotherapeutic effects of doxorubicin. *Nat Commun* **2013**, 4, 1908. DOI: 10.1038/ncomms2921.
32. Kwok, S. C.; Schelenz, S.; Wang, X.; Steverding, D., In vitro effect of DNA topoisomerase inhibitors on *Candida albicans*. *Med Mycol* **2010**, 48 (1), 155-60. DOI: 10.3109/13693780903114934.
33. Jung, W. H.; Stateva, L. I., The cAMP phosphodiesterase encoded by CaPDE2 is required for hyphal development in *Candida albicans*. *Microbiology* **2003**, 149 (Pt 10), 2961-76. DOI: 10.1099/mic.0.26517-0.
34. Shapiro, R. S.; Robbins, N.; Cowen, L. E., Regulatory circuitry governing fungal development, drug resistance, and disease. *Microbiology and molecular biology reviews : MMBR* **2011**, 75 (2), 213-67. DOI: 10.1128/membr.00045-10.
35. Nantel, A.; Dignard, D.; Bachewich, C.; Harcus, D.; Marcil, A.; Bouin, A. P.; Sensen, C. W.; Hogues, H.; van het Hoog, M.; Gordon, P.; Rigby, T.; Benoit, F.; Tessier, D. C.; Thomas, D. Y.; Whiteway, M., Transcription profiling of *Candida albicans* cells undergoing the yeast-to-hyphal transition. *Molecular biology of the cell* **2002**, 13 (10), 3452-65.
36. Staab, J. F.; Sundstrom, P., Genetic organization and sequence analysis of the hypha-specific cell wall protein gene HWP1 of *Candida albicans*. *Yeast* **1998**, 14 (7), 681-6. DOI: 10.1002/(sici)1097-0061(199805)14:7<681::aid-yea256>3.0.co;2-8.
37. Staab, J. F.; Bradway, S. D.; Fidel, P. L.; Sundstrom, P., Adhesive and mammalian transglutaminase substrate properties of *Candida albicans* Hwp1. *Science* **1999**, 283 (5407), 1535-8.
38. Birse, C. E.; Irwin, M. Y.; Fonzi, W. A.; Sypherd, P. S., Cloning and characterization of ECE1, a gene expressed in association with cell elongation of the dimorphic pathogen *Candida albicans*. *Infect Immun* **1993**, 61 (9), 3648-55.

39. Moyes, D. L.; Wilson, D.; Richardson, J. P.; Mogavero, S.; Tang, S. X.; Wernecke, J.; Hofs, S.; Gratacap, R. L.; Robbins, J.; Runglall, M.; Murciano, C.; Blagojevic, M.; Thavaraj, S.; Forster, T. M.; Hebecker, B.; Kasper, L.; Vizcay, G.; Iancu, S. I.; Kichik, N.; Hader, A.; Kurzai, O.; Luo, T.; Kruger, T.; Kniemeyer, O.; Cota, E.; Bader, O.; Wheeler, R. T.; Gutschmann, T.; Hube, B.; Naglik, J. R., Candidalysin is a fungal peptide toxin critical for mucosal infection. *Nature* **2016**, 532 (7597), 64-8. DOI: 10.1038/nature17625.
40. Bar-Yosef, H.; Vivanco Gonzalez, N.; Ben-Aroya, S.; Kron, S. J.; Kornitzer, D., Chemical inhibitors of *Candida albicans* hyphal morphogenesis target endocytosis. *Sci Rep* **2017**, 7 (1), 5692. DOI: 10.1038/s41598-017-05741-y.
41. Wolfert, M. A.; Roychowdhury, A.; Boons, G. J., Modification of the structure of peptidoglycan is a strategy to avoid detection by nucleotide-binding oligomerization domain protein 1. *Infect Immun* **2007**, 75 (2), 706-13. DOI: 10.1128/iai.01597-06.
42. Polke, M.; Leonhardt, I.; Kurzai, O.; Jacobsen, I. D., Farnesol signalling in *Candida albicans* – more than just communication. *Critical Reviews in Microbiology* **2018**, 44 (2), 230-243. DOI: 10.1080/1040841X.2017.1337711.
43. Rocha, C. R.; Schroppel, K.; Marcus, D.; Marcil, A.; Dignard, D.; Taylor, B. N.; Thomas, D. Y.; Whiteway, M.; Leberer, E., Signaling through adenylyl cyclase is essential for hyphal growth and virulence in the pathogenic fungus *Candida albicans*. *Mol Biol Cell* **2001**, 12 (11), 3631-43.
44. Sudbery, P. E., Growth of *Candida albicans* hyphae. *Nature reviews. Microbiology* **2011**, 9 (10), 737-48. DOI: 10.1038/nrmicro2636.

Chapter 4

CACYR1-LRR BINDS BACTERIAL DERIVED CARBOHYDRATES

4.1 Introduction

Since the 1950s, it has been known that blood serum is a potent inducer of hyphae formation in *C. albicans*¹. However, it was not until 2008 that the molecules in serum responsible for hyphae induction were identified as fragments of the bacterial cell wall². The bacterial cell wall is comprised of a mesh-like polymer known as peptidoglycan. Peptidoglycan is composed of two conserved carbohydrates (N-acetylglucosamine and N-acetylmuramic acid) linked together by penta-peptide chains³. Peptidoglycan is a common pathogen-associated molecular pattern (PAMP). In mammals, innate immune receptors, such as toll-like receptors (TLRs) and NOD-like receptors (NLRs), bind these PAMPs to initiate an immune response. Often the binding of these molecules occurs in a leucine rich repeat domain (LRR)⁴. After identifying the ability of peptidoglycan to trigger hyphae growth, the Wang and colleagues hypothesized a homologous protein was present in *C. albicans* performing a similar function². Using the sequence of the LRR domain of Nod2, a human NLR, to search the *C. albicans* genome database, Cyr1 was identified as a match with 40% sequence similarity².

Employing an affinity purification assay using biotinylated muramyl dipeptide (MDP) and GST-LRR purified from *E. coli*, Wang and colleagues proved their hypothesis by showing the LRR domain bound MDP. Although the Wang and

colleagues were able to demonstrate the direct interaction between the LRR domain and MDP, their affinity purification assay possessed several limitations. The assay provides only qualitative data on the interaction and was unable to define the affinity or kinetics of the binding event. Since this seminal finding in 2008, there have been no additional studies reported on this important interaction.

The seminal findings lead to two important questions: How promiscuous is the binding site for MDP? What is the strength of this interaction? Interestingly, acetylation on the amine at the 2 position of the carbohydrate of MDP increases the concentration of compound needed for 50% true hyphae to 4 mM compared to 30.64 μ M when the amine is unprotected². This would imply that the free amine is important for hydrogen bonding when the binding event occurs. Additionally, the initiation of hyphae growth by micromolar concentrations of the monosaccharide peptidoglycan fragments is intriguing. Most interactions between monosaccharides and proteins have K_d values in the millimolar range⁵. Traditionally, it has been thought that multivalent binding is required for biologically relevant carbohydrate interactions⁶.

In order to truly understand how *C. albicans* regulate morphology in response to bacteria, quantitative biophysical assays are necessary to determine the molecular mechanism of carbohydrate recognition by the LRR. In this chapter, I discuss the development of a surface plasmon resonance (SPR) assay and a fluorescence polarization (FP) assay to determine the promiscuity and the binding affinity of the LRR domain to bacterial derived ligands.

4.2 Materials and Methods

4.2.1 Materials

Alkane thiol reagents were purchased from SensoPath Technologies. Gold sensor chips were purchased from GE Health Care. A solution of 0.5% SDS was purchased from GE Healthcare Life Sciences. All other chemicals were purchased from Sigma-Aldrich, unless otherwise indicated. Muramyl tripeptide (**4.1**) was synthesized by my colleague Siaviash Mashayekh. 6-Bodipy-MDP (**4.8**) was synthesized by Dr. James Melynyk. Synthetic considerations are not included here but can be found in the resulting publication⁷.

4.2.2 Protein Expression and Purification

4.2.2.1 MBP-LRR

MBP-LRR was expressed and purified from *E. coli* as described in Chapter 2 (Materials and Methods 2.2.5-2.2.6). After refolding, the purified protein was dialyzed overnight against 1 L SPR assay buffer (50 mM Sodium Phosphate with 150 mM NaCl, pH 6.5).

4.2.2.2 Free MBP-tag expression and purification

The empty modified pMAL-c5x was transformed into BL21 (DE3) *E. coli* cells (Agilent Technologies). The free MBP-tag was expressed in 1 L LB media cultures containing carbenicillin (100 µg/mL). Cultures were grown at 30 °C until an OD₆₀₀ of 0.8 was reached. 1 mM of IPTG was added and the cultures were incubated

overnight at 18 °C. *E.coli* cells were pelleted by centrifugation at 5,000 rpm for 10 minutes. The supernatant was discarded and pellets stored at -80 °C until use.

A 1 L pellet was resuspended in 30 mL lysis buffer (50 mM sodium phosphate, pH 7.9 containing 150 mM NaCl and 10 mM imidazole) with 2 protease inhibitor tablets. The suspension was lysed on ice using sonication with an amplitude setting of 50% with pulsing 1s on and 1s off for 3 min total. The lysate was cleared by centrifugation at 15,000 rpm for 15 minute and the pellet was discarded.

The free MBP-tag was purified utilizing Fast-Protein Liquid Chromatography (FPLC) (Biorad) with a 5 mL HisTrap HP column (GE Healthcare). The column was equilibrated with 5 column volumes of lysis buffer, 5 column volumes of elution buffer (50 mM sodium phosphate, pH 7.9 containing 150 mM NaCl and 500 mM imidazole), and finally 10 column volumes of lysis buffer at a flow rate of 1 mL/min before the sample was applied. 25 mL of supernatant was applied to the column at a rate of 1 mL/min. The column was then washed with 5 column volumes of lysis buffer at a rate of 1 mL/min. Free MBP-tag was eluted with an gradient of 0-100% elution buffer over 20 column volumes. Fractions containing free MBP-tag were dialyzed against 1 L of SPR assay buffer.

4.2.3 Surface Plasmon Resonance

Conditions for preparing the SPR chip, mixed-SAM and running the SPR assay were adapted from Grimes et al.⁸ and Schaefer and Melnyk et al.⁹. The BIAcore 3000 instrument was used for all SPR studies described in this manuscript The cassettes described below were docked into the BIAcore 3000.

4.2.3.1 Preparation of Gold Thiol Chip (Mixed SAM)

The gold chip (GE Healthcare Life Sciences) was immersed in a solution of a mixture of thiols (1% mole fraction of hexa(ethylene glycol)-carboxylic acid (EG)₆CO₂H)-terminated thiol in tri(ethylene glycol) ((EG)₃OH)-terminated thiol) (2 mM total concentration) for 12 h. The chip was removed, rinsed with ethanol, and dried under a stream of nitrogen. The chip was then mounted onto a cassette following the protocol from the SIA Kit (GE Healthcare Life Sciences).

4.2.3.2 Immobilization of Compounds

For immobilization of the compounds **4.1** and **4.2**, a flow rate of 5 μ L/min was used. Fresh solutions of NHS (0.1 M) and EDC (0.4 M) in distilled water were prepared. Activation of the surface was achieved by equilibration with PBS, followed by the transformation of the surface carboxylic acid groups into NHS esters by passing a mixture of 0.05 M NHS and 0.20 M EDC in water over the surface for 7 min (the mixture is prepared by the automated robotics of the BIAcore 3000 using the DILUTE command). The system was then returned to PBS (2 min), and the solution of **4.1** was injected to flow cell 2, the solution of **4.2** was injected to flow cell 3 and the ethanolamine solution was injected to flow cell 4 for 7 min. This resulted in the formation of an amide bond by the displacement of the NHS esters. Following the coupling procedure all flow cells were cleaned by washing with 0.5% SDS at 10 μ L/min for 3 min.

4.2.3.3 Equilibrium Analysis

Solutions (1, 5, 10, 25, 50, 100, 150, 250, 500, and 1000 nM) of purified MBP-LRR were prepared by diluting stocks with SPR assay buffer. MBP-LRR solutions were applied to chip surface at a flow rate of 3 $\mu\text{L}/\text{min}$ for 20 min, washed with 1X PBS for 10 min, 0.5% SDS for 3 min, and 1X PBS for an additional 10 min. Binding of MBP-LRR to the chip surface was recorded in response units (RU), 1170 s after protein injection. Free MBP tag was used as a negative protein control.

4.2.3.4 Equilibrium Binding Analysis

Data was analyzed using Scrubber 2 (BioLogic Software), and binding curves were generated with Prism 6 (Graphpad). Sensograms were referenced to the ethanolamine capped lane and blank injections of SPR assay buffer to correct for non-specific binding. The K_D values were determined by plotting the RU at equilibrium as a function of varying ligand concentration and fitting the resulting points to a single site binding model given by¹⁰:

$$y = \frac{y_{max}(x)}{K_D + x}$$

4.2.3.5 Competition Assays

150 nM MBP-LRR was incubated with 0.15, 0.6, 2.4, or 9.6 μM **4.1-4.4** (Figure 4.1). Corresponding blanks were made with equal amounts of ligands to control for any changes in refractive index due to the small molecule. Samples were applied to the Biacore chip as described above. Relative responses were calculated by dividing the response of the MBP-LRR small molecule mixture by the response of apo

MBP-LRR Reported response levels are the average of three trials. 9.6 μM alanine (4.5), glutamate (4.6), and chloramphenicol (4.7) were used as negative competition controls.

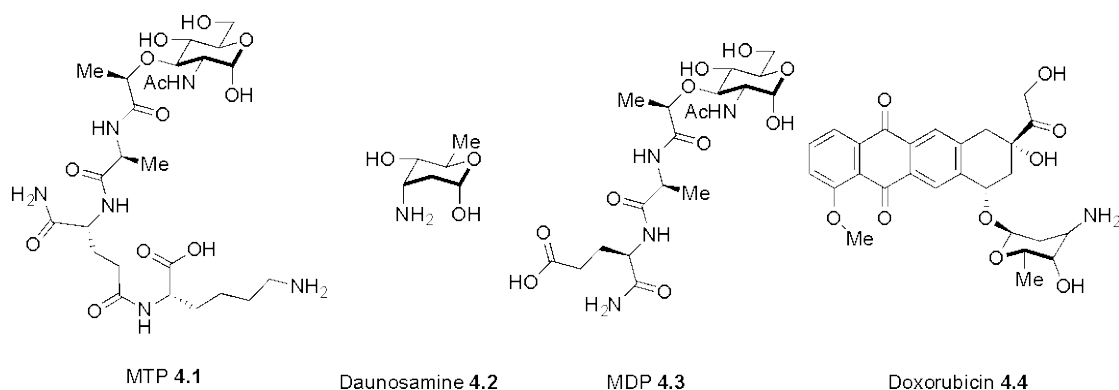


Figure 4.1 – Bacterial derived carbohydrates used in SPR assay

4.2.4 Fluorescence Polarization

4.2.4.1 Assay Setup

2000 nM MBP-LRR stock solutions were prepared in Blank buffer (50 mM Sodium Phosphate with 150 mM NaCl, pH 6.5), Total Binding Buffer (50 mM Sodium Phosphate with 150 mM NaCl and 100 nM 6-Bodipy-MDP (4.8), pH 6.5), or Non-specific binding buffer (50 mM Sodium Phosphate with 150 mM NaCl, 100 nM 6-Bodipy-MDP (4.8), and 100 μM MDP (4.3), pH 6.5). 1:2 serial dilutions were performed with each buffer until the MBP-LRR was at a concentration of 15.6 nM. 100 μL of each concentration was into the wells of a 96 well plate. The plate was protected from light and incubated at room temperature for 1 hr. Polarization was measured at 520 nm using a POLARstar Omega plate reader (BMG Labtech). Raw

perpendicular and parallel polarization data was obtained from the accompanying MARS data analysis software.

4.2.4.2 Data Analysis

Corrected polarization data was obtained by subtracting polarization values of the blank samples from the polarization values of Total and Non-specific samples. Anisotropy was calculated using the formula¹¹:

$$\frac{(I_{\parallel} - I_{\perp})}{(I_{\parallel} + 2 I_{\perp})} \times 1000.$$

Specific binding was determined by subtraction Anisotropy values of the non-specific samples from the total binding samples. Data was graphed in Prism 6 and fit using the parameters for one site binding.

4.3 Results and Discussion

4.3.1 Fluorescence Polarization

Previously, fluorescent polarization (FP) was used to demonstrate MDP binding to the LRR domain of Nod2¹². Knowing that the LRR domains of Cyr1 and Nod2 bind the similar ligands and have high sequence similarity, attempts were made to develop a FP assay for Cyr1.

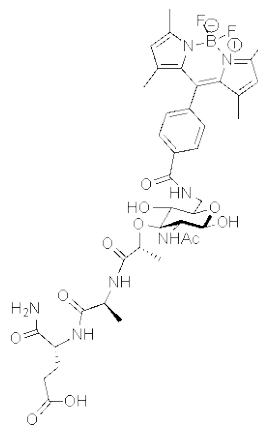


Figure 4.2 – 6-Bodipy-MDP (**4.8**) was used as a fluorophore in the FP assay.

In order to perform an FP assay with Cyr1-LRR, a ligand with a fluorescent molecule was needed. Previously, Dr. James Melynk synthesized a MDP derivative with a bodipy fluorophore attached to the 6-position (Figure 4.2, **4.8**) and this compound was utilized in the FP assay. 100 nM of **4.8** was incubated with serial dilutions of MBP-LRR ranging from 15.6 to 2000 nM. To account for non-specific binding, additional samples were prepared with 1000-fold excess unlabeled MDP (**4.1**). Samples were incubated for 1 hour to reach equilibrium and polarization values were obtained using a POLARstar Omega plate reader.

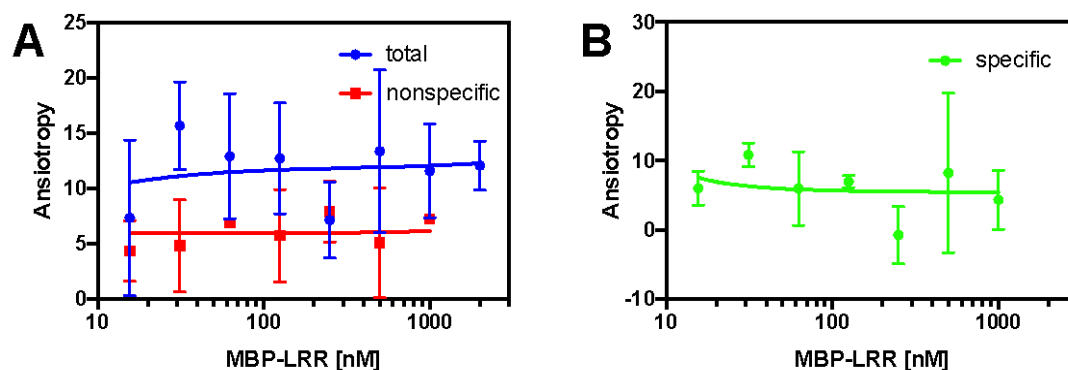


Figure 4.3- Results of Fluorescence polarization binding assay. A) Total and nonspecific binding anisotropy B) Specific Binding Anisotropy. The lack of change in anisotropy indicates the 6-bodipy MDP is not specifically binding MBP-LRR.

Polarization values were converted to anisotropy using the formula:

$$\frac{(\parallel - \perp)}{(\parallel + 2 \perp)} \times 1000$$

Comparing anisotropy to molar concentration of MBP-LRR generates a binding curve from which a K_d value can be determined. Unfortunately, anisotropic values did not change with increasing concentrations of MBP-LRR (Figure 4.3). Additionally, inclusion of 1000-fold excess of unlabeled MDP was unable to increase anisotropy values, indicating that the unlabeled MDP was incapable of affecting binding of 6-Bodipy MDP (4.8). We hypothesized the assay failed because either the bodipy moiety caused non-specific binding or the bodipy on the six position of MDP blocked binding to the LRR. The inability of free MDP to increase anisotropy values supports the hypothesis that 6-Bodipy MDP is non-specifically binding to the LRR. If this is the case, it is likely to be due to the hydrophobic bodipy fluorophore and

aggregating to the hydrophobic surface of the LRR domain. To optimize the assay, testing of additional fluorescent probes is needed. To test the hypothesis of the bodipy moiety blocked binding, we sought to develop a surface plasmon resonance assay. We chose to pursue the development of an SPR based assay, which would eliminate the need to fluorescently label the ligands.

4.3.2 Surface Plasmon Resonance (SPR)

4.3.2.1 Assay Design

Surface plasmon resonance (SPR) is a powerful assay, which eliminates the need for a fluorescent label on the ligand. This technique has gained prominence since its debut in the early 1990's¹³. SPR works by exploiting the evanescent wave phenomenon, in which an electromagnetic field is generated by the total internal reflection of light at the interface of a metallic surface and a solution¹⁴. In a typical SPR set up, a polarized light is directed through a prism with a high reflective index and onto the surface on which the ligand is immobilized. The angle of reflection is determined by the refractive index of the solution near the surface. Binding events change the refractive index, which can be evaluated by measuring the change in the angle of reflective light due to the alterations of the refractive index. These instruments provide incredible sensitivity with detections limits as low as 10 pg/mL.

In developing an SPR assay for Cyr1, it was important to choose a method of ligand coupling that would be both robust and highly sensitive. First, a decision had to be made of whether to attach the protein or the carbohydrate to the surface. Coupling the protein to the surface can be achieved by chemical immobilization, using aldehyde

or EDC/NHC chemistry, or affinity capture, employing antibodies or affinity fusion tags¹⁵. While protein attachment has advantages, such as being able to use crude samples employing affinity capture - coupling the LRR to the surface was not ideal. Due to the requirements of low ionic strength coupling buffers, 5-10 mM, the relatively unstable LRR likely would have aggregated. Additionally, the Ni-NTA/His tag interaction is not robust and it has been demonstrated that protein can be removed from the surface of an SPR chip with a 30 minute buffer wash¹⁶. It was decided that coupling the carbohydrates to the chip would be more practical. Coupling the carbohydrate has the distinct advantages of increasing the sensitivity of the assay. By attaching the smaller molecule, binding of the protein creates a larger SPR response, which can be attributed to the larger shift in refractive index of the solution at the chip surface. Using the 10 pg/mL as a guide, LRR binding could be detected at concentrations as low as 110 fM. It was decided to attach the bacterial carbohydrates to the surface and use the LRR in solution to determine binding affinity (Figure 4.4)

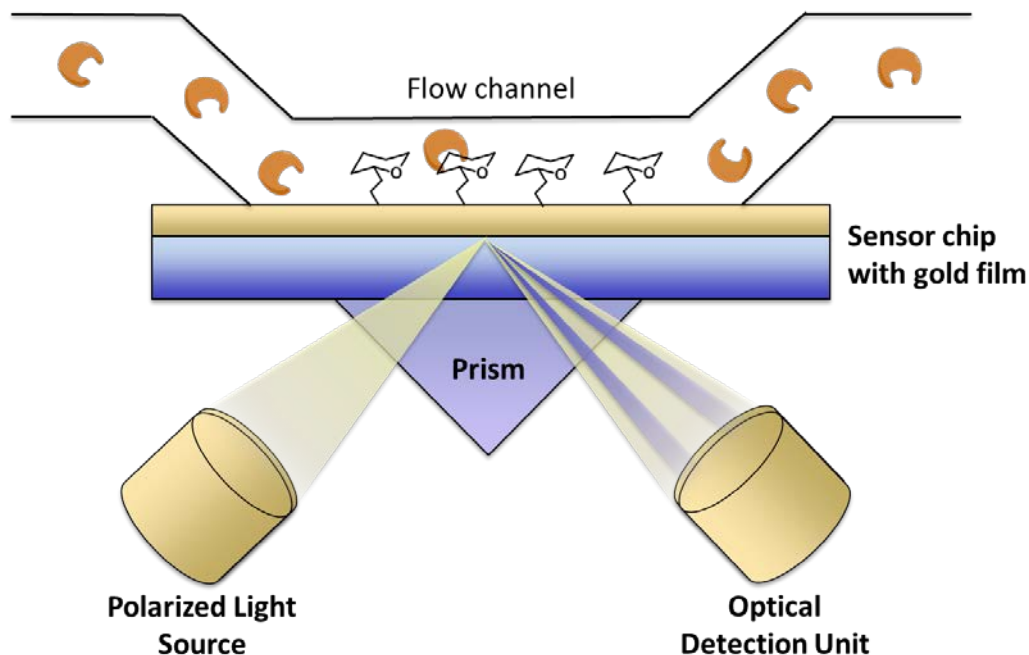


Figure 4.4 – SPR Assay. The bacterial carbohydrates are covalently coupled to the gold surface. The LRR domain is flowed over the chip and binding events are detected by measuring the change in refractive index occurring at the surface solution interface. Figure adapted from Cooper, *Nat Rev Drug Discov*¹⁴.

4.3.2.2 Chip Generation

Previously, our lab had designed an SPR assay to measure the binding affinity for Nod2 to peptidoglycan fragments⁸. In these experiments, peptidoglycan was attached to the SAMs through an amine modification installed on the six position of the carbohydrate. To test Cyr1-LRR's affinity for bacterial-derived carbohydrates, no synthetic modifications were needed. Coupling to the surface was achieved using the amine in the lysine in the peptide chain of MTP or the amine at the third position of daunosamine. A self-assembled monolayer (SAM) was formed by soaking the gold chip in a solution of PEG-thiols containing 1% carboxylic acid terminated PEG-thiols.

The gold chip was then loaded into the Biacore instrument for coupling of the ligands. Using methods developed by George Whitesides, NHS/EDC chemistry was used to couple the ligands to the alkanethiolates SAM¹⁷. Applying 1-ethyl-3-(3-dimethylaminopropyl) carbodiimide (EDC) to the surface followed by N-hydroxysuccinimide (NHS) converted the carboxylic acids to reactive NHS esters (Figure 4.5). MTP, lane 2, and daunosamine, lane 3, were applied to the chip, with their respective amines displacing the NHS esters to form stable amide bonds. Ethanolamine was applied to lane 4 to be used as a reference lane.

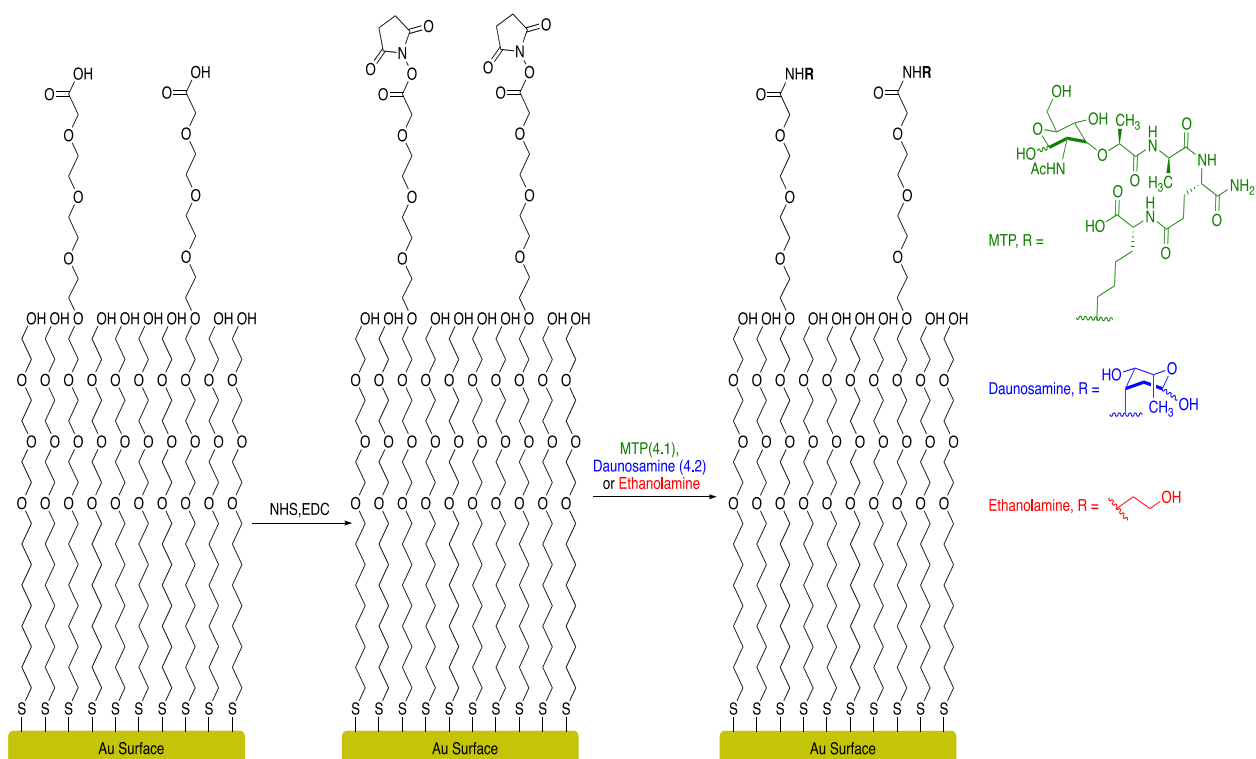


Figure 4.5 – Attachment of MTP and Daunosamine utilizing NHS/EDC coupling chemistry.

4.3.2.3 MTP and Daunosamine binding

To determine the binding affinity of Cyr-LRR for daunosamine (**4.2**) and MTP (**4.1**), purified MBP-LRR (Chapter 2) was diluted to concentrations ranging from 1 to 1000 nM. Each concentration of MBP-LRR was applied to the chip at a flow rate of 3 $\mu\text{L}/\text{min}$ for 20 minutes to allow for binding to reach equilibrium. A binding sensogram was generated for daunosamine and MTP with non-specific binding subtracted as measured by the response of the ethanolamine lane (Figure 4.6).

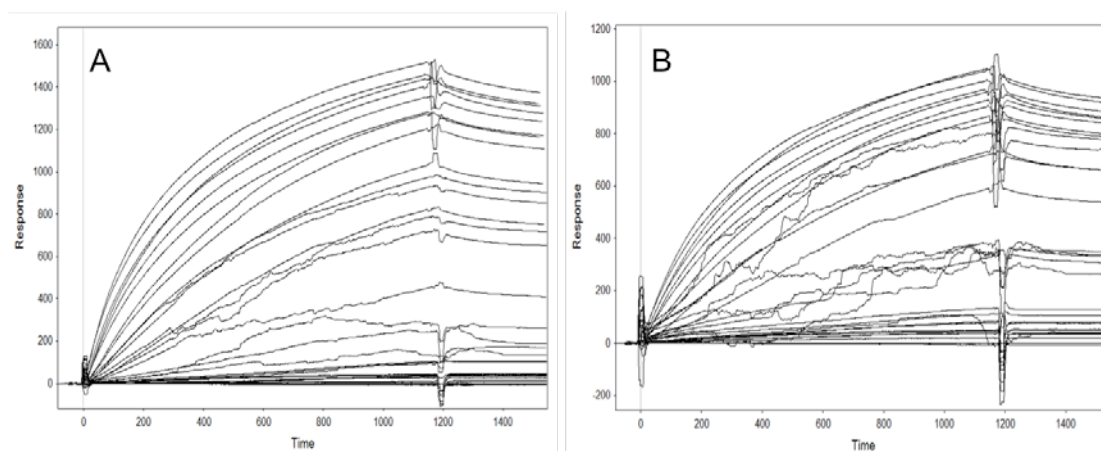


Figure 4.6 - Raw Sensogram of MBP-LRR binding to A) MTP (**4.1**) and B) daunosamine (**4.2**).

The response units at equilibrium (~ 1170 s) was plotted against molar concentration of MBP-LRR and fit to a single site-binding model (Materials and Methods 4.2.3.4) to determine dissociation constants (K_d) for MTP (**4.1**) and daunosamine (**4.2**) (Figure 4.7). MBP-LRR bound to MTP with a K_d of 176 ± 68 nM and to daunosamine with a K_D of 287 ± 88 nM, much lower than the millimolar affinities typically expected for monosaccharide-protein interactions. Interestingly,

both MTP and daunosamine had similar binding affinities, despite the large difference in ability to induce hyphae formation as demonstrated in chapter 3. This difference between binding and activation could be caused by interactions occurring between the amino acids in the active site of the protein and the increased number of hydrogen bond donors and acceptors on the peptide stem of MDP. To support this hypothesis, additional controls were needed to validate the SPR assay, and rule out non-specific interactions.

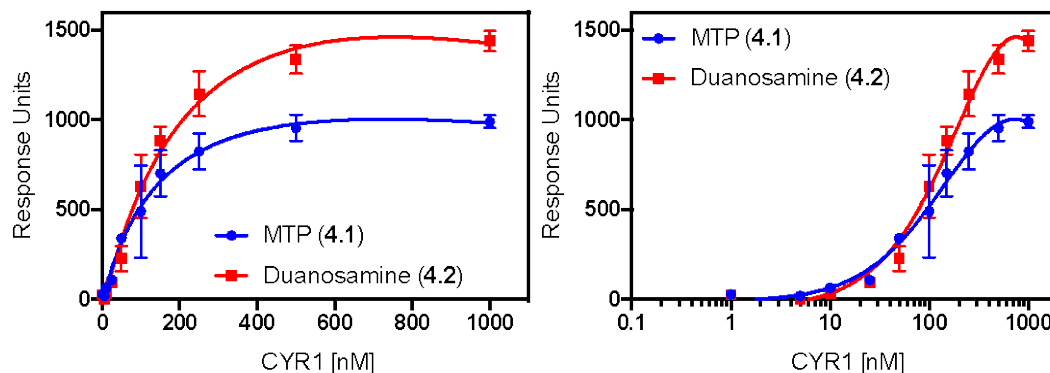


Figure 4.7 – MBP-LRR binds to MTP (4.1) ($K_D = 176 \pm 68$ nM) and to daunosamine (4.2) ($K_D = 287 \pm 88$ nM) with nanomolar affinity

4.3.2.4 MBP Control

To ensure that the observed K_d values were the result of the carbohydrates binding to the LRR and not the fusion partner, free MBP-tag was purified (Materials and Methods 4.2.2.2; Figure 4.8.) and binding to the carbohydrates was tested using the SPR assay described. The free MBP tag was diluted to 715 nM in SPR assay buffer and three samples were tested. Free MBP-tag showed markedly reduced

binding to either MTP or daunosamine (Figure 4.9). Response levels were 10% of what was observed when MBP-LRR was applied to the surface. This result indicates that the observed K_d values are due to the LRR domain and not the MBP tag binding the ligands. It also indicates that the surface is not non-specifically absorbing any protein that is used in the assay. However, the control by itself does not assure that the Cyr1-LRR is not absorbing to the surface rather than binding with MTP and daunosamine.

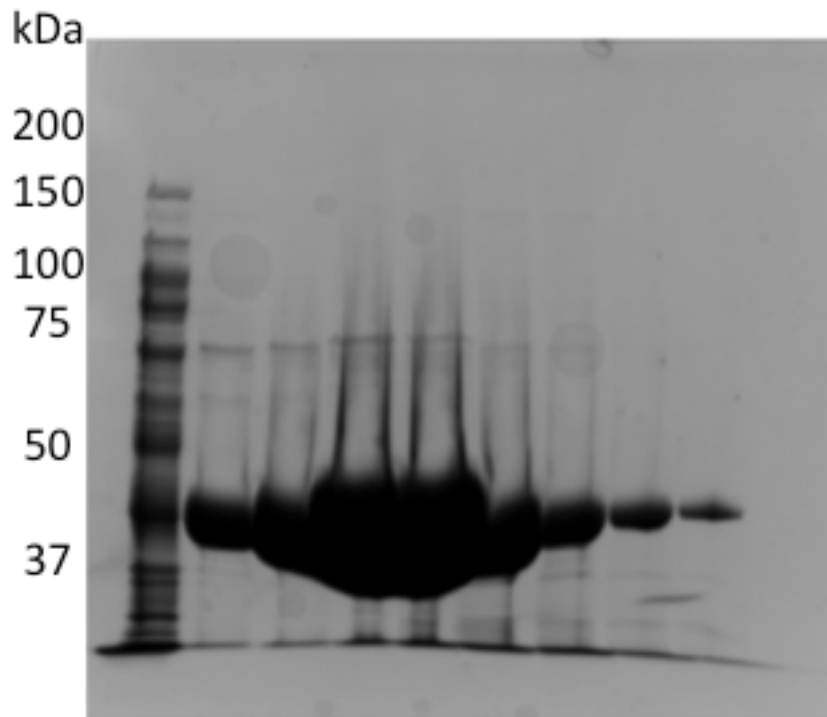


Figure 4.8 – Purified MBP-tag. Protein bands between the 37 kDa and 50 kDa molecular weight markers are consistent with the 42 kDa molecular weight of MBP. Lane 1: supernatant; Lanes 2-9: Free MBP-tag

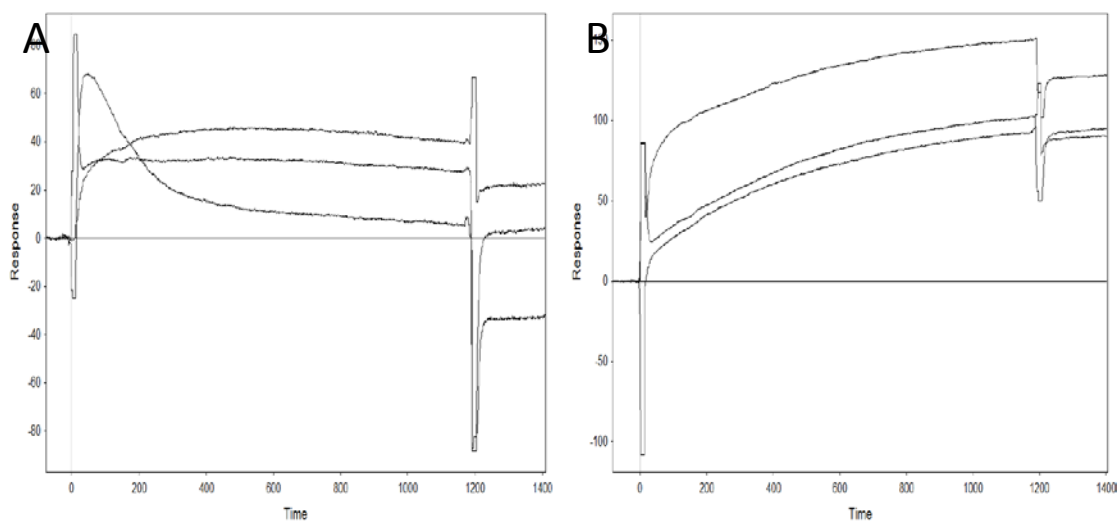


Figure 4.9 – Raw sensogram shows decreased binding of free MBP-tag to either A) MTP or B) Daunosamine

4.3.2.5 Competition assay

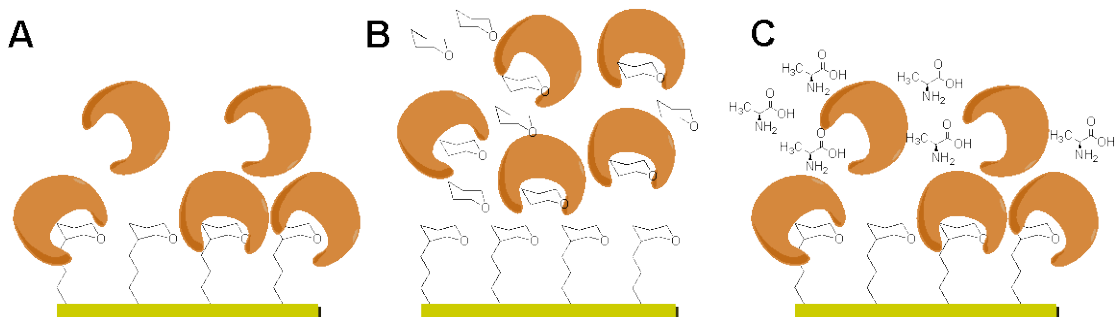


Figure 4.10 – Experimental design of competition assay. **A)** With no free ligand present the LRR can bind carbohydrates tethered to the surface. **B)** Preincubation with free ligand inhibits LRR binding to the surface **C)** Preincubation with a small molecule that does not bind the LRR has not effect on surface binding.

To confirm that the observed K_d values were a result of Cyr1-LRR's affinity for the bacterial-derived carbohydrate and not the result of non-specific absorption to the chip surface, a competition assay was performed (Figure 4.10). Prior to applying the protein to the chip surface, MBP-LRR was incubated with increasing concentration – between 0.15 μ M and 9.6 μ M - of MTP (**4.1**) or daunosamine (**4.2**). If the observed binding responses were the result of specific interactions between the LRR and the carbohydrates, incubating the protein with free ligand prior to the assay should reduce or eliminate the binding response. Response levels were recorded and results were compared to response levels of apo MBP-LRR, LRR not incubated with free ligand. Preincubation with 9.6 μ M MTP (**4.1**) decreased binding responses to MTP (**4.1**) and daunosamine (**4.2**) by $41.48 \pm 21.93\%$ and $49.47 \pm 19.74\%$ of apo levels respectively. A similar effect was observed when MBP-LRR was preincubated with daunosamine. Compared to apo levels, a $43.69 \pm 24.32\%$ decrease in binding response to MTP (**4.1**) and a $43.46 \pm 23.84\%$ decrease in binding response to daunosamine (**4.2**) was observed with a preincubation of 9.6 μ M daunosamine (**4.2**) (Figure 4.11). While a drastic reduction in binding response was observed, the addition of gross excess of free ligand was not able to completely eliminate binding to the surface. We hypothesize that the remaining binding response can be attributed to the kinetics of the interaction, where the protein is disassociating from the free ligand in solution and interaction with immobilized ligand in the flow path. The ability of free MTP or daunosamine to inhibit binding to each other on the surface suggests that Cyr1-LRR contains a single binding site for carbohydrates.

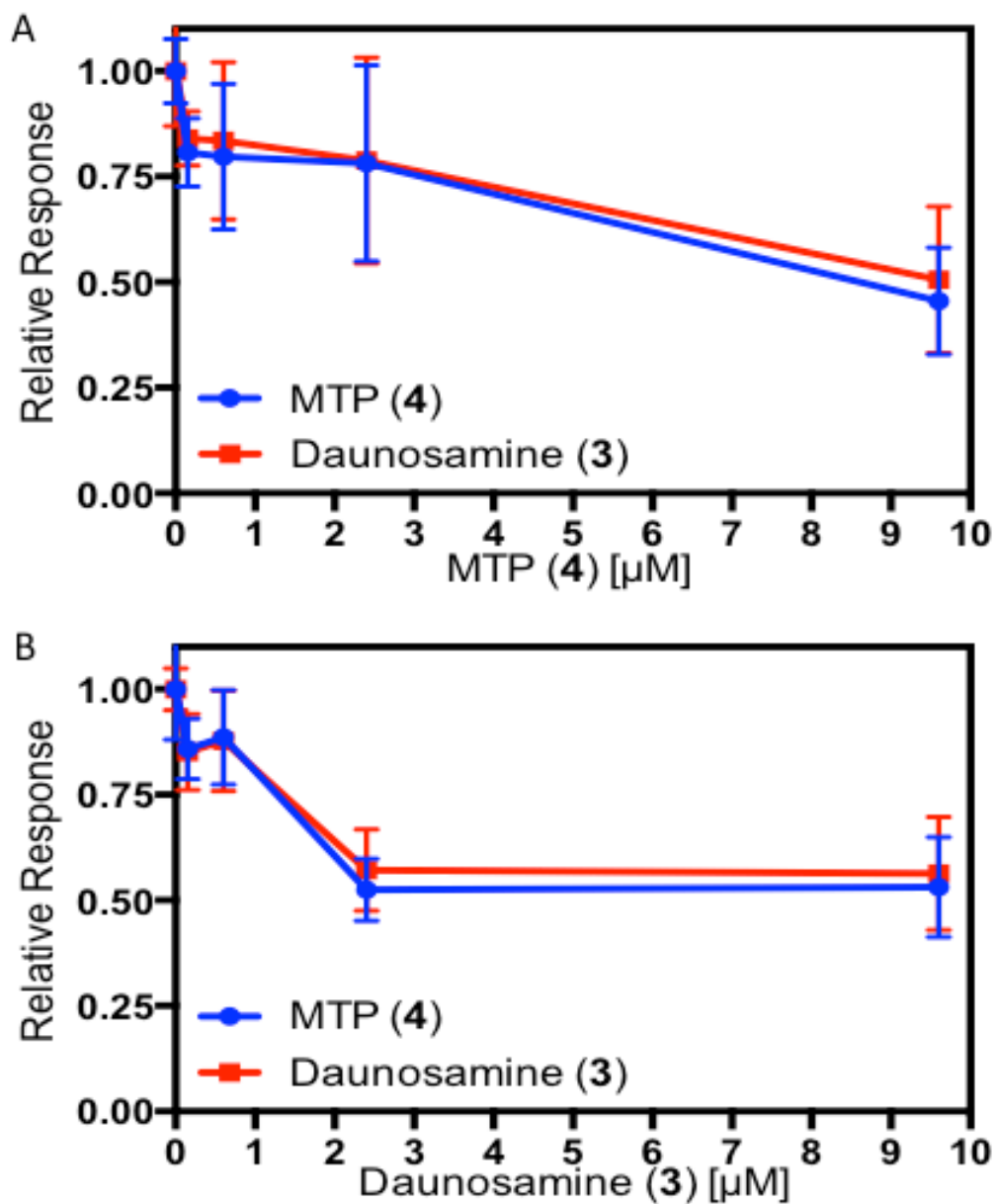


Figure 4.11- Preincubation with A) MTP or B) Daunosamine is capable of decreasing MBP-LRR binding by 50%. Binding was reported as a relative response, dividing each sample by the response of apo MBP-LRR (no preincubation with ligands). The relative response was set to 1 and values less than one indicate that the compound is capable of competing binding.

With the knowledge that daunosamine and MTP competitively inhibit binding to each other, we hypothesized that Cyr1 contained a single promiscuous binding site for carbohydrates. To support this hypothesis, additional ligands were examined utilizing the competition assay to probe the promiscuity of MBP-LRR. MDP – a peptidoglycan fragment similar to MTP – and doxorubicin – a *Streptomyces peucetius* natural product containing daunosamine – were preincubated with MBP-LRR prior to injection on the Biacore. MDP was capable of reducing binding of Cyr1-LRR to MTP and daunosamine by $55.40 \pm 26.91\%$ and $58.52 \pm 21.93\%$ of apo levels respectively. Preincubation with doxorubicin was perhaps the most effective at inhibiting binding, as MTP binding was decreased to $38.66 \pm 16.00\%$ and daunosamine binding levels were $33.13 \pm 16.89\%$ (Figure 4.12). It is unsurprising, that MDP inhibits binding to the surface to the same extent as MTP, due to the fact that MDP is only one amino acid shorter and otherwise are identical. This would suggest similar binding contacts for both MDP and MTP as the lysine in MTP is tethered to the chip. The large decrease observed due to doxorubicin can be attributed to the increased sterics of the aromatic rings blocking the binding site. However, this cannot be confirmed without obtaining a crystal structure of doxorubicin bound to the LRR. The ability of each of the four compounds to decrease the binding response to MTP and daunosamine supports our hypothesis that Cyr1-LRR contains a single binding site for the bacterial derived carbohydrates.

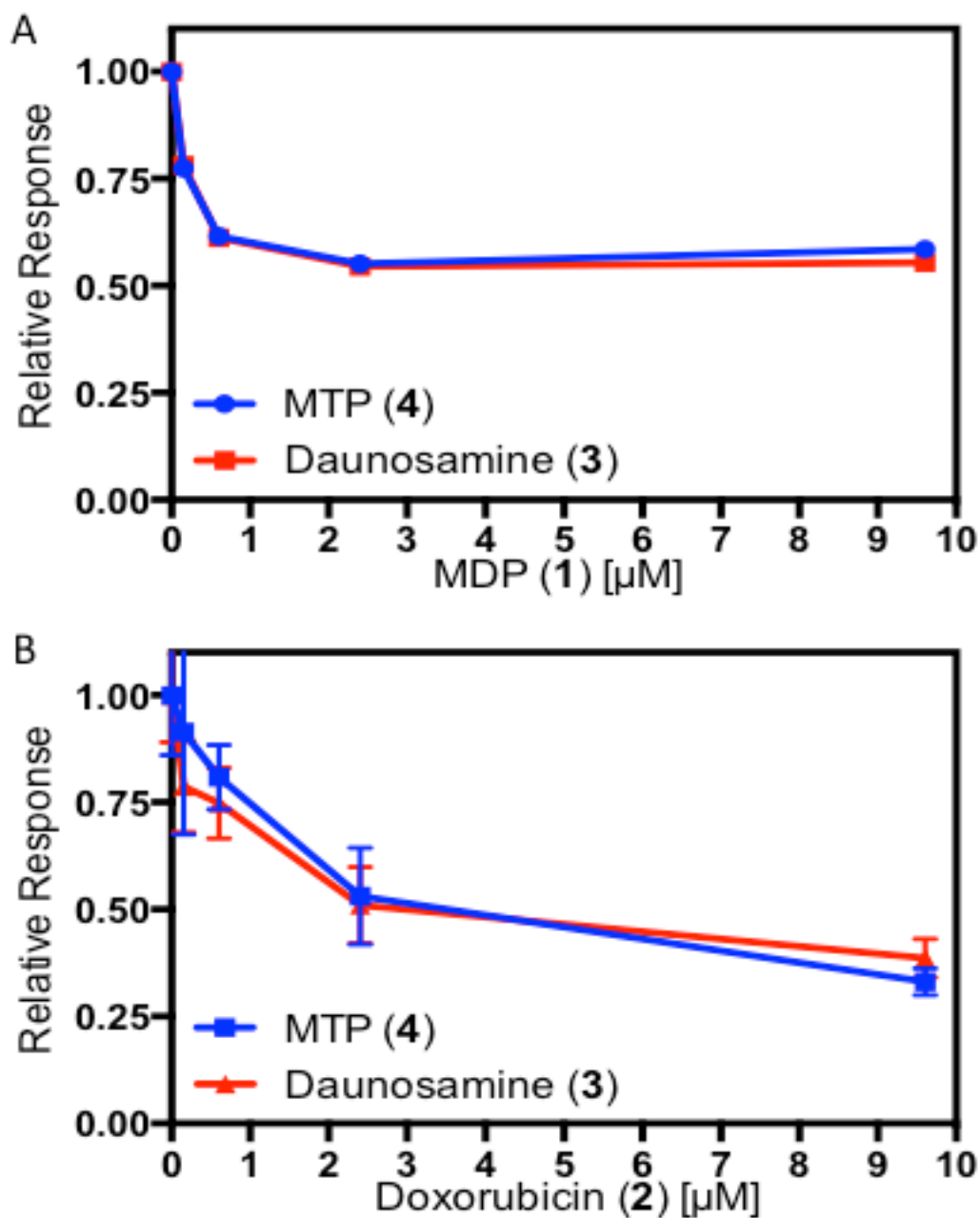


Figure 4.12- MBP-LRR binding to MTP and daunosamine can be competed away by A) MDP and B) Doxorubicin. Binding was reported as a relative response, dividing each sample by the response of apo MBP-LRR (no preincubation with ligands). The relative response was set to 1 and values less than one indicate that the compound is capable of competing binding.

4.3.2.6 Nonbinding Competition Control

While the competition assay showed that the observed binding responses were not caused by absorption to the surface and suggest a single binding pocket, an additional control identifying compounds that do not bind the LRR was needed to confirm specificity. Three compounds not containing carbohydrates were tested in the competition assay (Figure 4.13). Individual amino acids alanine and glutamate, which are present in the peptide stem of MDP and MTP, as well as chloramphenicol – a natural antibiotic product produced by *Streptomyces venezuelae* – were tested for their ability to inhibit MBP-LRR binding to MTP and daunosamine.

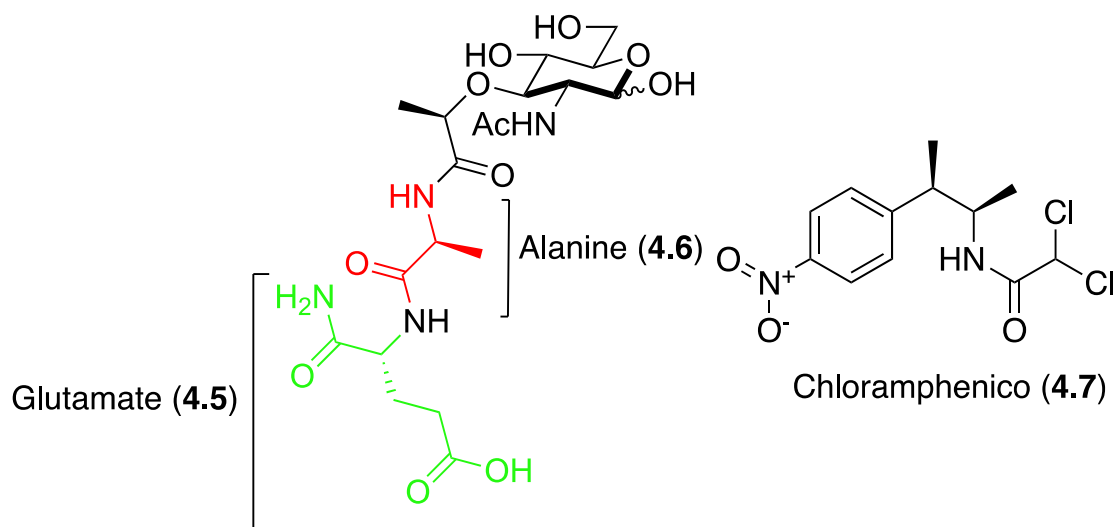


Figure 4.13- Chloramphenicol, a natural product for *Streptomyces* not containing a carbohydrate, and the individual amino acids (alanine and glutamate) forming the peptide stem of MDP were tested for the ability to inhibit MBP-LRR binding to carbohydrates.

9.6 μM of alanine, glutamate, and chloramphenicol were preincubated with 150 nM MBP-LRR. The competition with high concentration of MTP and daunosamine were repeated as positive competition controls. The response levels at equilibrium were compared to that of the apo protein. Again MTP and daunosamine caused approximately a 50% reduction in binding response. Alanine, glutamate, and chloramphenicol had no effect on MBP-LRR binding (Figure 4.14). The inability to bind individual amino acids and chloramphenicol, supports the hypothesis that while the binding site in the LRR is promiscuous it does show selectivity for carbohydrates.

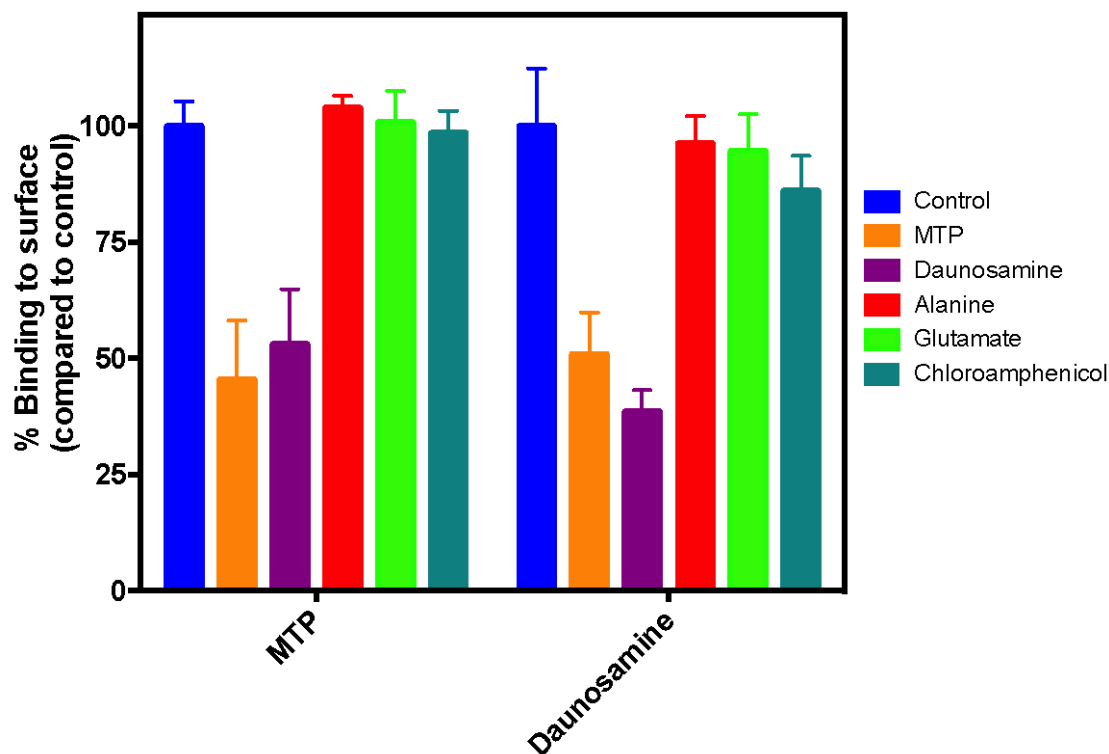


Figure 4.14 –MBP-LRR was incubated with 9.6 μM of each compound prior to being used in the SPR assay. Results were reported as the % binding to the surface. Calculated by dividing each sample by the response of control (no ligand). The control sample was set to 100% and values less than 100% indicate that the compound is capable of inhibiting binding. The non-carbohydrate compound did not inhibit binding.

4.4 Conclusions

Previously, the Wang and colleagues demonstrated that the LRR domain of Cyr1 was capable of binding MDP². However, they provided no biochemical characterization of this interaction in the seminal publication. Since the initial publication of their findings there have been no follow up studies further investigating the nature of the reported interactions. Intrigued that micromolar concentrations of a monosaccharide were capable of inducing hyphae formation in *C. albicans*, we sought

to understand the molecular nature of this binding event. In this chapter, I describe the development of two assays to determine the binding affinity of Cyr1 for bacterial derived carbohydrates. Using an SPR assay we were the first to demonstrate that Cyr1 bound daunosamine and doxorubicin via the LRR domain. Excitingly, daunosamine and MTP bound Cyr1 with K_d values of approximately 200 nM, much lower than the typical mM values expected for protein-carbohydrate interactions.

In the FP assay, binding was unable to be detected between the LRR and the 6-bodipy MDP (**4.8**). However, despite the lack of binding observed in the initial trials, additional iterations should be pursued. The MDP fluorophore needs to be optimized before definitely concluding that the assay is not working. It is possible that the bodipy fluorophore on the 6-position blocks the molecule from entering the binding site on the LRR domain. Taking clues from the binding of LRR to MTP on the surface of the SPR assay, attaching the fluorophore to the alanine may be better tolerated. To control for non-specific binding, a less hydrophobic fluorophore – such as fluorescein- should be used.

The lack of binding in the FP assay does not discredit the results seen in the SPR analysis. In developing the SPR assay, we were the first group to independently confirm the interaction between Cyr1 and peptidoglycan fragments. It was determined that MTP (**4.1**) bound the LRR domain with a K_d value of 176 ± 68 nM. Interestingly, this is orders of magnitude tighter than is expected for monosaccharide binding. Using the competition analysis, it was demonstrated that modifications of the peptides on peptidoglycan are well tolerated, as both MTP (**4.1**) and MDP (**4.2**) bound the LRR. Additionally, despite reports that the *Streptomyces* natural product –

doxorubicin - affected hyphae formation¹⁸, there has been no indication of which pathway was involved. We were the first to demonstrate that doxorubicin and its sugar moiety, daunosamine, directly interacted with the LRR domain of Cyr1. Finally, the ability of all carbohydrates tested to inhibit binding to daunosamine and MTP, suggests a single promiscuous binding site for carbohydrates.

This SPR assay provides a powerful tool to identify molecules that bind to Cyr1. Further studies aim to identify additional compounds that bind Cyr1 and inhibit hyphae formation. Continuing to expand the compounds that inhibit hyphae formation and gaining additional insight into the biological characterizations of these interactions have the potential aid in the development of therapeutics to combat deadly systemic *C. albicans* infections.

REFERENCES

1. Reynolds, R., The filament inducing property of blood for *Candida albicans* : its nature and significance. *Clin. Res. Proc.* **1956**, *4*, 40.
2. Xu, X. L.; Lee, R. T.; Fang, H. M.; Wang, Y. M.; Li, R.; Zou, H.; Zhu, Y.; Wang, Y., Bacterial peptidoglycan triggers *Candida albicans* hyphal growth by directly activating the adenylyl cyclase Cyr1p. *Cell Host Microbe* **2008**, *4* (1), 28-39. DOI: 10.1016/j.chom.2008.05.014.
3. Rogers, H. J., Peptidoglycans (mucopeptides): structure, function, and variations. *Ann N Y Acad Sci* **1974**, *235* (0), 29-51.
4. Ng, A.; Xavier, R. J., Leucine-rich repeat (LRR) proteins: integrators of pattern recognition and signaling in immunity. *Autophagy* **2011**, *7* (9), 1082-4.
5. Luo, J.; Xu, Z.-K., Protein–Carbohydrate Interactions on the Surfaces of Glycosylated Membranes. In *Proteins at Interfaces III State of the Art*, American Chemical Society: 2012; Vol. 1120, pp 253-275. DOI: doi:10.1021/bk-2012-1120.ch011
10.1021/bk-2012-1120.ch011.
6. Reynolds, M.; Pérez, S., Thermodynamics and chemical characterization of protein–carbohydrate interactions: The multivalency issue. *Comptes Rendus Chimie* **2011**, *14* (1), 74-95. DOI: <https://doi.org/10.1016/j.crci.2010.05.020>.
7. Burch, J. M.; Mashayekh, S.; Wykoff, D. D.; Grimes, C. L., Bacterial Derived Carbohydrates Bind Cyr1 and Trigger Hyphal Growth in *Candida albicans*. *ACS Infect Dis* **2018**, *4* (1), 53-58. DOI: 10.1021/acsinfecdis.7b00154.
8. Grimes, C. L.; Ariyananda Lde, Z.; Melnyk, J. E.; O'Shea, E. K., The innate immune protein Nod2 binds directly to MDP, a bacterial cell wall fragment. *J Am Chem Soc* **2012**, *134* (33), 13535-7. DOI: 10.1021/ja303883c.
9. Schaefer, A. K.; Melnyk, J. E.; Baksh, M. M.; Lazor, K. M.; Finn, M. G.; Grimes, C. L., Membrane Association Dictates Ligand Specificity for the Innate Immune Receptor NOD2. *ACS chemical biology* **2017**. DOI: 10.1021/acscchembio.7b00469.

10. Hein, P.; Michel, M. C.; Leineweber, K.; Wieland, T.; Wettschureck, N.; Offermanns, S., Receptor and binding studies. In *Practical Methods in Cardiovascular Research*, Springer: 2005; pp 723-783.
11. Lakowicz, J. R., *Principles of fluorescence spectroscopy*. Springer: New York, 2006.
12. Mann, J. K.; Shen, J.; Park, S., Enhancement of Muramyl Dipeptide-Dependent NOD2 Activity by a Self-Derived Peptide. *Journal of cellular biochemistry* **2017**, *118* (5), 1227-1238. DOI: 10.1002/jcb.25778.
13. Nguyen, H. H.; Park, J.; Kang, S.; Kim, M., Surface plasmon resonance: a versatile technique for biosensor applications. *Sensors (Basel)* **2015**, *15* (5), 10481-510. DOI: 10.3390/s150510481.
14. Cooper, M. A., Optical biosensors in drug discovery. *Nat Rev Drug Discov* **2002**, *1* (7), 515-28. DOI: 10.1038/nrd838.
15. Fischer, M. J. E., Amine Coupling Through EDC/NHS: A Practical Approach. In *Surface Plasmon Resonance: Methods and Protocols*, Mol, N. J.; Fischer, M. J. E., Eds. Humana Press: Totowa, NJ, 2010; pp 55-73. DOI: 10.1007/978-1-60761-670-2_3.
16. Khan, F.; He, M.; Taussig, M. J., Double-hexahistidine tag with high-affinity binding for protein immobilization, purification, and detection on ni-nitrilotriacetic acid surfaces. *Anal Chem* **2006**, *78* (9), 3072-9. DOI: 10.1021/ac060184l.
17. Lahiri, J.; Isaacs, L.; Tien, J.; Whitesides, G. M., A Strategy for the Generation of Surfaces Presenting Ligands for Studies of Binding Based on an Active Ester as a Common Reactive Intermediate: A Surface Plasmon Resonance Study. *Analytical Chemistry* **1999**, *71* (4), 777-790. DOI: 10.1021/ac980959t.
18. Kwok, S. C.; Schelenz, S.; Wang, X.; Steverding, D., In vitro effect of DNA topoisomerase inhibitors on *Candida albicans*. *Med Mycol* **2010**, *48* (1), 155-60. DOI: 10.3109/13693780903114934.

Chapter 5

CONCLUSIONS AND FUTURE DIRECTIONS

5.1 Introduction

With the launch of the National Institute of Health's Human Microbiome project, the importance of the microorganisms residing in and on the human body rapidly came into focus¹. The bacterial composition of the microbiome has been implicated in disease states including asthma, allergies, diabetes, cancer, and Crohn's disease²⁻⁶. While the impact of bacterial species in the microbiome has been widely studied, there is a smaller population of fungi, the mycobiome, whose importance to human health is not as well understood. Similar to bacterial species, recent studies have implicated the mycobiome in maintaining proper health⁷. Interestingly, fungal composition can mediate inflammation in mouse colitis models by regulating bacterial populations⁸. While it has been demonstrated that fungi can help regulate bacterial populations, these interactions are not always beneficial to the host. *Candida albicans*, commonly found in the gastrointestinal tract, has been demonstrated to form mixed biofilms with bacterial pathogens including *Pseudomonas aeruginosa*, *Staphylococcus epidermis*, *Staphylococcus aureus*, and *Streptococcus mutans*⁹⁻¹³.

Normally, *C. albicans* is a benign member of the human microflora. However, under certain conditions, it can turn pathogenic and becomes the most common cause of human fungal infections¹⁴. *C. albicans* pathogenicity is regulated by a morphological switch from budding yeast to filamentous hyphae¹⁵. Hyphae formation

is a complex process regulated by the interaction of several signaling cascades¹⁶. Of central importance is the cAMP-PKA pathway, as genetic knockouts of the lone adenylyl cyclase, Cyr1, abolishes hyphae formation¹⁷. In a seminal 2008 paper, Wang and colleagues demonstrated that via its leucine rich repeat (LRR) domain, Cyr1 can bind peptidoglycan fragments and activate hyphae formation¹⁸. However, since this discovery there has been no further characterization of the interaction. In this thesis, I have described methods to obtain recombinant LRR and the development of assays that work towards elucidating the molecular mechanism of the interaction between the LRR domain and bacterial carbohydrates.

5.2 Conclusions

5.2.1 Characterization of the Leucine Rich Repeat (LRR) Domain of the *Candida Albicans* Adenylyl Cyclase (*CaCyr1*)

The interaction between Cyr1 and peptidoglycan was first discovered with a pull-down assay using biotinylated muramyl dipeptide (MDP) and a GST-LRR construct expressed and purified from *E.coli* by Wang and coworkers¹⁸. While this paper first highlighted this interaction, expression conditions, purification techniques, and characterization of the purified protein were not described¹⁸. To further study this interaction, I first sought to develop an assay to quantify the binding of MDP to the LRR, it was necessary to obtain recombinant LRR. In chapter 2, I describe two methods I developed to obtain the pure protein. Initial attempts were made to purify a GST fusion protein spanning amino acids 480-900 of Cyr1, the same described by Wang and co-workers. Early purification attempts resulted in the co-purification of the chaperone proteins, DnaK and GroEL. Incubating the lysate with aliquots of denatured

proteins and washing the column with buffers containing ATP effectively removed these impurities. Despite obtaining pure GST-LRR, yields were low as much of the protein remained in the insoluble fraction.

I next sought to increase solubility. To accomplish this, I switched the fusion partner from a GST tag to a MBP tag. Unfortunately, a large portion of the protein still remained insoluble and was expressed in inclusion bodies. At this point, I started to investigate the possibility of isolating the protein from the inclusion bodies. The inclusion bodies containing MBP-LRR were washed, solubilized with urea, and purified using IMAC chromatography. The purified protein was successfully refolded by dialysis against buffers containing high concentrations of arginine. Analysis by circular dichroism determined the refolded protein contained 60.3% α -helix and 16.7% β -strand secondary structure. This was identical to MBP-LRR purified from the soluble fraction, indicating that the proper conformation was obtained after refolding. Purifying the protein while denatured ensured that no peptidoglycan fragments contaminated the sample. This method can be used as a guide to express and purify other peptidoglycan binding proteins in an *E. coli* system.

5.2.2 Bacterial Derived Carbohydrates Trigger Hyphae Formation in *C. albicans*

It has been demonstrated that peptidoglycan can trigger hyphae formation in *C. albicans*¹⁸. Minor changes such as an acetyl group capping the amine at the two position of the carbohydrate greatly effects the concentration necessary to elicit a hyphae response¹⁸. In order understand how *C. albicans* responds to bacteria, I sought to determine the minimum components of peptidoglycan necessary for hyphae

formation. In chapter 3, I described three assays used to show the effects of peptidoglycan fragments and bacterial natural products.

A brightfield microscopy assay illustrated the necessity of the carbohydrate moiety in inducing hyphae formation. The peptide portion of peptidoglycan was not significant as altering the length and stereochemistry of the peptide stem had no effect on the amount of hyphae formation. I discovered carbohydrates besides those found in peptidoglycan can trigger hyphae formation. Daunosamine, the sugar moiety of the *Streptomyces* natural product doxorubicin, elicited a morphological change. ELISA experiments showed increased cAMP levels when *C. albicans* cultures were exposed to MTP or daunosamine indicating these carbohydrates are activating Cyr1 and the cAMP-PKA pathway. Finally, RT-PCR experiments showed increased expression of hyphae specific genes, Ece1 and Hwp1, when cells were exposed to peptidoglycan fragments. Together this data demonstrates *C. albicans*' ability to recognize bacterial carbohydrates to regulate morphology and ultimately virulence.

While it has long been known that blood serum could initiate hyphae formation in *C. albicans*, it was not until 2008 that the molecules responsible was identified as fragments of peptidoglycan¹⁸⁻¹⁹. Due to the exclusive reliance on an innate defense system, it is unsurprising that *C. albicans* would evolve a mechanism to recognize the highly conserved peptidoglycan as a means to identify and respond to bacterial threats. Similar to *C. albicans*, other species of filamentous fungi, including *Pseudoplectania nigrella*, *Coprinopsis cinerea*, and *Chalaropsis* sp., possess proteins capable of binding peptidoglycan or the precursor, Lipid II²⁰. The ability of MDP to initiate hyphae formation in *C. albicans* further highlights peptidoglycan as a microbe-

associated molecular pattern (MAMP), which is capable of triggering an immune response in a diverse set of organisms, from signal cellular fungi to incredibly complex organisms such as humans.

In addition to confirming the ability of peptidoglycan fragments to trigger hyphae formation, the work in chapter 3 was the first to demonstrate that daunosamine is capable of effecting *C. albicans* morphology. Although it has previously been shown that the anthracycline, doxorubicin, effects *C. albicans* growth, our study is the first to demonstrate that specifically the carbohydrate moiety is responsible for this effect²¹. Although other bacterial small molecules, such as the quorum sensing molecules tyrosol and 3-oxo-C12-homoserine lactone, have been demonstrated to affect *C. albicans* hyphae, daunosamine is the first carbohydrate not found in peptidoglycan shown to affect *C. albicans* morphology. The main findings of chapter 3 expand the scope of bacterial molecules (**Table 5.1**) capable of effecting *C. albicans* hyphae formation.

Table 5.1 – Bacterial molecules demonstrated to effect *C. albicans* growth and morphology

Molecule	Bacterial Source	Reference
N-acetyl-glucosamine	Various	Simonetti <i>et al</i> ²² , Leberer <i>et al</i> ¹⁷
Muramyl Dipeptide	Various	Xu <i>et al</i> ¹⁸ , Burch <i>et al</i> ²³
Muramyl Tripeptide	Gram positive	Burch <i>et al</i> ²³
Tyrosol	Various	Chen <i>et al</i> ²⁴
homoserine lactone	<i>Pseudomonas aeruginosa</i>	Hall <i>et al</i> ²⁵
Doxorubicin	<i>Streptomyces peucetius</i>	Kwok <i>et al</i> ²¹ Burch <i>et al</i> ²³
Daunosamine	<i>Streptomyces</i> sp.	Burch <i>et al</i> ²³

5.2.3 CaCYR1-LRR Binds Bacterial Derived Carbohydrates

In the 2008 paper identifying the interaction between peptidoglycan and Cyr1, only qualitative data on the binding event was given¹⁸. Since this work was published, there has no biochemical characterization of this important interaction reported in the literature. Intrigued by the ability of peptidoglycan fragments to initiate hyphae formation, we sought to determine the molecular basis for the interaction. In chapter 4, I described the development of an SPR assay used to determine the binding affinity of the LRR domain of Cyr1 for bacterial derived carbohydrates. Using this technique, we were the first to demonstrate doxorubicin and daunosamine directly interacted with Cyr1. Cyr1-LRR bound to both daunosamine and MTP with K_d values of approximately 200 nM. This is an exciting result as typical monosaccharide-protein interactions can be expected to have K_d values on the high micromolar to millimolar scale and it had been hypothesized that polyvalent interactions are need for carbohydrate interactions to be biologically relevant²⁶⁻²⁷. Competition assays demonstrated that doxorubicin, MDP, MTP, and daunosamine were competitive inhibitors for LRR binding to MTP and daunosamine on the surface. From this data we hypothesize the LRR contains a single carbohydrate-binding site. This binding site is intriguing as it shows high affinity binding but is promiscuous to the identity of the carbohydrate.

The mid-nanomolar binding affinity of Cyr1 for the various carbohydrates is intriguing as it is generally hypothesized that multivalency is needed to achieve the binding strength necessary for a biologically relevant interaction²⁸. In lectins, a common class of carbohydrate proteins, carbohydrate ligands interact with shallow polar binding sites found on the protein. The strength of the interaction relies on

multiple hydrogen bonds enhanced by CH- π stacking with aromatic interactions. This generally results in binding strengths in the micro- to millimolar range²⁸⁻²⁹. While these weak carbohydrate-protein interactions are very common, there are several examples where low micromolar and nanomolar binders have been observed. Variable lymphocyte receptors, LRR repeat proteins found in jawless vertebrates, have been demonstrated to bind the disaccharide Thomsen-Friedenreich antigen with an affinity of 8 nM³⁰. The tight binding of the disaccharide is attributed to four tryptophan residues near the binding site, which form a hydrophobic cage that stabilizes the interaction and excludes water molecules³¹. While a similar mechanism could be enhancing carbohydrate binding to Cyr1 LRR, the proposed hydrophobic cage is unlikely to be formed exclusively by tryptophan residues as only one is present in the purified construct.. If a hydrophobic cage is contributing to ligand binding strength is likely due to phenylalanine residues, the LRR of Cyr1 contains 14 phenylalanine residues grouped into three clusters on the protein (Figure 5.1). With the reliance of CH- π interactions in carbohydrate-protein binding, I hypothesize that one of the three phenylalanine rich sites is the binding pocket for carbohydrates on the LRR.

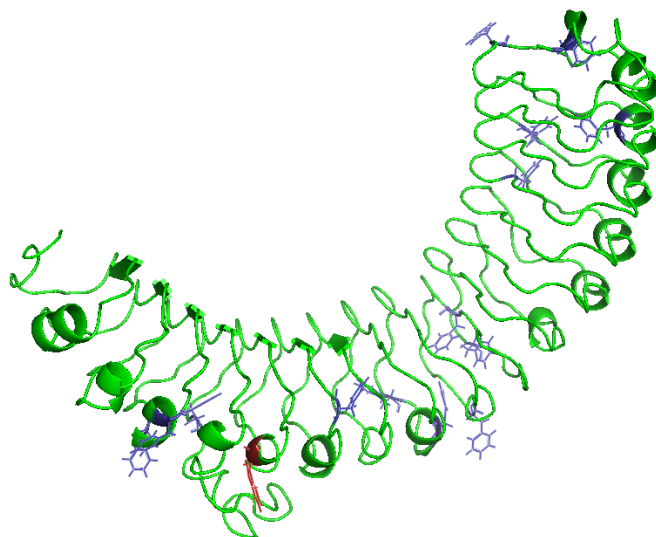


Figure 5.1 – The LRR domain of Cyr1 contains 14 phenylalanine residues (blue) and 1 tryptophan residue (red) organized into three hydrophobic clusters. Due to the reliance of CH- π interactions to stabilize carbohydrate-protein binding, these hydrophobic pockets potentially form Cyr1's binding site.

In addition to the residues present in the binding site of the protein, the structure of the carbohydrate is critical in determining the binding strength of the carbohydrate-protein interaction. Using the WW domain of Pin1 protein as a model, it has been demonstrated that variation in the stereochemistry and substituents on a pyranose ring can affect the strength of carbohydrate protein interactions. However, while variations did cause the strength of the interaction to fluctuate, all carbohydrates tested stabilized the protein suggesting that carbohydrate binding is promiscuous³². This supports the hypothesis that Cyr1 contains a single binding site capable of interacting with a variety of carbohydrates. We observed only a small fluctuation when the stereochemistry of the carbohydrate was altered between daunosamine and the muramic acid moiety of MDP. In the development of drugs to inhibit *E. coli* FmlH

and human galectin-3, the addition of aromatic groups, heterocycles, biphenyls and/or other natural products greatly enhance the affinity for the carbohydrate ligand compared to the naturally occurring variant³³⁻³⁴. The ability of these proteins to accept ligands containing large steric groups further supports the hypothesis that Cyr1 contains a single binding site and can explain how the LRR domain can bind the both the daunosamine and the much larger doxorubicin.

5.3 Future Directions

5.3.1 Improved LRR Solubility

In chapter 2, I described methods to obtain pure Cyr1-LRR as a fusion protein containing either a GST or a MBP tag. To further characterize the protein, it would be desirable to obtain a construct with no fusion partner. Unfortunately, attempts to remove the fusion tag from the construct containing amino acids 480-900 of Cyr1 resulted in insoluble protein. Looking at homology models of the protein (Figure 5.2), it appears that the purified construct could be truncating as many as eight repeats, indicated by the conserved motif of β -strands linked to α -helices. Of particular significance are the repeats missed at the N-terminus, as it has been demonstrated that LRR domains fold via an N-terminal polarized pathway. In Internalin B, deletion of the first repeat decreases the rate of folding and stability of the protein³⁵. Having possibly deleted the first LRR of Cyr1 may decrease the stability of the protein. Additionally, capping domains are often present before the first and after the last LRR. These capping domains are often cysteine rich³⁶; analysis of the sequence of Cyr1 shows cysteines present in the predicted first and last repeats. To test the hypothesis of

the LRR domain predicted by domain databases³⁷ being truncated, I propose expressing and purify a construct containing amino acids 370-1135 of Cyr1.

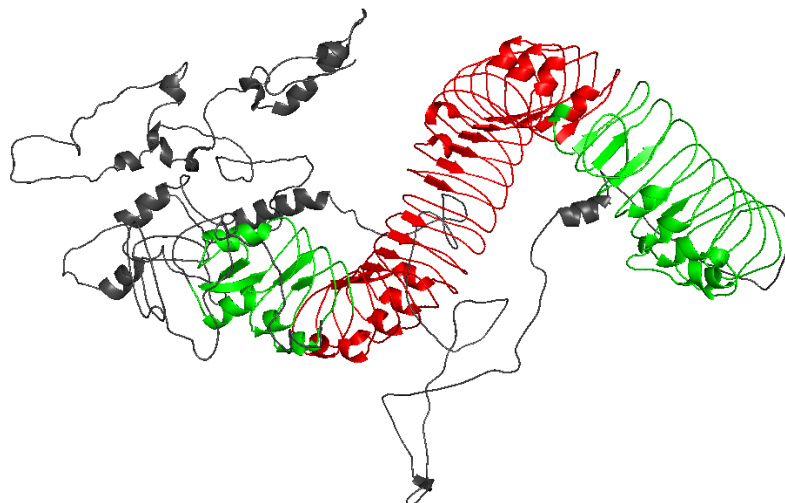


Figure 5.2 – Homology model of Cyr1. Residues 480-900 (red) indicate the predicted LRR domain from the SMART database. Residues 370 -1135 (green) show repeats truncated in the purified construct

5.3.2 Predicting the Carbohydrate Binding Pocket

To elucidate the molecular mechanism of carbohydrate binding to Cyr1 it is necessary to identify the binding site. The LRR domain of Cyr1 demonstrates mid-nanomolar binding affinity for MTP and daunosamine, which is curious, as typical monosaccharide-protein interactions are much weaker²⁷. Identifying the residues responsible for this tight interaction can help expand the understanding of protein-carbohydrate interactions. Examinations of crystal structures of carbohydrate binding

proteins have identified increased prevalence of aromatic residues in their binding pockets²⁹. These aromatic residues provide specificity and increased strength by engaging in CH- π interactions with the carbohydrates. Of the aromatic residues, tryptophan is the most common amino acid found in the vicinity of carbohydrates²⁹. Looking at the sequence of the purified LRR domain, only one tryptophan residue is present at residue 760 (Figure 5.3). Due to the prevalence of tryptophan residues in carbohydrate binding, I hypothesize that this residue may be critical for binding of peptidoglycan fragments. Our lab has previously demonstrated, that mutating a conserved tryptophan in Nod2 results in a 4-fold decrease in binding affinity for MDP³⁸. I propose purifying a W730A mutant to examine the importance of this residue.

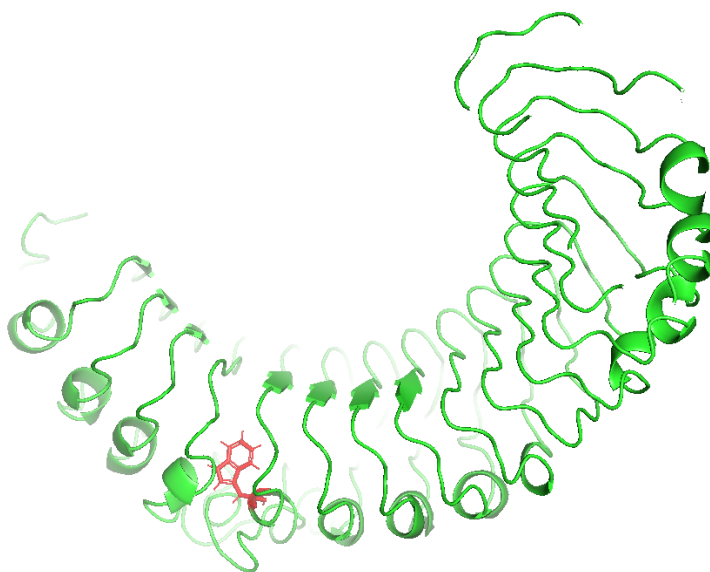


Figure 5.3 – The LRR domain of Cyr1 contains a single tryptophan residue at position 730. Mutational analysis can be employed to assess the importance of this residue in carbohydrate binding.

5.3.3 Photoactivatable Crosslinking

Pioneering work by James Paulson demonstrated the potential of carbohydrates with photoactivatable moieties to identify protein carbohydrate interactions³⁹. Since this seminal work, Jen Kohler has reported the synthesis of many monosaccharaides with diazirine crosslinkers⁴⁰⁻⁴¹. The small size of the diazirine allows for their incorporation into sugars with minimum interference in binding interactions. When diazirine crosslinkers are exposed to UV-light, elemental nitrogen is released and a carbene is formed. Through C-H or N-H insertion a stable bond is created between the carbohydrate crosslinker and the interacting protein⁴⁰⁻⁴¹. Inspired by Jen Kohler's work, a former member of the Grimes' group, Dr. James Melnyk, synthesized MDP derivatives appended with diazirine and azide moities. Dr. Melnyk proposed photocrosslinking MDP to Nod2 then utilizing the azide handle clicking on a fluorophore for visualization using in-gel fluorescence.

I propose using these photoactivatable MDP crosslinkers to identify the binding site in Cyr1. Mass spectrometric analysis has been used to elucidate binding residues in protein-protein interactions. After crosslinking, the complexes are digested with trypsin and proteomic mass spectrometry can identify crosslinked peptide fragments⁴². Similar techniques could be used to identify the MDP's binding site in Cyr1 (Figure 5.4). Identifying the binding site could elucidate the mechanism by which LRR proteins are able achieve nanomolar binding affinities for carbohydrates.

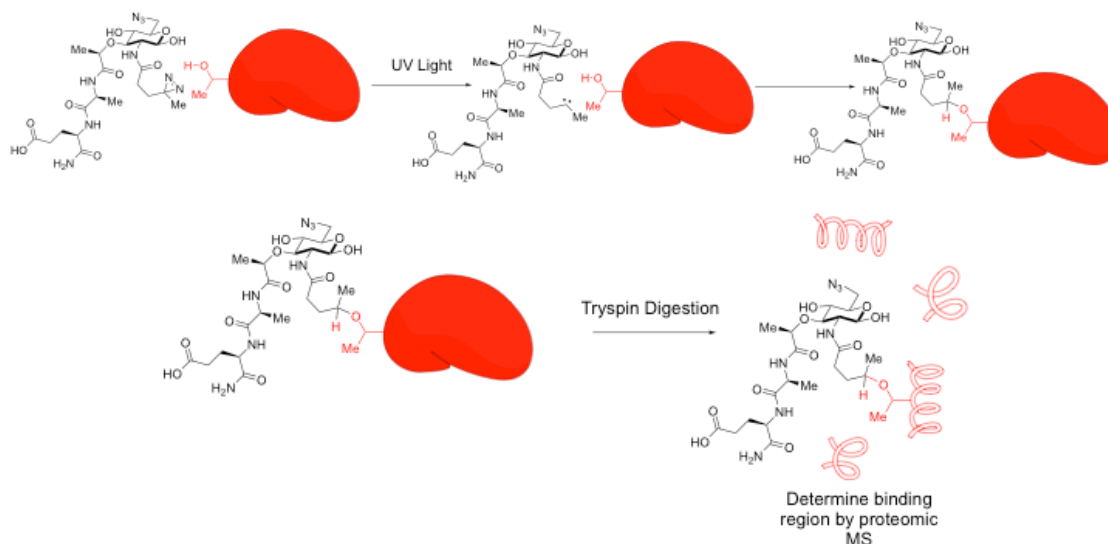


Figure 5.4 – Proposed mass spectrometry experiments to identify the MDP's binding site on Cyr1. The LRR domain would be incubated with photoactivatable MDP. After exposure to UV light, the protein will be digested with trypsin and analyzed by proteomic mass spectrometry

5.4 Summary

The findings presented in this thesis further the understanding of how microorganisms located in the human body are able to recognize and respond to different species on a molecular level. Using microscopy, ELISA, and qPCR assays, I demonstrated that the common human fungal pathogen *Candida albicans* undergoes a morphological switch in the presence of carbohydrates derived from the bacterial cell wall. The change from budding yeast to filamentous hyphae has been linked to biofilm formation and the penetration of epithelial barriers which leads to systemic infection⁴³. Utilizing recombinant protein obtained from *E. coli* inclusion bodies, a SPR assay was developed which demonstrated that the carbohydrates directly interacted with the LRR domain of Cyr1. This work not only is the first to characterize the binding strength of CYR1 and the peptidoglycan fragment, MTP, but is also the first to report the binding

of doxorubicin and its sugar moiety, daunosamine, by Cyr1. These carbohydrates ligands can be used as leads for the development of glycomimetic antifungal drugs, which are being explored as a new class of antibiotics to combat drug resistant microbes⁴⁴⁻⁴⁷. While this work is scratching the surface of this field, laying the foundation is an essential building block towards new paradigm shifting breakthroughs. The growing interest in this field will have positive impacts on the fields of science and medicine as more and more research is done on these key interactions.

On a larger biological scale, this thesis provides further insight to the molecular understanding of LRR domains and protein-carbohydrate binding. The SPR assay utilized revealed the LRR of Cyr1 is capable of binding stereochemically diverse carbohydrates and is tolerant to large substituents attached to the carbohydrate. Most interestingly these monosaccharides have mid-nanomolar binding affinities, providing further evidence challenging the hypothesis that only polysaccharide can form strong biologically relevant interactions²⁸. These results lay the inspiration for future research focusing on further investigating the scope and root cause of these unexpected interactions.

REFERENCES

1. Peterson, J.; Garges, S.; Giovanni, M.; McInnes, P.; Wang, L.; Schloss, J. A.; Bonazzi, V.; McEwen, J. E.; Wetterstrand, K. A.; Deal, C.; Baker, C. C.; Di Francesco, V.; Howcroft, T. K.; Karp, R. W.; Lunsford, R. D.; Wellington, C. R.; Belachew, T.; Wright, M.; Giblin, C.; David, H.; Mills, M.; Salomon, R.; Mullins, C.; Akolkar, B.; Begg, L.; Davis, C.; Grandison, L.; Humble, M.; Khalsa, J.; Little, A. R.; Peavy, H.; Pontzer, C.; Portnoy, M.; Sayre, M. H.; Starke-Reed, P.; Zakhari, S.; Read, J.; Watson, B.; Guyer, M., The NIH Human Microbiome Project. *Genome research* **2009**, *19* (12), 2317-23. 10.1101/gr.096651.109
2. Huang, Y. J.; Boushey, H. A., The microbiome in asthma. *The Journal of allergy and clinical immunology* **2015**, *135* (1), 25-30. 10.1016/j.jaci.2014.11.011
3. Ling, Z.; Li, Z.; Liu, X.; Cheng, Y.; Luo, Y.; Tong, X.; Yuan, L.; Wang, Y.; Sun, J.; Li, L.; Xiang, C., Altered fecal microbiota composition associated with food allergy in infants. *Appl Environ Microbiol* **2014**, *80* (8), 2546-54. 10.1128/AEM.00003-14
4. Schwabe, R. F.; Jobin, C., The microbiome and cancer. *Nature reviews. Cancer* **2013**, *13* (11), 800-12. 10.1038/nrc3610
5. Lauro, M. L.; Burch, J. M.; Grimes, C. L., The effect of NOD2 on the microbiota in Crohn's disease. *Current Opinion in Biotechnology* **2016**, *40*, 97-102. <http://dx.doi.org/10.1016/j.copbio.2016.02.028>
6. Wang, B.; Yao, M.; Lv, L.; Ling, Z.; Li, L., The Human Microbiota in Health and Disease. *Engineering* **2017**, *3* (1), 71-82. <https://doi.org/10.1016/J.ENG.2017.01.008>
7. Huseyin, C. E.; O'Toole, P. W.; Cotter, P. D.; Scanlan, P. D., Forgotten fungi-the gut mycobiome in human health and disease. *FEMS Microbiol Rev* **2017**, *41* (4), 479-511. 10.1093/femsre/fuw047

8. Qiu, X.; Zhang, F.; Yang, X.; Wu, N.; Jiang, W.; Li, X.; Li, X.; Liu, Y., Changes in the composition of intestinal fungi and their role in mice with dextran sulfate sodium-induced colitis. *Scientific Reports* **2015**, *5*, 10416. 10.1038/srep10416
9. Adam, B.; Baillie, G. S.; Douglas, L. J., Mixed species biofilms of *Candida albicans* and *Staphylococcus epidermidis*. *J Med Microbiol* **2002**, *51* (4), 344-9. 10.1099/0022-1317-51-4-344
10. Hogan, D. A.; Kolter, R., *Pseudomonas-Candida* interactions: an ecological role for virulence factors. *Science* **2002**, *296* (5576), 2229-32. 10.1126/science.1070784
11. Metwalli, K. H.; Khan, S. A.; Krom, B. P.; Jabra-Rizk, M. A., *Streptococcus mutans*, *Candida albicans*, and the human mouth: a sticky situation. *PLoS Pathog* **2013**, *9* (10), e1003616. 10.1371/journal.ppat.1003616
12. Pierce, G. E., *Pseudomonas aeruginosa*, *Candida albicans*, and device-related nosocomial infections: implications, trends, and potential approaches for control. *J Ind Microbiol Biotechnol* **2005**, *32* (7), 309-18. 10.1007/s10295-005-0225-2
13. Schlecht, L. M.; Peters, B. M.; Krom, B. P.; Freiberg, J. A.; Hansch, G. M.; Filler, S. G.; Jabra-Rizk, M. A.; Shirliff, M. E., Systemic *Staphylococcus aureus* infection mediated by *Candida albicans* hyphal invasion of mucosal tissue. *Microbiology* **2015**, *161* (Pt 1), 168-181. 10.1099/mic.0.083485-0
14. Pappas, P. G.; Kauffman, C. A.; Andes, D. R.; Clancy, C. J.; Marr, K. A.; Ostrosky-Zeichner, L.; Reboli, A. C.; Schuster, M. G.; Vazquez, J. A.; Walsh, T. J.; Zaoutis, T. E.; Sobel, J. D., Clinical Practice Guideline for the Management of Candidiasis: 2016 Update by the Infectious Diseases Society of America. *Clin Infect Dis* **2016**, *62* (4), e1-50. 10.1093/cid/civ933
15. Gow, N. A. R.; Yadav, B., Microbe Profile: *Candida albicans*: a shape-changing, opportunistic pathogenic fungus of humans. *Microbiology* **2017**, *163* (8), 1145-1147. 10.1099/mic.0.000499
16. Sudbery, P. E., Growth of *Candida albicans* hyphae. *Nature reviews. Microbiology* **2011**, *9* (10), 737-48. 10.1038/nrmicro2636

17. Rocha, C. R.; Schroppel, K.; Harcus, D.; Marcil, A.; Dignard, D.; Taylor, B. N.; Thomas, D. Y.; Whiteway, M.; Leberer, E., Signaling through adenylyl cyclase is essential for hyphal growth and virulence in the pathogenic fungus *Candida albicans*. *Mol Biol Cell* **2001**, *12* (11), 3631-43.
18. Xu, X. L.; Lee, R. T.; Fang, H. M.; Wang, Y. M.; Li, R.; Zou, H.; Zhu, Y.; Wang, Y., Bacterial peptidoglycan triggers *Candida albicans* hyphal growth by directly activating the adenylyl cyclase *Cyr1p*. *Cell Host Microbe* **2008**, *4* (1), 28-39. 10.1016/j.chom.2008.05.014
19. Reynolds, R., The filament inducing property of blood for *Candida albicans* : its nature and significance. *Clin. Res. Proc.* **1956**, *4*, 40.
20. Kunzler, M., Hitting the sweet spot-glycans as targets of fungal defense effector proteins. *Molecules (Basel, Switzerland)* **2015**, *20* (5), 8144-67. 10.3390/molecules20058144
21. Kwok, S. C.; Schelenz, S.; Wang, X.; Steverding, D., In vitro effect of DNA topoisomerase inhibitors on *Candida albicans*. *Med Mycol* **2010**, *48* (1), 155-60. 10.3109/13693780903114934
22. Simonetti, N.; Strippoli, V.; Cassone, A., Yeast-mycelial conversion induced by N-acetyl-D-glucosamine in *Candida albicans*. *Nature* **1974**, *250*, 344. 10.1038/250344a0
23. Burch, J. M.; Mashayekh, S.; Wykoff, D. D.; Grimes, C. L., Bacterial Derived Carbohydrates Bind *Cyr1* and Trigger Hyphal Growth in *Candida albicans*. *ACS Infect Dis* **2018**, *4* (1), 53-58. 10.1021/acsinfecdis.7b00154
24. Chen, H.; Fujita, M.; Feng, Q.; Clardy, J.; Fink, G. R., Tyrosol is a quorum-sensing molecule in *Candida albicans*. *Proceedings of the National Academy of Sciences of the United States of America* **2004**, *101* (14), 5048-52. 10.1073/pnas.0401416101
25. Hall, R. A.; Turner, K. J.; Chaloupka, J.; Cottier, F.; De Sordi, L.; Sanglard, D.; Levin, L. R.; Buck, J.; Muhlschlegel, F. A., The quorum-sensing molecules farnesol/homoserine lactone and dodecanol operate via distinct modes of action in *Candida albicans*. *Eukaryot Cell* **2011**, *10* (8), 1034-42. 10.1128/EC.05060-11
26. Reynolds, M.; Pérez, S., Thermodynamics and chemical characterization of protein-carbohydrate interactions: The multivalency issue. *Comptes Rendus Chimie* **2011**, *14* (1), 74-95.
<https://doi.org/10.1016/j.crci.2010.05.020>

27. Hudson, K. L., Introduction. In *Carbohydrate-Based Interactions at the Molecular and the Cellular Level*, 2018, 10.1007/978-3-319-77706-1_1pp 1-34.
28. Hudson, K. L., The Nature of Protein–Carbohydrate Interactions. In *Carbohydrate-Based Interactions at the Molecular and the Cellular Level*, 2018, 10.1007/978-3-319-77706-1_3pp 57-86.
29. Hudson, K. L.; Bartlett, G. J.; Diehl, R. C.; Agirre, J.; Gallagher, T.; Kiessling, L. L.; Woolfson, D. N., Carbohydrate-Aromatic Interactions in Proteins. *J Am Chem Soc* **2015**, *137* (48), 15152-60. 10.1021/jacs.5b08424
30. Hong, X.; Ma, M. Z.; Gildersleeve, J. C.; Chowdhury, S.; Barchi, J. J., Jr.; Mariuzza, R. A.; Murphy, M. B.; Mao, L.; Pancer, Z., Sugar-binding proteins from fish: selection of high affinity "lambodies" that recognize biomedically relevant glycans. *ACS chemical biology* **2013**, *8* (1), 152-60. 10.1021/cb300399s
31. Luo, M.; Velikovskiy, C. A.; Yang, X.; Siddiqui, M. A.; Hong, X.; Barchi, J. J., Jr.; Gildersleeve, J. C.; Pancer, Z.; Mariuzza, R. A., Recognition of the Thomsen-Friedenreich pancarcinoma carbohydrate antigen by a lamprey variable lymphocyte receptor. *The Journal of biological chemistry* **2013**, *288* (32), 23597-606. 10.1074/jbc.M113.480467
32. Hsu, C. H.; Park, S.; Mortenson, D. E.; Foley, B. L.; Wang, X.; Woods, R. J.; Case, D. A.; Powers, E. T.; Wong, C. H.; Dyson, H. J.; Kelly, J. W., The Dependence of Carbohydrate-Aromatic Interaction Strengths on the Structure of the Carbohydrate. *J Am Chem Soc* **2016**, *138* (24), 7636-48. 10.1021/jacs.6b02879
33. Kalas, V.; Hibbing, M. E.; Maddirala, A. R.; Chugani, R.; Pinkner, J. S.; Mydock-McGrane, L. K.; Conover, M. S.; Janetka, J. W.; Hultgren, S. J., Structure-based discovery of glycomimetic FmlH ligands as inhibitors of bacterial adhesion during urinary tract infection. *Proceedings of the National Academy of Sciences of the United States of America* **2018**, *115* (12), E2819-E2828. 10.1073/pnas.1720140115
34. Zetterberg, F. R.; Peterson, K.; Johnsson, R. E.; Brimert, T.; Hakansson, M.; Logan, D. T.; Leffler, H.; Nilsson, U. J., Monosaccharide Derivatives with Low-Nanomolar Lectin Affinity and High Selectivity Based on Combined Fluorine-Amide, Phenyl-Arginine, Sulfur-pi, and Halogen Bond Interactions. *ChemMedChem* **2018**, *13* (2), 133-137. 10.1002/cmdc.201700744

35. Courtemanche, N.; Barrick, D., The leucine-rich repeat domain of Internalin B folds along a polarized N-terminal pathway. *Structure* **2008**, *16* (5), 705-14. 10.1016/j.str.2008.02.015
36. Bella, J.; Hindle, K. L.; McEwan, P. A.; Lovell, S. C., The leucine-rich repeat structure. *Cell Mol Life Sci* **2008**, *65* (15), 2307-33. 10.1007/s00018-008-8019-0
37. Schultz, J.; Copley, R. R.; Doerks, T.; Ponting, C. P.; Bork, P., SMART: a web-based tool for the study of genetically mobile domains. *Nucleic acids research* **2000**, *28* (1), 231-4.
38. Lauro, M. L.; D'Ambrosio, E. A.; Bahnson, B. J.; Grimes, C. L., Molecular Recognition of Muramyl Dipeptide Occurs in the Leucine-rich Repeat Domain of Nod2. *ACS Infect Dis* **2017**, *3* (4), 264-270. 10.1021/acsinfectdis.6b00154
39. Han, S.; Collins, B. E.; Bengtson, P.; Paulson, J. C., Homomultimeric complexes of CD22 in B cells revealed by protein-glycan cross-linking. *Nature Chemical Biology* **2005**, *1*, 93. 10.1038/nchembio713
40. McCombs, J. E.; Zou, C.; Parker, R. B.; Cairo, C. W.; Kohler, J. J., Enhanced Cross-Linking of Diazirine-Modified Sialylated Glycoproteins Enabled through Profiling of Sialidase Specificities. *ACS chemical biology* **2016**, *11* (1), 185-192. 10.1021/acscchembio.5b00775
41. Tanaka, Y.; Kohler, J. J., Photoactivatable Crosslinking Sugars for Capturing Glycoprotein Interactions. *Journal of the American Chemical Society* **2008**, *130* (11), 3278-3279. 10.1021/ja7109772
42. Leitner, A.; Faini, M.; Stengel, F.; Aebersold, R., Crosslinking and Mass Spectrometry: An Integrated Technology to Understand the Structure and Function of Molecular Machines. *Trends in biochemical sciences* **2016**, *41* (1), 20-32. <https://doi.org/10.1016/j.tibs.2015.10.008>
43. Sardi, J. C.; Scorzoni, L.; Bernardi, T.; Fusco-Almeida, A. M.; Mendes Giannini, M. J., Candida species: current epidemiology, pathogenicity, biofilm formation, natural antifungal products and new therapeutic options. *J Med Microbiol* **2013**, *62* (Pt 1), 10-24. 10.1099/jmm.0.045054-0
44. AlFindee, M. N.; Zhang, Q.; Subedi, Y. P.; Shrestha, J. P.; Kawasaki, Y.; Grilley, M.; Takemoto, J. Y.; Chang, C. T., One-step synthesis of carbohydrate esters as antibacterial and antifungal agents. *Bioorg Med Chem* **2018**, *26* (3), 765-774. 10.1016/j.bmc.2017.12.038

45. Ernst, B.; Magnani, J. L., From carbohydrate leads to glycomimetic drugs. *Nat Rev Drug Discov* **2009**, 8 (8), 661-77. 10.1038/nrd2852
46. Vandeputte, P.; Ferrari, S.; Coste, A. T., Antifungal resistance and new strategies to control fungal infections. *Int J Microbiol* **2012**, 2012, 713687. 10.1155/2012/713687
47. Delso, I.; Valero-Gonzalez, J.; Marca, E.; Tejero, T.; Hurtado-Guerrero, R.; Merino, P., Rational Design of Glycomimetic Compounds Targeting the *Saccharomyces cerevisiae* Transglycosylase Gas2. *Chem Biol Drug Des* **2016**, 87 (2), 163-70. 10.1111/cbdd.12650

Appendix

REPRINT PERMISSIONS

Chapters 2, 3, and 4 are largely adapted from the following publication:

Burch, J. M.; Mashayekh, S.; Wykoff, D. D.; Grimes, C. L., Bacterial Derived Carbohydrates Bind Cyr1 and Trigger Hyphal Growth in *Candida albicans*. *ACS Infect Dis* **2018**, *4* (1), 53-58. DOI: 10.1021/acsinfecdis.7b00154. (<https://pubs.acs.org/doi/abs/10.1021/acsinfecdis.7b00154>)

Dear Dr. Burch:

Thank you for contacting ACS Publications Support.

Your permission request is granted and there is no fee for this reuse. In your planned reuse, you must cite the ACS article as the source, add this direct link (<https://pubs.acs.org/doi/abs/10.1021/acsinfecdis.7b00154>) and include a notice to readers that further permissions related to the material excerpted should be directed to the ACS.

I hope this information helped. Please let me know if I can be of further assistance.

Sincerely,

Kryxie J. Ramirez
ACS Customer Services & Information
<https://help.acs.org/>

Dear jburch@udel.edu,

Incident Information:

Incident #: 2441691

Date Created: 2018-12-18T03:14:22

Priority: 3

Customer: jburch@udel.edu

Title: Rights for Bacterial Derived Carbohydrates Bind Cyr1 and Trigger Hyphal Growth in Candida albicans

Description: I like like to request permission to reuse the entire contents of the article Bacterial Derived Carbohydrates Bind Cyr1 and Trigger Hyphal Growth in Candida albicans (<https://pubs.acs.org/doi/abs/10.1021/acsinfecdis.7b00154>). I am the first author on the paper and would like to include the paper in my thesis at the University of Delaware.

Thank You,
Jason Burch